SYNTHESIS, CHARACTERIZATION AND MATRIX METALLOPROTEINASE INHIBITION OF DOXYCYCLINE MODIFIED DENTAL ADHESIVES

Jadesada Palasuk

Submitted to the faculty of the University Graduate School
in partial fulfillment of the requirements
for the degree
Doctor of Philosophy
in the School of Dentistry,
Indiana University

February 2016

Accepted by the Graduate Faculty, Indiana University, in partial fulfillment of the requirements for the degree of Doctor of Philosophy.

L. Jack Windsor, Ph.D., Co-chair

Marco C. Bottino, D.D.S., M.S., Ph.D., Co-chair

Doctoral Committee

Jeffrey A. Platt, D.D.S., M.S.

Chao-Hung Lee, Ph.D.

October 23, 2015

Saulo Geraldeli, D.D.S., M.S., Ph.D.

DEDICATION

I dedicate this dissertation to my parents for their unconditional love, support and encouragement.

ACKNOWLEDGEMENTS

Completing a Ph.D. is very challenging. This dissertation would not have been completed without the support of many people. First and foremost, I would like to express my deepest appreciation to my co-mentors, Dr. L. Jack Windsor and Dr. Marco C. Bottino for their continuous support of my Ph.D. study and dissertation, as well as for their patience, motivation, and knowledge. I deeply appreciate them for giving me the opportunities to study and work in their lab, and to gain a lot of expertise from them. Without their guidance, expertise and support, this would not have been possible.

Beside my co-mentors, I would like to thank Dr. Jeffrey A. Platt, Dr. Saulo Geraldeli, and Dr. Chao-Hung Lee for their evaluation of my dissertation and being on my doctoral research committee.

My appreciation is also expressed to Dr. Richard Gregory and Dr. Fengyu Song for their help and support, to Dr. Bruce Cooper from Bindley Bioscience Center, Purdue University, who taught and assisted me with the HPLC and mass spectrometry analysis, and Sabrina and Krzysztof who helped me with parts of this project.

In addition, I thank my friends and colleague P Nok, Nui and Beth for their friendship and for times that I spent with them.

I take this opportunity to thank the Ministry of Science and Technology (Thailand) for the financial support throughout my master and Ph.D. studies at Indiana University School of Dentistry and the Delta Dental Foundation for the financial support of this project.

Finally, my deeply gratitude is given to my parents and my brother for supporting me spiritually throughout my life.

Jadesada Palasuk

SYNTHESIS, CHARACTERIZATION AND MATRIX METALLOPROTEINASE INHIBITION OF DOXYCYCLINE MODIFIED DENTAL ADHESIVES

The biodegradation of the hybrid layer of dental restorations is due in part to the degradation of the demineralized collagen by matrix metalloproteinases (MMPs). During the bonding procedure, phosphoric acid/acidic primers activate MMPs that degrade denuded type I collagen. As a result, the hybrid layer loses its integrity overtime, leading to the failure of the resin composite restoration. This study aimed to evaluate doxycycline (DOX) for its effects on preventing the degradation of the hybrid layer through the modification of the dental adhesive with aluminosilicate clay nanotubes (HNT) loaded with doxycycline.

Doxycycline was encapsulated into HNT at three distinct concentrations (10%, 20% and 30% DOX, w/v). The increases in the concentration of doxycycline significantly increased the amount of doxycycline that was encapsulated into HNT and the drug loading into the HNT. Conversely, the encapsulation efficiency was significantly decreased with the increases in concentration of doxycycline. The modified adhesives were fabricated by incorporation of DOX-encapsulated HNT into a commercially available dental adhesive (Adper Scotchbond Multi-Purpose, SBMP). The degree of conversion (DC), Knoop microhardness, doxycycline release profiles, the biological activity (antibacterial and anti-MMP activity), and cytocompatibility of the modified adhesives were investigated. There were no statistically significant differences ($p > 0.05$) in DC and Knoop microhardness compared to the control (SBMP). None of the adhesive

eluates was cytotoxic to the human dental pulp stem cells. Although higher concentrations of doxycycline led to a higher release of doxycycline from the modified adhesives, the differences were not significant ($p = 0.259$) among the groups (10%, 20% and 30% DOX). A significant growth inhibition of *S. mutans* and *L. casei* by direct contact illustrated successful encapsulation of doxycycline into the modified adhesives. Doxycycline released from the modified adhesives did not inhibit the growth of both cariogenic bacteria but inhibited MMP-1 activity. The results suggested that subantimicrobial levels of doxycycline were gradually released. The immediate microtensile bond strengths were not significantly different from those of the control (SBMP), suggesting no negative effect of doxycycline on dentin bonding (only 10% DOX were investigated). The long-term resin-dentin bond durability should be evaluated.

L. Jack Windsor, Ph.D., Co-chair

Marco C. Bottino, D.D.S., M.S., Ph.D., Co-chair

TABLE OF CONTENTS

LIST OF TABLES

LIST OF FIGURES

LIST OF ABBREVIATIONS

10-MDP	10-methacryloxydecyl dihydrogen phosphate
4-MET	4-methacryloxyethyl trimellitic acid
ANOVA	Analysis of Variance
APMA	4-aminophenylmercuric acetate
Bis-EMA	Bisphenol A polyethylene glycol diemthacrylate
Bis-GMA	Bisphenol A glycidyl dimethacrylate
BisHPPP	Bis-hydroxy-propoxy-phenyl-propane
CHX	Chlorhexidine
DC	Degree of conversion
DEJ	Dentin-enamel junction
DMEM	Dulbecco's Modified Eagle's Medium
DMP-1	Dentin matrix protein-1
DMSO	Dimethyl sulfoxide
DOX	Doxycycline
DPP	Dentin phosphoprotein
DSP	Dentin sialoprotein
ECM	Extracellular matrix
EGCG	Epigallocatechin gallate
EGDMA	Ethylene glycol dimethacrylate
FITC	Fluorescein isothiocyanate
hDPSCs	Human dental pulp stem cells
HEMA	2-hydroxyethyl methacrylate

HNT	Aluminosilicate clay nanotubes (Halloysite nanotubes)
HPLC	High-pressure liquid chromatography
KHN	Knoop hardness number
L. casei	*Lactobacilli casei*
MA	Methacrylic acid
MDPB	12-methacryloyloxydodecylpyridinium bromide
MMPs	Matrix metalloproteinases
NIH	National Institute of Health
PBS	Phosphate buffer saline
PENTA	Dipentaerythritol pentaacrylate monophosphate
Phenyl-P	2-methacryloxyethyl phenyl hydrogen phosphate
RTT	Rat tail tendon
S. mutans	*Streptococcus mutans*
SBMP	Adper Scotchbond Multi-Purpose
SD	Standard deviation
SDD	Subantimicrobial dose doxycycline
SDS-PAGE	Sodium dodecyl sulfate-polyacrylamide gel electrophoresis
SEM	Scanning electron microscopy
SiC	Silicon carbide
SUP	Supernatant
TEG	Triethylene glycol
TEGDMA	Triethylene glycol dimethacrylate
TEGMA	Triethylene glycol methacrylate

TEM	Transmission electron microscopy
UDMA	Urethane dimethacrylate
WST-1	Water-Soluble Tetrazolium-1

INTRODUCTION

According to a report of the World Health Organization (WHO), dental caries is one of the world's major diseases affecting 60–90% of children and most adults (Petersen and Lennon, 2004). Resin composites have become one of the materials of choice for direct restoration because of superior esthetics and minimally invasive preparations, compared to traditionally used amalgam restorations with mercury concerns. However, resin composite restorations have an average lifetime of only 5.7 years (Liu et al., 2011) and an average annual failure rate of 2.2% (Manhart et al., 2004; Mjor et al., 2000). Replacement of defective dental restorations costs approximately five billion dollars per year in the US (Jokstad et al., 2001). Secondary caries that develops at the margin of the restoration is the primary reason for restoration replacement (Mjor et al., 2000). Kermanshahi et al. reported that degradation of the hybrid layer of a dental restoration increased bacterial microleakage (Kermanshahi et al., 2010). As a consequence, the degradation of the hybrid layer may contribute to recurrent caries or failure of the restorations. Since the hybrid layer of resin-enamel bonding is more durable than that of resin-dentin bonding (Loguercio et al., 2008), this study focused mainly on the resin-dentin bonding and the degradation of the hybrid layer at the resin-dentin interface.

Anatomy of teeth

Enamel

Enamel is the hard-mineralized tissue that covers the crown of teeth. Enamel is formed by ameloblasts starting at the dentin-enamel junction (DEJ) and proceeding outward to the tooth surface. Enamel covers the anatomic crowns of teeth and varies in thickness in different areas and is the hardest substance of the human body. Enamel is a

highly mineralized crystalline structure consisting of approximately 95–98% by weight and 90–92% by volume inorganic components. Hydroxyapatite crystal makes up the highest amount of the mineral content in enamel. The remaining components of enamel are organic matrix and water of approximately 1–2% and 4% by weight, respectively. The organic matrices of enamel are mainly amelogenins and enamelins that are resorbed during tooth maturation (Sakaguchi and Powers, 2012). Enamel is structurally arranged as prisms or rods of approximately 5 μm in diameter (Roberson et al., 2006; Sakaguchi and Powers, 2012). The numbers of rods are approximately 5 million for mandibular incisors and 12 million for maxillary molars. Enamel rods generally orient perpendicularly to the DEJ and the tooth surface except in the cervical region where they are aligned outward in a slightly apical direction (Roberson et al., 2006).

Dentin-Pulp Complex

The dentin and the dental pulp are considered as a biologic entity named the "dentin-pulp complex" because of their common mesenchymal origin, conjugated evolution, and highly related interactions (Vitalariu et al., 2005). Dentin is a mineralized connective tissue formed by odontoblasts. The body of odontoblasts is located in the pulp chamber but their cytoplasmic processes are extended toward the dentinal tubules. Therefore, dentin is considered a living tissue and can respond to external stimuli (i.e., caries, trauma) creating different forms of dentin such as secondary, reparative or tertiary, and sclerotic dentin.

Mature dentin contains 50% inorganic structures, 30% organic structures, and 20% water by weight. Like enamel, the inorganic component is primarily hydroxyapatite crystals. The organic components are mainly type I collagen and noncollagenous proteins

such as dentin matrix protein 1 (DMP 1), dentin phosphoprotein (DPP), and dentin sialoprotein (DSP) (Mazzoni et al., 2009). One of the main structures of dentin is dentinal tubules that are small canals created by odontoblasts during dentin formation or dentinogenesis. Dentinal tubules extend from the DEJ to the pulp chamber covering the entire width of dentin. Each dentinal tubule also contains the cytoplasmic extension of odontoblasts that extends approximately one third of the dentin thickness (Goracci et al., 1999). In addition to main tubules, dentin also contains a branching and anastomosing system (Mjor and Nordahl, 1996). The density and number of dentinal tubules and branching are different in different locations. The number of branches of dentinal tubules was particularly abundant in locations where the density of tubules was low. Three types of branches have been identified: major branches (0.5–1 μm in diameter), fine branches (0.3–0.7 μm in diameter), and microbranches (25–200 nm in diameter).

Dentin is typically pale yellow and is slightly harder than bone. There are two main types of dentin: intertubular and peritubular dentin (Summitt et al., 2006). Intertubular dentin is the main structural component of dentin. It is the hydroxyapatite crystal embedded in type I collagen matrix. Peritubular dentin is densely packed hydroxyapatite crystals that wrap around dentinal tubule walls. After primary dentin is formed, mineral deposition of dentin gradually decreases the tubule lumen of dentin. The rate of deposition may increase in response to external stimuli such as caries or trauma.

Cementum

Cementum is a hard-mineralized tissue secreted by cementoblasts and is present on the surface of the roots. By weight, cementum consists of 45–50% inorganic components that are primarily hydroxyapatite crystals and 55–50% organic matrix and

water. The organic contents are mainly type I collagen. Cementum is classified into two main types: cellular and acelluar cementum (Gonçalves et al., 2005). Acellular cementum is located on the coronal half of the root surface. It does not contain cementocytes in its structure. Cellular cementum is present predominantly on the apical half of root surfaces and contains cementocytes embedded in a collagenous matrix of intrinsic collagen fibers. Cellular cementum plays a crucial role in adaptive response to external stimuli (i.e. repair process) and maintaining the tooth in proper position. Thickness of cementum can increase in response to occlusal wear and passive eruption of the root (Roberson et al., 2006).

Bonding to dental substrates

Bonding mechanism

Adhesive dentistry has evolved since Buonocore first introduced orthophosphoric acid-etching to improve the adhesion of acrylic resin to enamel in 1955 (Buonocore, 1955). Nevertheless, the basic principle of adhesion to tooth substrate remains unchanged. The bonding to tooth substrate is based on an exchange process that involves the removal of mineral content from dental hard tissue followed by the application and infiltration of an adhesive resin/dentin bonding agent. This results in micromechanical interlocking that is believed to be a prerequisite for good bonding in clinical settings (Van Meerbeek et al., 2003). The micromechanical interlocking was first demonstrated in 1982 by Nakabayashi et al. (Nakabayashi et al., 1982). This process is referred to as "hybridization" or the formation of the hybrid layer (De Munck et al., 2005; Wang and Spencer, 2003). The hybrid layer is the zone that resin monomers flow and polymerize into the acid-etched dentin creating a micromechanical interlocking for resin-dentin

bonding. In the hybrid layer, demineralized collagen matrix (type I collagen) serves as a scaffold for the infiltration of hydrophilic resin monomers. Wang et al. reported that the quality of the hybrid layer that unites the resin composite with the underlying dentin is directly related to the durability of the resin-dentin bond (Wang and Spencer, 2003). Ideally, the adhesive resin should completely infiltrate into the space generated by the removal of mineral by acid etching. If the creation of the hybrid layer is imperfect, it will lead to limited resin-dentin bond durability and severely shortens the lifespan of a resin composite restoration (Liu et al., 2011).

Current adhesive systems can be classified into two major categories based on two distinct mechanisms: removing (etch-and-rinse adhesives) and modifying smear layer (self-etch adhesives) (Breschi et al., 2008).

Etch-and-rinse adhesive systems

The etch-and-rinse adhesives involve simultaneous enamel and dentin etching using 30–40% phosphoric acid (pH ~ 0.5–1) for a predetermined period of time (15–30 seconds). Subsequently, the etched enamel and dentin are rinsed off, and a primer (an adhesion promoting agent) and eventually an adhesive resin are applied either separately (three-step etch-and-rinse adhesives) or in combination (two-step etch-and-rinse adhesives). The role of the primer is to remove water that occupies interfibrillar spaces after etching and rinsing, and to facilitate resin infiltration by increasing the hydrophobicity of the dentin. Generally, primers are composed of hydrophilic monomers dissolved in an appropriate solvent. The hydrophilic monomers include 2-hydroxyethyl methacrylate (HEMA) and dipentaerythritol pentaacrylate monophosphate (PENTA). The solvents are ethanol, water, acetone or a combination of these solvents. After the

application of primer, the solvent is removed by air-drying, and the more hydrophobic dentin is copolymerized with the adhesive resin creating a 5–8 μm thick hybrid layer. Since a rinsing step is required for etch-and-rinse adhesives, the smear layer, the smear plugs, and the demineralized inorganic component of dentin will not be part of the hybrid layer after bonding (Pashley et al., 2011).

Initially, the etch-and-rinse adhesive was introduced as a dry bonding technique where the cavity wall was air-dried after acid etching and rinsing until the enamel margin appeared as a chalky-like color. This results in a relatively dry enamel surface that is needy for bonding. If the demineralized dentin is over-dried, the interfibrillar spaces of the collagen network that are essential for resin infiltration will collapse. As a consequence, the resin-enamel bond strength is high but the resin-dentin bond strength is very low (Pashley et al., 2011). The other shortcomings associated with the dry bonding technique are dentin hypersensitivity, microleakage, and secondary caries (Pashley et al., 2011).

To overcome the limitation of the dry bonding technique, Kanca introduced the concept of wet bonding (Kanca, 1992). He found that water is an excellent rewetting agent. When the demineralized dentin is moist prior to the application of primer and adhesive resins, the resin-dentin bond strength is improved with less post-operative sensitivity (Pashley et al., 2011).

Both clinical and *in vitro* studies showed that the three-step etch-and-rinse adhesive system provided a superior outcome in terms of effectiveness of bonding compared to other systems, especially the one-step self-etch adhesive systems (De Munck et al., 2003; De Munck et al., 2005; Peumans et al., 2005; Rosa et al., 2015; Van

Meerbeek et al., 2010). Therefore, the three-step etch-and-rinse adhesive is considered a gold standard for dental adhesion and is often used as a control to compare the performance of new adhesives (Van Meerbeek et al., 2010).

Self-etch adhesive systems

Unlike etch-and-rinse adhesives, self-etch adhesives do not require a separate etching step because the acidic primers of self-etch adhesives diffuse into the smear layer, etching and priming the dentin simultaneously. Since no rinsing is required, the smear layer is partially dissolved and later copolymerized with the adhesive resin, becoming part of the hybrid layer (Koibuchi et al., 2001; Prati et al., 1998; Tay et al., 2000). One of the main advantages of this approach is fewer incidences of post-operative sensitivity, compared to the etch-and-rinse adhesives, due to less aggressive acid etching of dentin and the presence of a partially dissolved smear layer that obstructs dentinal tubules. Generally, hybrid layers created by self-etch adhesives range from 1–2 μm in thickness, depending upon the acidity of the monomers used (Van Meerbeek et al., 2011). It has been reported that the number of resin tags, not the length of resin tags or thickness of the hybrid layer, plays a major role in dentin bonding (Lohbauer et al., 2008; Yoshiyama et al., 1995).

Based on the pH or intensity of acid demineralization, self-etch adhesives are subdivided into four types: ultra mild (pH > 2.5), mild (pH ~ 2), intermediate (pH = 1–2) and strong (pH < 1) (Van Meerbeek et al., 2011). Like etch-and-rinse adhesives, strong self-etch adhesives completely dissolve the hydroxyapatite from dentin but unlike etch-and-rinse adhesives, the hydroxyapatite is not rinsed off. This results in relatively deep dentin hybridization several micrometers thick, and the dissolved calcium and phosphate

that remain in the demineralized dentin are not stable in an aqueous environment. As a result, the resin-dentin bond is compromised with less hydrolytic stability (Van Meerbeek et al., 2011).

On the other hand, the mild self-etch adhesives partially demineralize dentin creating submicron-thick hybrid layers, in which substantial amount of hydroxyapatite remains around exposed collagen. Generally, the acidic monomers of self-etch primers and adhesives are esters from the reaction of a bivalent alcohol with methacrylic acid and phosphoric/carboxylic acid derivatives (Yoshida et al., 2004). Moreover, self-etch adhesives also contain specific functional monomers that facilitate chemical bonding to the remaining hydroxyapatite.

The chemical interaction between dentin and self-etch adhesives occurs through the ionic bond formed between the calcium in hydroxyapatite and the carboxylic/phosphate group of the functional monomers in the acidic primer [i.e., 10-methacryloxydecyl dihydrogen phosphate (10-MDP), 4-methacryloyloxyethyl trimellitic acid (4-MET), and 2-methacryloxyethyl phenyl hydrogen phosphate (phenyl-P) (De Munck et al., 2005; Lohbauer et al., 2008; Yoshida et al., 2004)]. According to the Adhesion-Decalcification (AD) concept, the functional monomers first chemically or ionically bond to calcium in the hydroxyapatite. This step occurs together with the release of phosphate (PO_4^{3-}) and hydroxide (OH^-) into the adhesive suspension. This ionic bond may either decompose and demineralize the tooth surface, or remain stable and chemically bond with calcium depending on the stability of the resulting calcium-monomer complex (Van Landuyt et al., 2008). Yoshida et al chemically characterized the bond formation and the stability of the bond of three common functional monomers (10-

MDP, 4-MET and phenyl-P) with synthetic hydroxyapatite using x-ray photoelectron spectroscopy (XPS) and atomic absorption spectrophotometry, and the interactions of these monomers with dentin ultra-morphologically using transmission electron microscopy (Yoshida et al., 2004). They found that the chemical bond created by the 10-MDP monomer is very effective and stable as confirmed by the lower dissolution rate of its calcium salt in water. The bonding potential of 4-MET was substantially lower. The monomer phenyl-P and its bonding to hydroxyapatite did not appear to be hydrolytically stable. The results suggest additional roles of functional monomers in acidic primers that contribute to their adhesive potential to dentin other than micromechanical interlocking (Yoshida et al., 2004).

The self-etch adhesives are typically supplied as two-step or one-step adhesives depending on whether the self-etch primer and the adhesive are provided separately or supplied in one bottle. One-step self-etch adhesives are subdivided into single component (all-in-one) and two components that need to be mixed prior to use. The single component self-etch adhesives provide several advantages including fewer technical demands and shorter application time. However, this adhesive is a combination of hydrophilic and hydrophobic monomers that has been reported to have shortcomings including reduced immediate bonding strength, increased nanoleakage, high water sorption (due to the high hydrophillic HEMA content), limited bonding durability, phase separation, formation of water bubbles when the solvent starts to evaporate, and poor clinical performance (Van Meerbeek et al., 2011).

Degradation of hybrid layer

The ultimate goal of resin-dentin bonding is to create a complete resin infiltration into the demineralized dentin matrix. However, incomplete infiltration of resin monomers into demineralized dentin normally occurs and possibly contributes to the formation of less durable resin-dentin bonds compared to bonding to enamel (Liu et al., 2011). It has been suggested that resin-dentin bonds are degraded extensively leading to restoration failure (Tjaderhane et al., 2013b). The degradation of resin-dentin bonds can be observed by the loss of bond strength to dentin and increased nanoleakage at the hybrid layer.

The loss of dentin bond strength after aging (i.e., 6–12 months) has been reported in many studies. Bond strength tests are most commonly used to evaluate the effectiveness of the resin-dentin bond. The rationale behind these tests is that the stronger the adhesion between resin and dentin, the better it will resist the stress during function. The microtensile bond strength test is the most widely used bond strength testing method because of the following reasons: (1) this test is more sensitive to artificial aging than the other tests [i.e., fracture toughness, and nanoleakage tests]; (2) multiple microtensile beams can be obtained from one tooth; and (3) unlike the microtest methods (shear bond strength test), the microtensile bond strength test creates more uniform stress distribution at the interface (De Munck et al., 2005).

It was reported that the microtensile bond strength significantly decreases with increasing water storage time (De Munck et al., 2012). The duration and technique of aging varied among studies (i.e., aging by water storage, thermocycling, occlusal loading and *in vivo* degradation studies). The most commonly used artificial aging technique is storage in water or artificial saliva at 37°C for a period of time. This period ranges from a

few months (Armstrong et al., 2001; Armstrong et al., 2003; Shono et al., 1999) to 3–4 years (De Munck et al., 2003; Reis et al., 2008) or longer (Armstrong et al., 2004; Fukushima et al., 2001). Some studies reported a significant reduction in bond strength even after a short period of aging (Armstrong et al., 2001; Armstrong et al., 2003; De Munck et al., 2003). The decrease in bond strength could be attributed to the degradation of hybrid layer.

Nanoleakage is defined as the diffusion of nanometer-sized molecules (i.e., silver nitrate) within adhesive resin, demineralized dentin, or the hybrid layer in the absence of gap formation (Sano et al., 1995a; Sano et al., 1995b). The term nanoleakage was used because the spaces that allow the leakage are approximately 20–200 nm compared to 10–20 μm for microleakage (Sano, 2006). The spaces of nanoleakage are too small for bacterial penetration. However, they are large enough for the penetration of water and enzymes. Therefore, nanoleakage could be a channel for degradation of the hybrid layer (Sano, 2006). There are two types of nanoleakage: reticular and spotted types (Tay et al., 2002). The *reticular type* is related to incomplete resin infiltration and degradation of the hybrid layer, while the *spotted type* results from the adsorption of silver nitrate by hydrophilic and/or acidic functional groups of the adhesive resin (Sano, 2006; Tay et al., 2002; Tay et al., 2004). As the degradation occurs at the hybrid layer, reticular patterns of nanoleakage are observed, especially at the bottom of the hybrid layer (Breschi et al., 2010; Carrilho et al., 2007; Talungchit et al., 2014).

Nanoleakage indicates incomplete resin infiltration. Theoretically, discrepancies between the depths of demineralization and resin infiltration should not be observed, especially when using self-etch adhesives because they demineralize dentin and

simultaneously replace it with resin monomers. However, several studies demonstrated nanoleakage at the bottom of the hybrid layer even with self-etch adhesives (Carvalho et al., 2005; Wang and Spencer, 2005; Yuan et al., 2007). It is speculated that this is a manifestation of incomplete resin infiltration into the demineralized collagen network (Carvalho et al., 2005; Yuan et al., 2007) or continuous etching (Wang and Spencer, 2005). Moreover, the excess water in dentin and/or dentinal tubules also inhibits polymerization of acidic monomer. As a result, the acidic monomer will continue to demineralize the surrounding dentin and the nanoleakage could be observed (Wang and Spencer, 2005).

The demineralized dentin that is not fully infiltrated by resin monomers is normally occupied by water that may contribute to the deterioration of the hybrid layer through two main mechanisms.

Degradation of adhesive resin by esterases and hydrolysis

Resin based dental materials (i.e., resin composite, adhesive resin) generally consist of inorganic filler, polymer matrix, and a silane coupling agent; the latter is used to improve the bonding between fillers and the polymer matrix. The most commonly used polymer matrices in dentistry are methacrylate-based resins (Figure 1) that contain ester linkages such as bisphenol A diglycidyl ether diemthacrylate (Bis-GMA), bisphenol A polyethylene glycol dimethacrylate (Bis-EMA), ethylene glycol dimethacrylate (EGDMA), urethane dimethacrylate (UDMA), triethylene glycol dimethacrylate (TEGDMA), and 2-hydroxyethyl methacrylate (HEMA). The ester linkages are vulnerable to hydrolysis by esterases in the oral cavity. When the ester linkages of adhesive resin breakdown, the parent molecules are converted into carboxylic acid and

alcohol. Figure 2 illustrates the biodegradation of the dental monomer Bis-GMA to Bis-hydroxy-propoxy-phenyl-propane (BisHPP) and methacrylic acid (MA). Figure 3 demonstrates the biodegradation of the dental monomer TEGDMA to Triethylene glycol (TEG) and methacrylic acid (MA).

Hydrolysis is a chemical reaction that involves the breakdown of chemical bonds with water. Hydrolysis can be catalyzed by enzymes (i.e., esterases) and this process is called biodegradation. Studies reported that human saliva contains esterases that can degrade resin composite and adhesive resin (Jaffer et al., 2002). These enzymes may originate from salivary glands, microorganisms, inflammatory responses, and human cells such as human gingival/pulp fibroblasts (Gregson et al., 2009; Jaffer et al., 2002) and mononuclear phagocytic cells (monocytes and macrophages) (Bourbia et al., 2013). Kermanshahi et al. reported that resin composite that is bonded to dentin can be degraded when it is exposed to salivary esterase enzymes (Kermanshahi et al., 2010). They observed an increased depth of bacteria penetration between dentin and resin composite in the specimens that were exposed to esterases for 90 days compared to those that were not exposed. The results of this study suggest that biodegradation of the hybrid layer increases bacterial microleakage (Kermanshahi et al., 2010).

The degradation products of resin composite and adhesive resin include methacrylic acid (MA), triethylene glycol (TEG), and bishydroxy-propoxy-phenyl-propane (BisHPPP) (Finer and Santerre, 2003; Khalichi et al., 2009; Shokati et al., 2010; Van Landuyt et al., 2011). These products induce human cells (gingival/pulp fibroblasts) to release hydrolytic enzymes and cytokines/growth factors resulting in the increased degradation of these materials (Gregson et al., 2008; Gregson et al., 2009).

These degradation products (i.e., MA, TEG) also regulate the growth and gene expression of oral bacteria. Khalichi et al. evaluated the effects of triethylene glycol (TEG) and methacrylic acid (MA) on the growth of *Streptococcus mutans* (*S. mutans*, NG8 and JH1005) and *Streptococcus salivarius* (*S. salivarius*, AT2) at pH 5.5 and 7.0. Results of their study revealed that both TEG and MA affected the growth of *S. mutans* and *S. salivarius* in a concentration and pH dependent manner (Khalichi et al., 2004). In addition, a study conducted by Hansel et al. showed that the eluates of TEGDMA and ethylene glycol dimethacrylate (EGDMA) increased the proliferation of *Lactobacillus acidophilus* and *Streptococcus sobrinus (S. Sobrinus) in vitro* (Hansel et al., 1998). Furthermore, degradation products of resin composite and adhesive resin (i.e., Bis-HPPP, TEG and MA) upregulate the expression of glucosyltransferase B (gtfB) of *S. mutans* that is used for the synthesis of extracellular glucans from sucrose and is involved in biofilm formation (Khalichi et al., 2009; Singh et al., 2009).

As a consequence, this degradation process compromises the resin-dentin interface, promotes water absorption and more hydrolytic degradation, increases bacterial microleakage (Kermanshahi et al., 2010), and contributes to recurrent caries, hypersensitivity, and inflammation (Finer and Santerre, 2004; Gregson et al., 2008).

Degradation of collagen fibrils by matrix metalloproteinases and other proteases

Among the enzymes trapped in dentin, the MMPs and cathepsins have recently gained much attention due to their possible roles in several physiological and pathological processes. Interest has been especially focused on the roles of MMPs in secondary caries and the degradation of the demineralized dentin that is infiltrated by an adhesive resin at the hybrid layer.

Matrix metalloproteinases

Matrix metalloproteinases (MMPs) are a family of zinc-dependent endopeptidases that are able to cleave multiple components of the extracellular matrix. MMPs play a vital role in the remodeling of extracellular matrix in physiological conditions such as embryogenesis, organ development, and wound healing. Under normal physiological conditions, the activities of MMPs are highly regulated at the level of transcription, activation of inactive pro-MMPs, interaction with specific extracellular matrix components, and inhibition of activated enzymes by endogenous inhibitors (Visse and Nagase, 2003). A loss of their control may result in pathological conditions such as arthritis, cancer, atherosclerosis, aneurysms, fibrosis as well as periodontal disease (Nagase et al., 2006; Song et al., 2006; Tallant et al., 2010; Visse and Nagase, 2003).

Structurally, MMPs consist of a prodomain, a catalytic domain, a hinge region, and a hemopexin domain. MMPs are either secreted from the cell or anchored to the cell membrane. Currently, 24 different MMPs have been identified in vertebrates, and 23 of them are found in humans (Visse and Nagase, 2003). Based on their substrate specificity, sequence similarity, and domain organization, MMPs can be classified into 6 main groups (Table 1) as follows: Collagenases (MMP-1, MMP-8, MMP-13), Gelatinases (MMP-2, MMP-9), Stromelysins (MMP-3, MMP-10, MMP-11), Matrilysins (MMP-7, MMP-26), Membrane-types MMPs (MMP-14, MMP-15, MMP-16, MMP-17, MMP-25), and other MMPs (MMP-12, MMP-19, MMP-21, MMP-28) (Nagase et al., 2006; Sbardella et al., 2012; Song and Windsor, 2005; Song et al., 2006; Tjaderhane et al., 2013b; Visse and Nagase, 2003). Although MMPs share common domain and structures, not all MMPs are able to digest fibrillar collagen Type I, II and III. Only collagenases

(MMP-1, MMP-8, MMP-13), gelatinase A (MMP-2), and MT1-MMP (MMP-14) are able to degrade fibrillar collagen. However, MMP-2 and MT1-MMP cannot cleave fibrillar collagen as efficiently as the true collagenases (MMP-1, MMP-8, MMP-13) (Feitosa et al., 2014; Song et al., 2006). The collagenolytic process of MMPs involves a three-step process, including binding, unwinding, and cleaving of the collagen. The first cleavage step of type I fibrillar collagen occurs at the specific cleavage site between Gly/Ile of α1(I) chain and between Gly/Leu bond α2(I), generating ¾ N-terminal and ¼ C-terminal fragments (Visse and Nagase, 2003). These fragments are further digested by gelatinases and other proteinases (Sbardella et al., 2012).

MMPs are responsible for degradation of extracellular matrix especially type I collagen that is a predominant dentin matrix component. MMPs play a crucial role during tooth development and are trapped in the mineralized dentin matrix (Nishitani et al., 2006). Studies reported that MMP-2 (Heikinheimo and Salo, 1995), MMP-3 (Hall et al., 1999), MMP-9 (Tjaderhane et al., 1998), MMP-8 (Palosaari et al., 2000), and MMP-20 (Llano et al., 1997; Palosaari et al., 2002; Sulkala et al., 2002) are expressed in human odontoblasts and pulp tissue. So far, MMP-1, MMP-2, MMP-3, MMP-8, MMP-9, MT1-MMP and MMP-20 have been found in dentin (Martin-De Las Heras et al., 2000; Mazzoni et al., 2011; Mazzoni et al., 2012; Mazzoni et al., 2015; Tjaderhane et al., 2015; van Strijp et al., 2003). MMPs are secreted as zymogens or inactive pro-MMPs. Pro-MMPs can be activated by proteases, other MMPs, heat, and low pH. The activation of MMPs occurs through the process called “cysteine switch” where the bond between a sulfhydryl group (–SH) of the amino acid cysteine at the pro-domain and Zn^{2+} ion of the catalytic domain is disrupted (Figure 4) resulting in the active forms of MMPs.

During the acid-etching procedure of dentin bonding, phosphoric acid of the etch-and-rinse adhesives or acidic primer of the self-etch adhesives not only demineralizes, but also activates pro-MMPs (Figure 4) (Liu et al., 2011; Zhang and Kern, 2009). Active MMPs digest the exposed collagen networks that are not completely infiltrated with resin monomers and deteriorate the hybrid layer overtime.

Mazzoni et al. investigated the MMP-2 and MMP-9 activities in dentin powder after treatment with different two-step etch-and-rinse and the one-step self-etch adhesives using gelatin zymography and enzyme activity assays (Biotrak^{TM} activity assay system) (Mazzoni et al., 2013). Their results showed that active MMP-2 and MMP-9 were increased after treatment with etch-and-rinse and self-etch adhesives. The results suggest that the acid released from the adhesive can activate endogenous MMP-2 and MMP-9 in human dentin. Mazzoni et al. also showed MMP-2 and MMP-9 are active at the hybrid layer (Mazzoni et al., 2012). Intense MMP activities were observed especially at the bottom of the hybrid layer, while the weaker activities were shown on the top of the hybrid layer.

These studies provided the evidence that acid etching is able to activate pro-MMPs. MMP activities may cause the loss of integrity of the hybrid layer due to collagen fibril degradation, especially at the bottom of the hybrid layer where incomplete resin infiltration normally occurs. This leads to dentinal fluid influx into the hybrid layer and hydrolytic degradation of both adhesive and collagen in the upper parts of the hybrid layer. Eventually, the complete destruction of the hybrid layer may contribute to secondary caries or failure of the restoration (Kermanshahi et al., 2010).

Cysteine cathepsins

Lysosomal cysteine proteases belong to the family of papain-like enzymes. Eleven cysteine cathepsins (cathepsin B, C, F, H, K, L, O, S, V, X and W) have been identified (Dickinson, 2002). Like MMPs, cysteine cathepsins participate in extracellular matrix degradation and remodeling including the breakdown of type I, II, III and IV collagen, laminin, fribronectin, and proteoglycans. The activities of cysteine cathepsins are regulated by endogenous cysteine protease inhibitors. Cathepsins may be activated autocatalytically during biosynthesis or by other proteases (Mach et al., 1994; Tjaderhane et al., 2013b). Cathepsins B, H, L, and C are expressed in all cells and tissues, whereas cathepsins S, V, X, O, K, F, and W are present in specific cell types (Obermajer et al., 2008). Cysteine cathepsins exist as exopeptidases (i.e., cathepsins B, L, and S) that cleave the non-helical telopeptide of collagen molecules. Only cathepsin K is able to cleave at multiple sites in the triple helix region of the collagen chain generating different fragments of collagen molecules (Garnero et al., 1998). Most of cysteine cathepsins work under acidic environments. However, some cysteine cathepsins can function at a pH close to neutral (i.e., cathepsin K). Cathepsin K has collagenolytic activity on type I collagen at pH 5.0–6.5 or gelatinolytic activity at pH 4.0–7.0 (Song et al., 2006).

Several cysteine cathepsin genes (i.e., cathepsin A, B, C, D, E, F, H, L, O, K and Z) have been shown to express in mature human odontoblasts and dental pulp tissues (Tersariol et al., 2010). Active cysteine cathepsins were also found in both carious (Nascimento et al., 2011; Vidal et al., 2014) and intact (Tersariol et al., 2010) dentin. Moreover, cathepsin B was detected in dentinal tubules. These findings indicate that

cysteine cathepsins may play an important role during dentinal caries development and degradation of the hybrid layer.

Strategies to prevent the degradation of the hybrid layer

In recent years, several approaches have been proposed to prolong the durability of the hybrid layer and overall clinical success of resin composite restorations. These strategies include the use of (1) MMP inhibitors, (2) collagen crosslinking agents, (3) ethanol wet bonding with hydrophobic resins, and (4) biomimetic remineralization (Liu et al., 2011; Tjaderhane et al., 2013a). One strategy that has been widely investigated is to hinder the collagenolytic activity of MMPs using protease inhibitors. These inhibitors include galardin (Breschi et al., 2010), chlorhexidine (Montagner et al., 2014; Santiago et al., 2013; Talungchit et al., 2014), carbodiimide (Mazzoni et al., 2014), epigallocatechin gallate (ECGC) (Khamverdi et al., 2015; Santiago et al., 2013), and doxycycline (Feitosa et al., 2014).

Breschi et al. investigated the effect of galardin (GM6001, a synthetic MMP inhibitor) on MMP activities. Galardin has a collagen-like backbone and contains a hydroxamate structure (R–CO–NH–OH, where R is an organic residue) (Breschi et al., 2010). The collagen-like backbone facilitates the binding of galardin to MMP, and hydroxamate inhibits MMP activity through chelation of Zn^{2+} at the MMP active site on the catalytic domain (Breschi et al., 2010). Galardin was found to have no negative effect on immediate microtensile bond strength (Breschi et al., 2010). After 1 year of aging in artificial saliva, microtensile bond strength was significantly decreased in the control compared to the galardin-treated group ($p<0.05$) (Breschi et al., 2010). Investigation of interfacial nanoleakage revealed reduced silver deposits in galardin-treated specimens

compared to the control ($p<0.05$) (Breschi et al., 2010). These results suggest that acid demineralization is able to activate trapped MMPs and the use of MMP inhibitors could provide some resistant to enzymatic degradation of the hybrid layer.

Santiago et al. evaluated the effects of dentin pretreatment with EGCG on the preservation of the resin-dentin bond of etch-and-rinse adhesives (Santiago et al., 2013). After 6 months of storage, a significant decrease in bond strength was observed in the control group. Dentin pretreatment with EGCG (0.02%, 0.1%, or 0.5%, w/v), as well as with 2% chlorhexidine (positive control), preserved the resin-dentin bond after 6 months of storage (Santiago et al., 2013).

Quaternary ammonium compounds such as benzakaonium chloride (BAC) and polymerizable quaternary ammonium methacrylates (QAMs) are able to inhibit MMP activities. 12-methacryloyloxydodecylpyridinium bromide (MDPB) has been incorporated into self-etch primers. Like chlorhexidine, MDPB has antibacterial and anti-MMP properties as they can chelate Zn^{2+} of MMPs. A study was conducted to investigate the effects of QAMs on MMP activities by incubating demineralized dentin beams with or without QAMs, and the loss of dry mass was determined after 30 days. The results showed a significant reduction in the loss of dry mass in the dentin beams incubated with QAMs (0.2–6.0% loss of dry mass) compared to the control (no QAMs, 29% loss of dry mass) (Tezvergil-Mutluay et al., 2011). The unique advantage of QAMs over other MMP inhibitors is that they can polymerize with resin monomers (Imazato et al., 2003) and will not leach out of the resin-dentin bond interface.

Chlorhexidine is one of the most commonly investigated MMP inhibitors that have been used to prevent the degradation of the hybrid layer. The results from an *in vitro*

study showed that the use of 2% or 0.2% chlorhexidine prevented the loss of bonding strength to dentin after aging (Montagner et al., 2014). Carrilho et al. treated dentin with 2% chlorhexidine after 37% phosphoric acid etching and showed a significantly higher microtensile bonding strength after 14 months compared to no treatment (Carrilho et al., 2007). Transmission electron microscopy (TEM) also revealed the progressive loss of hybrid layer integrity in the control group (Carrilho et al., 2007). These findings suggest that using MMP inhibitors can prevent hybrid layer degradation. However, the inhibitory effects of chlorhexidine on dentin bond durability were not observed for the longer period of aging (i.e., >18 months) (Dutra-Correa et al., 2013; Montagner et al., 2014; Sartori et al., 2013). Pallan et al. evaluated the mechanical properties of methacrylate-based resin incorporated with chlorhexidine (0.2–2.0%) (Pallan et al., 2012) and found that chlorhexidine had no negative impact on water sorption, but 2% chlorhexidine incorporation was found to decrease the degree of conversion. The flexural strength and modulus of elasticity were slightly increased compared to the control (no chlorhexidine) (Pallan et al., 2012).

A clinical study conducted in non-carious Class V lesions over 36 months revealed no improvement in the durability of adhesive restorations when chlorhexidine was used prior to an application of the adhesive (Sartori et al., 2013). The long-term clinical performance of 70 non-carious cervical lesions with and without the application of 2% chlorhexidine to demineralize dentin using split mouth design was also investigated. The restoration of the control group started debonding after 6 months of clinical function, while none of the restorations in the chlorhexidine treated group debonded until 12 months (Sartori et al., 2013). This observation suggested that

chlorhexidine stabilized the hybrid layer for up to 12 months. Therefore, a sustained release of MMP inhibitor could be an alternative option to provide a long-term and more stable resin-dentin bonding.

Doxycycline

Tetracycline is a group of broad-spectrum antibiotics that are used for treatment of several infectious diseases. There are several derivatives of tetracycline including minocycline, oxytetracycline, methacycline, and doxycycline (Kogawa and Salgado, 2012). Doxycycline (Figure 5) is a semi-synthetic derivative of tetracycline that was developed in the early 1960s and was first commercially available in 1967 (Tan et al., 2011). Doxycycline has activity against a broad range of bacteria including gram-positive and gram-negative and some protozoa (i.e., malaria). Doxycycline is also used as a prophylactic antibiotic (i.e., malaria), for treatments of sexually transmitted diseases and respiratory tract infections (Holmes and Charles, 2009). Three forms of doxycycline are commercially available: doxycycline hyclate, monohydrate, and hydrochloride (Kogawa and Salgado, 2012). The antibacterial properties of doxycycline occur through the inhibition of bacterial protein synthesis by binding to the 30S subunit of ribosome. This results in limited access to the t-RNA acceptor site in the mRNA-ribosome complex.

In addition to its antimicrobial properties, doxycycline has been found to inhibit MMPs at a sub-antimicrobial dose in the treatment of periodontal disease (Metzger et al., 2008). Doxycycline is the only host-modulating drug that has been approved by the Food and Drug Administration (FDA) and other national regulatory agencies in Europe and Canada as an adjunctive treatment for chronic periodontitis.

Since subantimicrobial dose of doxycycline (SDD) has no selective pressure on bacteria, no resistant strains would emerge (Greenstein, 1995; Pallasch, 2003). A commercially available subantimicrobial dose of doxycycline is Periostat® that is prescribed as 20 mg 2×/day (Sgolastra et al., 2011) compared to antibiotic-dose: 100 mg 1×/day of doxycycline (2×/day for the first day) (Prakasam et al., 2012). SDD is used to suppress host-derived MMPs in the periodontal lesion by inhibiting the pathologic degradation of collagens in periodontal tissues and to prevent complications of regularly administered doses of tetracycline [i.e., gastrointestinal disturbance, increased photosensitivity and drug resistance] (Gu et al., 2012). Doxycycline is also used as a locally delivered antibiotic such as Atridox™ (10% doxycycline hyclate, Atrix Laboratories, Fort Collins, CO). The inhibitory effect of doxycycline occurs through its binding to the Zn^{2+} located in the catalytic domain of MMPs.

Aluminosilicate clay nanotubes

Aluminosilicate clay nanotubes (Halloysite or Halloysite nanotubes, HNT) are naturally occurring clay that is formed by rolled kaolin (Lvov et al., 2014). Halloysite is a two-layered alumosilicate mineral with a 1:1 ratio of Al:Si and a stoichiometry of $Al_2Si_2O_5(OH)_4.nH_2O$ (Yah et al., 2012b). There are two forms of HNT: the anhydrous form ($Al_2Si_2O_5(OH)_4$) with an interlayer of 7 angstroms, and the hydrated form ($Al_2Si_2O_5(OH)_42H_2O$) with expanded interlayer spacing of 10 angstroms as a consequence of water occupied in the interlamellar space (Yah et al., 2012b). The inner surface of HNT has chemical properties similar to those of Al_2O_3 as it is formed by the octahedral sheet of Al–OH, while the outer surface has the chemical properties identical to those of SiO_2 resulting from siloxane groups (Si–O–Si) (Yah et al., 2012a). This

difference in chemical composition results in a negatively charged outer surface and a positively charged inner lumen. HNT has an outer diameter of approximately 50–70 nm, an inner diameter of approximately 10–15 nm, and a length between 500 and 1500 nm (Figure 6) (Wei et al., 2014).

HNT provides several advantages including having abundant hydroxyl groups, biocompatibility, hydrophilicity, high mechanical strength, very large surface areas, ease in purification and processing, being available in large quantities and much more cost-effective than many other nano-scaled fillers such as carbon nanotubes/nanofibers (Bottino et al., 2013; Chen et al., 2012; Li et al., 2014; Luo et al., 2013; Qi et al., 2012). As a result, HNT has been used for a large number of applications such as controlled release of protective agents (Ariga et al., 2011; Lvov et al., 2008; Veerabadran et al., 2009; Vergaro et al., 2010), biomimetic reaction vessels (Shchukin et al., 2005), adsorption agents, corrosion prevention agents (Shchukin and Möhwald, 2007), additives for improving thermal stability, and nucleating agents for crystallization of polymers (Luo et al., 2013).

The Young's modulus of HNT calculated using the geometric optimization protocol has been reported to be approximately 230–340 GPa (Guimaraes et al., 2010). Because of the high mechanical properties, biocompatibility and hydrophilicity, HNT has been used as reinforcing material in engineered composites (Qi et al., 2010; Qi et al., 2012; Qi et al., 2013; Ye et al., 2007) and polymers in dentistry (dental resin composite, adhesive resin) (Bottino et al., 2013; Chen et al., 2012).

A study conducted by Chen et al. (Chen et al., 2012) on resin composite impregnated with different amounts of HNT found that incorporation of 1% and 2.5% of

silanized HNT significantly improved the flexural strength and elastic modulus of Bis-GMA/TEGDMA resin composite. However, a high mass fraction of HNT (5%) did not increase these properties (Chen et al., 2012). The results suggested that the incorporation of HNT into Bis-GMA/TEGDMA resin composite could result in two opposite effects: the reinforcing effect due to highly separated and uniformly distributed HNT and the weakening effect due to agglomeration of HNT particles.

Similarly, it has been shown that the incorporation of nanofillers with different properties (chemical compositions, sizes, shapes and morphological characteristics) into adhesive resin would enhance the resin-dentin bond strength and the mechanical properties of the adhesive layer (Conde et al., 2009; Kim et al., 2005; Lohbauer et al., 2010; Miyazaki et al., 1995; Sadat-Shojai et al., 2010; Solhi et al., 2012). The nanoscale particle size and the increased surface area associated with HNT may reinforce the polymer matrix via crack deflection and localized plastic deformation around the fillers (Bottino et al., 2013). Furthermore, it has been suggested that nanofillers can infiltrate into the dentinal tubules, decreasing polymerization shrinkage, stiffening the adhesive layer, and ultimately strengthening the adhesive layer (Lohbauer et al., 2010; Sadat-Shojai et al., 2010).

The effects of HNT incorporated into the adhesive resin on degree of conversion, Knoop microhardness, and dentin shear bond strength have been reported (Bottino et al., 2013). HNT was incorporated into a commercially available three-step etch-and-rinse adhesive (Adper Scotchbond Multi-Purpose, SBMP) at five distinct concentrations (5%, 10%, 15%, 20% and 30%, w/v). The results revealed that incorporation of HNT at 30% (w/v) into the adhesive resin showed the highest dentin shear bond strength and Knoop

microhardness number, and was significantly higher than the control (unfilled adhesive). For the degree of conversion, incorporation of HNT up to 20% (w/v) had no negative effect. However, at 30% (w/v), DC was significantly decreased compared to the control. The results of this study suggested that the incorporation (5–30%, w/v) of HNT into adhesive resin had no negative effect on dentin shear bond strength and Knoop microhardness. However, due to a significant reduction in DC at 30% HNT-loading compared to the unfilled adhesive, HNT can be incorporated up to 20% (w/v) without compromising the physicochemical properties of adhesive resin.

Specific Aims

The ultimate goal of this study was to evaluate doxycycline (DOX), an FDA approved MMP inhibitor, for its effects on preventing hybrid layer degradation through the modification of dental adhesive with aluminosilicate clay nanotubes (HNT). Doxycycline was encapsulated into HNT, and DOX-encapsulated HNTs were incorporated into dental adhesive (Adper Scotchbond multi-purpose [SBMP], 3M ESPE). Physico-chemical and mechanical characteristics of the dental adhesive were first investigated. Then, doxycycline released from the dental adhesive was evaluated for its inhibition of MMP activity. The immediate microtensile bond strength of the resin-dentin bonding was evaluated (24 h bond strength).

The central hypothesis of this study was that doxycycline would be released overtime from the modified adhesives (DOX-loaded dental adhesive) at subantimicrobial levels, and the released doxycycline would inhibit MMP activity. These studies were accomplished under the following specific aims.

Specific aim 1: To investigate the anti-MMP activity and the microtensile bond strength of the modified adhesive (dental adhesive loaded with 10% DOX-encapsulated HNT).

This specific aim was mainly a proof of concept that the release of doxycycline from DOX-encapsulated HNT modified adhesive was at subantimicrobial levels and that the released doxycycline inhibited MMP activity without compromising the resin-dentin microtensile bond strength.

Specific aim 1A: To fabricate the modified adhesive (dental adhesive loaded with 10% DOX-encapsulated HNT) and to evaluate the antimicrobial activity of the doxycycline released from 10% DOX-encapsulated HNT modified adhesive.

Hypothesis: Doxycycline would be released from the modified adhesive at subantimicrobial levels and inhibit MMP activity.

Specific aim 1B: To evaluate the microtensile bond strength of the resin-dentin bonding after 24 h in artificial saliva.

Hypothesis: No significant differences in resin-dentin microtensile bond strength after 24 h in artificial saliva would be found between the modified adhesive groups and the control (SBMP).

Specific aim 2: To investigate the release of doxycycline from modified adhesives (dental adhesives loaded with 10%, 20% and 30% of DOX-encapsulated HNT) and the effect of the released doxycycline on MMP activity.

This specific aim included the experiments that were conducted in specific aim 1 with increasing concentrations of doxycycline (10%, 20% and 30% doxycycline). The encapsulation efficiency and the amount of released doxycycline were also determined.

Specific aim 2A: To encapsulate doxycycline into aluminosilicate clay nanotubes at three distinct concentrations (10% DOX, 20% DOX and 30% DOX, w/v) and to fabricate the modified adhesives.

Hypotheses: The incorporation of DOX-encapsulated HNT into dental adhesives would not significantly increase the degree of conversion and Knoop microhardness.

Specific aim 2B: To determine the amount of doxycycline released from modified adhesives and the effect of released doxycycline on MMP activity.

Hypotheses: Doxycycline would be released from the dental adhesive loaded with DOX-encapsulated HNT at subantimicrobial levels and inhibit MMP activity.

MATERIALS AND METHODS

Specific aim 1

Encapsulation of doxycycline into aluminosilicate clay nanotubes

Doxycycline hyclate (Sigma Aldrich, St. Louis, MO, USA) was dissolved at 10% (w/v) in phosphate buffered saline (PBS; pH 7.2, Fisher Scientific, Pittsburgh, PA, USA) at 50°C for 2 h under stirring conditions (Fisher Thermix, model 310T, Fisher Scientific).

The encapsulation process was modified from a previously reported procedure (Qi et al., 2010). Aluminosilicate clay nanotubes (HNT; Dragonite 1415JM, Applied Minerals Inc., New York, NY, USA) were sieved (<45 μm sieve) prior to use. HNT (1 g) was mixed in 10 mL of doxycycline, and sonicated for 2 h to enhance dispersion. Vacuum (25 in Hg) was applied and maintained for 1 h to remove any air between and within the HNT. The solution was then stirred for 1 h and vacuum was reapplied. Finally, the solution was dried in an incubator at 37°C for 5 days. The dried powder was ground and sieved (<45 μm) prior to use.

Fabrication of DOX-encapsulated nanotube modified adhesives

Three groups were investigated as follows:

1. Control: unmodified adhesive (SBMP without HNT and doxycycline),
2. HNT: SBMP + HNT
3. 10% DOX: SBMP + 10% DOX-encapsulated HNT.

The modified adhesives were fabricated by incorporating either HNT or DOX-encapsulated HNT into a commercially available three-step etch-and-rinse adhesive bonding system (Adper Scotchbond Multi-Purpose [SBMP]; 3M ESPE, St. Paul, MN, USA) at 15% (w/v). It was previously reported that HNT could be incorporated up to

20% (w/v) without jeopardizing the physico-chemical and bonding properties of the adhesive (Bottino et al., 2013). However, the modified adhesives were fabricated with 15% (w/v) because 20% HNT (w/v) resulted in high viscosity of the modified adhesive.

The DOX-encapsulated HNT powder was incorporated (75 mg of DOX-encapsulated nanotubes per 500 μL of adhesive) into the dental adhesive (SBMP) by mixing with a stirrer and a conical micropestle (Roti-Speed, Roth, Karlsruhe, Germany) followed by sonication (Ultrasonic cleaning L&R 2014, Mfg Co., Kearney, NJ, USA) for 1 h to further enhance HNT dispersion. The modified adhesives were fabricated with light-proof (amber) microcentrifuge tubes because of photosensitivity of doxycycline. All specimens were fabricated in a constant temperature room (23°C) with a filtered lighting system to minimize unintentional polymerization.

Degree of conversion

Degree of conversion (DC) was used to determine whether adhesive polymerization was affected by the incorporation of doxycycline. Disc-shaped specimens (7 × 0.24 mm, n = 5) were fabricated and light cured for 10 sec (manufacturer's recommendation), 20 sec, or 40 sec. A light-emitting diode curing system (DEMI LED, Kerr, Orange, CA, USA) with an approximate output irradiance of 1,300 mW/cm^2 was used, and the output was periodically monitored using a Cure Rite Visible Light Meter (Dentsply Caulk, Milford, DE, USA). The amounts of energy applied onto specimen disks during light curing of 10 sec, 20 sec and 40 sec were measured with a MARC Resin Calibrator (BlueLight analytics Inc, Halifax, NS, Canada) and were 10.92 J/cm^2, 22.49 J/cm^2 and 46.18 J/cm^2, respectively.

Prepared specimens were stored at room temperature for 24 h in a dark and dry condition. Degree of conversion was evaluated with Fourier transform infrared spectroscopy (FTIR; Jasco 4100, Jasco Corp., Tokyo, Japan) in attenuated total reflection mode. The area under 2 absorbance bands at 1,637 cm^{-1} (methacrylate group C=C) and 1,715 cm^{-1} (ester group C=O) was used in the following equation to calculate the degree of conversion:

$$DC\ (\%) = (1 - \frac{\text{Cured (area under 1637 cm}^{-1}\text{/area under 1715 cm}^{-1}\text{)}}{\text{Uncured (area under 1637 cm}^{-1}\text{/area under 1715 cm}^{-1}\text{)}}) \times 100$$

Antibacterial properties

In order to prove successful encapsulation of doxycycline in modified adhesives and to further support our hypothesis that the DOX-encapsulated HNT modified adhesives would release doxycycline at subantimicrobial levels, antimicrobial activity was assessed by agar diffusion testing.

Agar diffusion tests of the modified adhesive disks and the doxycycline containing eluates (PBS eluates) against *Streptococcus mutans* (*S. mutans*, UA159) were performed.

Antibacterial properties of the modified adhesive disks

Disk-shaped adhesive specimens (6.2 × 2 mm, n = 4 per group) were fabricated and light cured for 10 sec. Specimens were kept at room temperature for 24 h, and disinfected by ultraviolet light exposure (30 min/side). *S. mutans* was cultured aerobically in tryptic soy broth (Difco Laboratories, Detroit, MI, USA) for 24 h in 5% CO_2 at 37°C. Then, 100 μL of the bacterial suspension was swabbed onto blood agar plates to create a lawn of bacteria (Palasuk et al., 2014). The disinfected specimens were directly placed on blood agar plates (bioMerieus Inc., Durham, NC, USA) containing a freshly prepared

lawn of bacteria. The blood agar plates were incubated in 5% CO_2 at 37°C. After 72 h of incubation, the diameters (in mm) of the clear zones of growth inhibition were determined. Chlorhexidine (0.12%) and sterile PBS were used as positive and negative control, respectively.

Antibacterial properties of the doxycycline containing eluates

Disk-shaped specimens (5 mm × 2 mm, n = 4) were fabricated as previously described and individually incubated at 37°C in 10 mL of PBS (pH 7.2). One mL of aliquot containing doxycycline (leached from specimen disks) was collected at day 1, 7 and 14. An equal amount of sterile PBS was added to replace the removed volume. Aliquots were stored at −20°C until tested.

S. mutans was cultured and plated on blood agar plates as previously described. Each agar plate was divided into zones and a 10 μL aliquot from days 1, 7, and 14 were pipetted into the center of each zone (Palasuk et al., 2014). The blood agar plates were incubated in 5% CO_2 at 37°C. After 72 h of incubation, the diameters (in mm) of the clear zones of growth inhibition were determined. Chlorhexidine (0.12%) and sterile PBS were used as positive and negative control, respectively.

MMP mediated casein cleavage assays

Disk-shaped specimens (5 mm × 2 mm, n = 4) were fabricated, placed into 12-well plates and incubated in 2 mL of 50 mM Tris with 0.2 M NaCl, 10 mM $CaCl_2$, and 1 μM $ZnCl_2$ (pH 7.4). On days 1, 7, and 14, aliquots (500 μL) from the modified adhesives (doxycycline containing eluates) were collected. An equal volume of the buffer was added to keep the volume constant. Aliquots were stored at −20°C until tested. MMP-1 purified from human gingival fibroblast-conditioned media by anticollagenase affinity

chromatography (Windsor et al., 1994; Windsor et al., 1997) was activated with 4-aminophenylmercuric acetate (APMA, Sigma-Aldrich, St. Louis, MO, USA). The activation was performed by incubation of 10 mM APMA (10×) with purified MMP-1 (1:9 ratio by volume) at 37°C for 90 min.

APMA activated MMP-1 (100 μL) was incubated with β-casein (100 μL, 5 mg/mL) at 37°C (Windsor et al., 1994; Windsor et al., 1997) with or without the doxycycline containing eluates (200 μL, n = 4) in a total volume of 400 μL. Samples (65 μL) were periodically (0–120 min) removed, and the reaction was terminated by addition of 1,10-phenanthroline (10 μL, 200 mM) to a final concentration of 10 mM. Samples were resolved in 10% sodium dodecyl sulfate-polyacrylamide gel electrophoresis (SDS-PAGE), stained with Coomassie blue, and analyzed using ImageJ software (NIH, Bethesda, MD). The positive and negative controls were 0.1% doxycycline and Tris buffer, respectively.

Cytocompatibility

Cytotoxicity of modified adhesives with and without doxycycline, as well as control (SBMP), was evaluated on human dental pulp stem cells (hDPSCs).

Adhesive disks (5 × 2 mm; n = 4) were fabricated as previously described. The doxycycline containing eluates were prepared following the guidelines of the International Standards Organization (1993). In brief, a 1:2 ratio of the elution solution (low-glucose [1 g/L] Dulbecco's Modified Eagle's Medium [DMEM], Corning Cellgro, Manassas, VA, USA) and the adhesive disk volume (*i.e.*, 1 mL of DMEM to 2 mm^3) was used (Zhang et al., 2013a; Zhang et al., 2013b). The adhesive disks were disinfected by ultraviolet light exposure (30 min/side) and then individually immersed in 19.64 mL of

DMEM supplemented with 10% fetal bovine serum (FBS, Hyclone, Logan, UT, USA) and 1% penicillin-streptomycin (Sigma), placed in a shaker, and mixed at 37°C at 50 rpm for 24 h.

To mimic clinical conditions, the eluates were serially diluted as follows: 32-fold (1 mL of original eluate + 31 mL of DMEM), 64-fold, and 128-fold (Zhang et al., 2013a; Zhang et al., 2013b). The rationale was that the average daily salivary flow is of proximately 1000–1500 mL (Humphrey and Williamson, 2001). These dilutions corresponded to a total solution of 483 mL, 966 mL, and 1933 mL, respectively. This corresponded to approximately ½, 1, and 1.5 fold of the normal saliva amount per day, taking into account patients with reduced or increased saliva production.

Human dental pulp cells (hDPCs) were cultured in low-glucose DMEM (Corning Cellgro, Manassas, VA, USA) supplemented with 10% FBS (Hyclone, Logan, UT, USA) and 1% penicillin-streptomycin (Sigma). Cells at passages 3–8 were used in these experiments. Human DPSCs were seeded at the density of 3,000 cells per well in 96-well plates in 100 μL of culture medium (Feitosa et al., 2014). After 24 h of incubation at 37°C and 5% CO_2, the culture medium was removed and replaced with 100 μL of previously prepared DMEM eluates.

After 48 h, 15 μL of dye solution (CellTiter 96 Non-Radioactive Cell Proliferation Assay/MTT; Promega, Madison, WI, USA) was added to each well. After 4 h of incubation, 100 μL of Solubilization/Stop Mix was added into each sample. The optical density was measured at 570 nm after an overnight incubation, and the reading was subtracted by the background optical density measured at 680 nm. Blank wells were prepared using culture medium without cells. Positive (100% survival, untreated cells)

and negative (total cell death) controls were DMEM with cells but without the eluates (100% survival) and a 0.3% phenol solution (v/v), respectively.

The absorbance values of the treated cells were subtracted by the absorbance values of the blank, and the following equation was used to calculate cell proliferation:

$$\text{Cell proliferation (\%)} = \frac{\text{Absorbance value of treated cells}}{\text{Absorbance value of untreated cells}} \times 100$$

Dentin bonding

Thirty-six extracted non-carious human third molars (n = 12) stored in 0.1% thymol solution were used within 6 months of extraction with an Institutional Review Board approval (NS1004-03, Indiana University). Teeth were sectioned to expose mid-coronal dentin using a low-speed diamond disk (Buehler Ltd., Lake Bluff, IL, USA) and examined under a stereomicroscope (40×) for the absence of enamel. A midcoronal dentin surface was polished with SiC papers (240–600 grit) to create a flat surface and to standardize the smear layer. Teeth were then randomly assigned into 3 groups according to the types of dental adhesive used: unmodified adhesive (control, SBMP), HNT (SBMP + HNT), 10% DOX (SBMP + 10% DOX-encapsulated HNT). The bonding procedure was performed as recommended by the manufacturer's instruction. Briefly, dentin surfaces were etched with 37% phosphoric acid for 15 sec, rinsed with deionized water for 15 sec, air dried for 5 sec, primed, bonded, and polymerized (DEMI LED, Kerr, Orange, CA, USA). Teeth were incrementally restored with resin composite (~1–2 mm thick/increment; Z100, 3M ESPE). All specimen blocks were stored at 37°C in deionized water for 24 h.

Bonded specimens were cut perpendicular to the resin-dentin interface using a slow-speed water-cooled saw equipped with a diamond-impregnated disk (Isomet,

Buehler, Lake Bluff, IL, USA) to produce 0.8 × 0.8 mm beams. The beams were kept in artificial saliva at 37°C for 24 h.

Microtensile bond strength testing

The beams were placed in a notched Geraldeli jig (ODEME Biotechnology, Joacaba, SC, Brazil) for microtensile testing using cyanoacrylate resin (Loctite Superglue Control Gel, Henkel Corporation, Avon, OH, USA). All beams were loaded with tension in a universal testing machine (MTS Sintech Renew 1123, Eden Prairie, MN, USA) until fracture at a crosshead speed of 1 mm/min.

Failure mode analysis

Fracture surfaces (121 beams, 80% recovery) were examined under a stereomicroscope (40×). The types of failure were classified as cohesive failure in dentin, cohesive failure in resin composite, adhesive failure (within the adhesive layer), or mixed failure (combination of adhesive and cohesive failures).

Scanning electron microcopy (SEM)

Randomly selected fractured specimens were sputter coated with gold (Denton Vacuum Desk II cold sputter, Moorestown, NJ, USA) and imaged with a scanning electron microscope (SEM; JSM-5310LV, JEOL, Tokyo, Japan).

Statistical analysis

Data were analyzed using one-way ANOVA, except the microtensile bond strength data in which a mixed-model ANOVA was used. Tukey's test was used for *post hoc* comparisons. The level of significance was set at 0.05.

Specific aim 2

Encapsulation of doxycycline into aluminosilicate clay nanotubes

Doxycycline hyclate (Sigma Aldrich, St. Louis, MO, USA) was dissolved in 50 mM HEPES buffer (pH = 7.2) using a vortex mixer at three distinct concentrations (w/v) as follows:

1. 10% DOX: 0.5 g of doxycycline powder in 5 mL of 50 mM HEPES,
2. 20% DOX: 1.0 g of doxycycline powder in 5 mL of 50 mM HEPES
3. 30% DOX: 1.5 g of doxycycline powder in 5 mL of 50 mM HEPES.

During the encapsulation process, the weight of 15-mL polypropylene tubes, doxycycline, and HNT used for the encapsulation was recorded to determine encapsulated doxycycline and unencapsulated doxycycline.

Aluminosilicate clay nanotubes (HNT, <45 μm sieved) were mixed with doxycycline solution at 25% (w/v, 1.25 g in 5 mL of doxycycline solution) and sonicated for 2 h. Vacuum (25 in Hg) was applied and maintained for 1 h. The solution was mixed for 1 h using end-to-end mixer and vacuum was reapplied for another 1 h. Finally, the solution (DOX+HNT) was centrifuged at 3000 rpm for 10 min. The supernatants were collected and stored at −20°C for high-pressure liquid chromatography (HPLC) analysis. The pellets (DOX-encapsulated HNT) were dried in an incubator at 37°C for 7 days. The dried pellets were weighed, recorded, ground, and sieved (<45 μm) prior to use.

Encapsulation efficiency and drug loading

Incorporation of doxycycline into HNT was characterized by two techniques (n=5).

1. By dry weight

Since the amount of doxycycline that was added in each group (i.e., 0.5 g in 10% DOX, 1.0 g in 20% DOX and 1.5 g in 30% DOX), the dry weight of the pellets (DOX + HNT) and the amount of HNT added were known, the amounts of encapsulated doxycycline and unencapsulated doxycycline were calculated as follows:

Encapsulated DOX (mg) = DOX added (mg) + HNT added (mg) – pellet (mg)

Unencapsulated DOX (mg) = DOX added (mg) – encapsulated DOX (mg)

2. By High-pressure liquid chromatography (HPLC)

HPLC was used to determine doxycycline concentration in supernatant (SUP) after drug encapsulation. Since the volume of supernatant and the amount of doxycycline added in each group were known, the amounts of unencapsulated doxycycline (doxycycline in the supernatant) and encapsulated doxycycline were calculated as follows:

Unencapsulated DOX (mg) = conc. of DOX in SUP (mg/mL) × vol. of SUP (mL)

Encapsulated DOX (mg) = Amount of DOX added (mg) – unencapsulated DOX (mg)

High-pressure liquid chromatography (HPLC)

High-performance liquid chromatography (HPLC) equipped with a UV-Vis detector was used to determine the doxycycline content using maximal absorption peaks at 273 nm. HPLC analysis was performed on an Agilent 1100 system (Palo Alto, CA) using an Eclipse XDB-C18 chromatography column (3.5 μm, 150 × 4.6 mm) with a 10 μL injection volume. A binary mobile phase consisting of solvent systems A and B was used in an isocratic elution with 80:20 A:B. Mobile phase A was 50 mM $KHPO_4$ in dH_20 and mobile phase B was 100% acetonitrile. The HPLC flow rate was 1.0 mL/min and the total run time was 10 min. The retention time of doxycycline was 4.85 min. The

concentration of doxycycline was calculated from a standard curve of doxycycline (r^2 = 0.99984).

The percent of encapsulation efficiency and drug loading were calculated using the following equations (Patel et al., 2013):

$$\text{Encapsulation efficiency } (\%) = \frac{\text{Da} - \text{Ds}}{\text{Da}} \times 100$$

$$\text{Drug loading } (\%) = \frac{\text{Da} - \text{Ds}}{\text{Na}} \times 100$$

Where Da = total amount of drug added (g)

Ds = unencapsulated doxycycline (g) determined by HPLC (the amount of drug in supernatant after centrifugation) or by dry weight

Na = total of amount of HNT (1.25 g)

Fabrication of DOX-encapsulated nanotube modified adhesives

Three groups according to the concentrations of doxycycline and two control groups were investigated as follows:

1. Control: unmodified adhesive (SBMP without HNT and doxycycline),
2. HNT: SBMP + HNT (no doxycycline)
3. 10% DOX: SBMP + 10% DOX-encapsulated HNT
4. 20% DOX: SBMP + 20% DOX-encapsulated HNT
5. 30% DOX: SBMP + 30% DOX-encapsulated HNT

The modified adhesives were fabricated as previously described.

Degree of conversion

Degree of conversion (n = 5) was used to determine whether polymerization of the modified adhesives was affected by the incorporation of doxycycline and was evaluated as previously described.

Knoop microhardness

Microhardness is an alternative technique to determine the degree of conversion because of a strong positive correlation between microhardness and degree of conversion (Ferracane, 1985). This study determined the Knoop microhardness of the specimens with the same dimension as were used for drug release profiling to ensure that the release of doxycycline was not due to underpolymerization.

Disc-shaped specimens of the adhesive for all of the groups (6.2 × 1.0 mm, n = 5) were fabricated and light cured for 20 sec on each side and stored at room temperature for 24 h in the dark and dry condition. Specimens were embedded in self-cure epoxy resin (EpoxiCure®, Buehler, Lake Bluff, IL, USA) and polished with SiC paper (1200 grit) for 10 sec. Specimens were subjected to a microhardness test (M-400, Leco Corp., St. Joseph, Michigan USA) using a Knoop diamond indenter at a 50 gf load and 15 s dwell time. Five readings at different locations (at least 1 mm apart) were obtained from each specimen. The diagonal lengths were measured immediately after each indentation. The values were converted to KHN number (kg/mm^2).

Doxycycline release profile

Disc-shaped specimens of the adhesive for all the groups (6.2 × 1.0 mm, n = 6) were fabricated as previously described. Specimen disks were individually incubated at 37°C in 1 mL of phosphate buffer saline (PBS, pH 7.4). To collect doxycycline-

containing eluates, 150 μL aliquots were collected after 1, 7, 14, 21, and 28 days. An equal amount of sterile PBS was added to replace the removed volume. Aliquots were stored at −20°C until used.

Mass spectrometry

High performance liquid chromatography tandem mass spectrometry (HPLC-MS-MS, Agilent 6460 Triple Quadrupole LC/MS) was used to determine the concentration of doxycycline released from the specimen disks. The analysis was performed with an XBridge-C18 chromatography column (3.5 μm, 100 × 2.1 mm) with a 5 μL injection volume. The mobile phase consisted of 0.1% formic acid in deionized water (A) and 0.1% formic acid in acetonitrile (B) under an isocratic condition (A:B, 80:20). A flow rate of 0.30 mL/min was used. The mass spectrometer was operated in multireaction monitoring (MRM) mode. The transition for doxycycline was mass:charge (m/z) at 445.1 (MS1) and 428.1 (MS2). The concentration of doxycycline release was calculated from a standard curve of doxycycline ($r^2 = 0.99986$).

Doxycycline in specimen disk

The amount of doxycycline in one adhesive disk was determined by two techniques as follows:

1. Dissolve modified adhesive disk in dimethyl sulfoxide (DMSO)

Disc-shaped specimens of the adhesive for all the groups (6.2 × 1.0 mm, n = 3) were fabricated as previously described. Specimen disks were individually incubated at 37°C in 1 mL of DMSO to completely dissolve the adhesive after 48 h. The DOX+DMSO solutions were centrifuged at 4000 rpm for 5 minutes, and the supernatants that contained doxycycline were collected and stored at −20°C until used for mass

spectrometry analysis. This provided the amount of doxycycline that was incorporated into each adhesive disk (total doxycycline in the adhesive disk).

2. Dissolve 7.5 mg of DOX-encapsulated HNT powder in ethanol.

7.5 mg of DOX-encapsulated HNT powder (n = 5) was individually incubated at 37°C in 1 mL of ethanol for 48 h. The solutions were centrifuged at 4000 rpm for 5 minutes, and the supernatants that contained doxycycline were collected and stored at −20°C until used for mass spectrometry analysis.

Doxycycline remained in the adhesive disk after 4 months of incubation

After 4 months of incubation at 37°C in PBS, specimen disks were individually dissolved in DMSO and processed for mass spectrometry analysis as previously described. This provided the amount of doxycycline that remained in each adhesive disk.

Antibacterial properties

Agar diffusion tests against *Streptococcus mutans* (UA159) and *Lactobacilli casei* (ATCC 393) was performed as follows:

1. *Antibacterial properties of the adhesive disks (n = 3)*
2. *Antibacterial properties of doxycycline containing eluates (n = 3).*

The same PBS eluates that were used for doxycycline release profiling were also used for the agar diffusion tests as previously described.

Anti-matrix metalloproteinase activity assay

To evaluate anti-MMP activity of DOX-encapsulated nanotube-modified adhesives, doxycycline-containing eluates were collected in Tris buffer. The fluorescein isothiocyanate (FITC) labeled type I collagen cleavage assay was used to determine the MMP inhibition by the eluates collected in Tris buffer.

Doxycycline containing eluates in Tris buffer (Tris eluates)

Disk-shaped specimens of the adhesive for all the groups (6.2 × 1.0 mm, n = 4) were fabricated as previously described. After 24 h, specimen disks were individually incubated at 37°C in 1 mL of Tris buffer (50 mM Tris-HCl, 0.2 M NaCl, 5 mM $CaCl_2$, 1 μM $ZnCl_2$, and 15 mM NaN_3, pH 7.4). To collect doxycycline containing eluates, 150 μL aliquots were collected after 1, 7, 14, 21, and 28 days. An equal amount of tris buffer was added to replace the removed volume. Aliquots were stored at −20°C until tested.

Labeling type I collagen with fluorescein isothiocyanate

Rat-tail tendon (RTT) type I collagen was purified and labeled with fluorescein isothiocyanate (FITC, sigma-Aldrich) as previously described (Birkedal-Hansen et al., 2003). RTT was dissolved in 20 mM acetic acid at 4 mg/mL under a stirring condition at 4°C for 48 h. An equal volume (5 mL each) of 4 mg/mL of RTT and 20 mM acetic acid were mixed. After the addition of Dulbecco's Modified Eagle's Medium (DMEM, 10 mL), the mixture was neutralized with NaOH, immediately transferred into a 10-cm diameter dish, and incubated at 37°C overnight to form gels. Gels were washed twice with borate buffer (0.05 M $NaB_4O_7.10H_2O$, pH 9.3 and 0.04 M NaCl). The buffer was replaced with 10 mL borate buffer containing FITC (2 mg/mL), and the gels were incubated at room temperature for 30 min until the dye diffused into the gels. Then, the gels were washed with multiple changes of PBS for several days until the washing solution was clear of excess FITC. Gels were washed with deionized water to remove salt and re-dissolved in 5 mL 0.2 M acetic acid at 4°C. FITC labeled type I collagen was dialyzed using dialysis membrane (Spectra/Por 2 dialysis tubing, 12–14K MWCO) against 13 mM HCl.

Activation of matrix metalloproteinase-1

Human full-length matrix metalloproteinase I (MMP-1, 0.05 mg/mL, Abcam, Cambridge, MA, USA) was activated with 4-aminophenylmercuric acetate (APMA, Sigma-Aldrich, St. Louis, MO, USA). Briefly, 10 µL of MMP-1 was incubated with 10 µL of 10 mM APMA (10×, pH 7.4) and 80 µL of buffer (50 mM Tris-HCl, 0.2 M NaCl, 5 mM$CaCl_2$, 1 µM $ZnCl_2$ and 15 mM NaN_3) at 37°C for 90 min (Windsor et al., 1997). The activation was confirmed by western blot analysis.

Western blot analysis

After 90 min at 37°C, the activated and inactivated MMP-1 was mixed with loading buffer and resolved in 10% sodium dodecyl sulphate polyacrylamide gel electrophoresis (SDS-PAGE) at 120 V. The proteins were transferred onto nitrocellulose membranes (Bio-Rad) using blotting buffer (2 mM Tris-HCl, pH 8.3, 192 mM glycine, and 10% methanol) at 100 V for 60 min. The membranes were blocked with 5% (w/v) non-fat milk for 1 h in phosphate buffered saline (PBS) containing 0.1% Tween-20 and then incubated overnight at 4°C with the primary antibodies. The monoclonal Ab-5 (1 µg/mL, Clone III12b, Neomarkers, Fremont, CA, USA) for MMP-1 was used. The membranes were then incubated with secondary antibodies (HRP conjugated anti-rabbit IgG at 1:10,000 ratio, GE Healthcare Life Sciences, Piscataway, NJ, USA) for 1 h at room temperature. The immune complexes were detected using the Pierce Fast Western Blot Kit and SuperSignal West Pico Substrate (Thermo Scientific, Rockford, IL, USA) according to the manufacturer's protocol.

FITC labeled type I collagen cleavage assay

Doxycycline containing eluates in Tris buffer (150 μL, n = 4, 50 mM Tris-HCl, 0.2 M NaCl, 5 mM $CaCl_2$, 1 μM $ZnCl_2$ and 15 mM NaN_3, pH 7.4) were incubated with APMA activated MMP-1 for 30 min at room temperature. Then, Tris buffer (200 μL) and FITC labeled type I collagen (50 μL) were added and the mixture was incubated at 37°C for 120 min. The negative and positive controls were Tris buffer and 0.1% doxycycline, respectively. Samples (70 μL) were periodically (0–120 min) removed, and the reaction was terminated by addition of 1,10-phenanthroline (200 mM, 10 μL) to a final concentration of 25 mM. Sodium dodecyl sulfate polyacrylamide gel electrophoresis (SDS-PAGE) sample buffer was added (1:1). Samples were boiled for 10 min and resolved in 8% SDS-PAGE (150 V, 3 h). The fluorescent signals were captured using Bio-Rad imaging system (Gel Doc™ XR imaging system). The fluorescence intensity at 0 min and 120 min incubation was analyzed with ImageJ software (National Institutes of Health, Bethesda, MD, USA). The percent of FITC labeled RTT of buffer (negative control), 0.1% doxycycline (positive control), and DOX eluates was calculated as follows:

$$\text{Cleaved RTT (\%)} = \left(1 - \frac{\text{Fluorescent density at 2 h}}{\text{Fluorescent density at 0 h}}\right) \times 100$$

The inhibition bydoxycycline containing eluates was calculated using the following equation.

$$\text{Inhibition (\%)} = \frac{\text{Cleaved RTT in buffer (\%)} - \text{cleaved RTT of DOX eluates (\%)}}{\text{Cleaved RTT in buffer (\%)}} \times 100$$

Cytocompatibility

Adhesive disks (6.2 × 1 mm; n = 4) were fabricated and the doxycycline containing eluates were prepared by individually immersing the specimen disks in 15.1 mL of low glucose (1g/L) DMEM supplemented with 10% FBS (Atlanta Biologicals, Lawrenceville, GA, USA), 100 U/mL penicillin (Sigma-Aldrich, St. Louis, MO, USA), 50 mg/mL gentamicin (Invitrogen Life Technologies, Carlsbad, CA, USA) under shaking conditions (50 rpm) at 37°C for 24 h.

Cytotoxicity of the adhesive eluates was evaluated on human dental pulp stem cells (hDPSCs) using water-soluble tetrazolium-1 (WST-1, Roche Diagnostics, Indianapolis, IN, USA) according to the manufacturer's instruction (Zhang et al., 2010) and as previously described.

Transmission electron microscopy (TEM)

TEM was used to evaluate the interface between resin composite and modified adhesive. Disk-shaped specimens (7 × 2 mm) were fabricated using a custom-made silicone mold (Exaflex putty, GC America Inc., Alsip, IL, USA). Briefly, resin composite was placed into the mold and light cured for 40 sec followed by the application of modified adhesive (HNT without doxycycline) and light curing for 20 sec. The adhesive without HNT (SBMP) was used as a control. Specimens were cut to produce approximately 2 × 2 × 2 mm beams using a diamond disk and processed according to the standard TEM protocols as described below:

1. Fixation: specimens were fixed in fixative (Karnovsky) for 24 h and rinsed in 0.1 M sodium cacodylate buffer for ½ h.

2. Post-fixation: specimens were placed in 1% osmium tetroxide in 0.1 M sodium cacodylate buffer (pH 7) at room temperature for 1 h followed by rinsing with 0.1 M sodium cacodylate buffer (pH=7) for ½ h.
3. Dehydration: specimens were dehydrated in ascending concentrations of ethanol: 30%, 50%, 70%, 85%, 90%, and 100% (1 h for each concentration)
4. First infiltration/embedding: dehydrated specimens were infiltrated with 100% propylene oxide, 1:1, 1:2 and 1:3 of 100% propylene oxide, and 100% embedding resin at room temperature (1 h each), respectively.
5. Dehydrated specimens were embedded in resin and polymerized for 48 h at 60°C.
6. The resin blocks were first thick sectioned at 1–2 microns with glass knives using an Ultracut UCT (Leica, Bannockburn, IL). These sections were used as a reference to trim blocks for thin sectioning.
7. The resin blocks were thin sectioned using a diamond knife (Diatome, Electron Microscopy Sciences, Hatfield, PA) at 70–90 nm thick (silver to pale gold using color interference). The sections were then placed on copper mesh grids.
8. After drying on filter paper for a minimum of 1 hour, the sections were examined using a transmission electron microscope Tecnai BioTwin (FEI, Hillsboro, OR, USA).

Statistical analysis

Data were analyzed using One-way Analysis of Variance (ANOVA) followed by Tukey's test for multiple comparisons. A significance level was set at $\alpha=0.05$. Results were summarized as the mean and standard deviation.

RESULTS

Specific aim 1

Degree of conversion

Table 2 and Figure 7 show the results of degree of conversion of the control (SBMP) and modified adhesives that were polymerized for 10 sec, 20 sec,or 40 sec. Generally, increasing the curing times increased the degree of conversion: 60.68–64.10% (10 sec), 63.74–69.70% (20 sec), and 70.79–72.62% (40 sec). However, no statistically significant differences in the degree of conversion were found ($p > 0.05$) with each curing time between the modified adhesives and the control (SBMP).

Agar diffusion test

Representative images of agar diffusion test of control (SBMP) and modified adhesive disks against *S. mutans* at 72 h of incubation are shown in Figure 8. No growth inhibition was observed for the control (SBMP, Figure 8A) and HNT (Figure 8B). The mean inhibition zone of 10% DOX adhesive disks was 12.0 ± 0.0 mm (Figure 8C). The results indicated successful encapsulation and release of DOX from the modified adhesive (10% DOX). The mean inhibition zone of 0.12% chlorhexidine (positive control, Figure 8D) was 21.0 ± 1.0 mm and no inhibition was seen with sterile PBS (negative control).

Eluates from control (SBMP), HNT, and 10% DOX adhesive disks incubated up to 14 days in PBS did not inhibit bacterial growth (data not shown).

Cytocompatibility

Cytotoxicity of adhesive eluates from specimen disks tested on human dental pulp stem cells (hDPSCs, Figure 9) showed no significant differences ($p = 0.225$) among

groups and dilutions tested compared to the control (100% survival, no adhesive eluates, $p > 0.05$). Human DPSC viability ranged from 92.0–107.8% indicating no toxicity of the adhesive eluates to hDPSCs.

MMP mediated casein cleavage assays

MMP mediated casein cleavage assays (Figure 10) demonstrated that doxycycline containing eluates from 14 days (10% DOX) inhibited 13.4% of the MMP-1 activity compared to 48% by 0.1% DOX (positive control). Conversely, the eluates from days 1 and 7 (10% DOX) showed 0% inhibition, whereas eluates from HNT modified adhesives ranged from 0–1.8% inhibition.

Microtensile bond strength and failure mode analysis

Mean microtensile bond strengths (Table 3) were 44.6 ± 15.2 MPa (HNT), 51.7 ± 23.3 MPa (SBMP), and 54.3 ± 19.1 MPa (10% DOX). Statistical analysis revealed no significant differences in microtensile bond strengths among the groups ($p = 0.07$). The modes of failure were predominantly mixed (52.78–60.98%, Table 3) followed by adhesive failure (23.26–31.71%), cohesive failure in resin composite (2.44–19.44%), and cohesive failure in dentin (2.78–11.63%).

Scanning electron microscopy (SEM) analysis

Representative SEM micrographs of the fractured surfaces are shown in Figure 11. At high magnification, rod-like structures indicating the presence of halloysite nanotubes were found in HNT group (Figure 11A, 11B) and 10% DOX (Figure 11C, 11D).

Specific aim 2

Encapsulation efficiency and drug loading

Results of doxycycline encapsulation determined by HPLC and by dry weight are shown in Table 4 and Table 5, respectively. As determined by HPLC (Table 4), the doxycycline that was encapsulated into HNT was 0.24 ± 0.00 g for 10% DOX, 0.36 ± 0.01 g for 20% DOX, and 0.47 ± 0.02 g for 30% DOX. The encapsulation efficiency was 47.08 ± 1.68% for 10% DOX, 36.24 ± 0.54% for 20% DOX, and 31.54 ± 1.05% for 30% DOX. The drug loading (DOX: HNT ratio) was 19.17 ± 0.28% for 10% DOX, 29.05 ± 0.48% for 20% DOX, and 37.85 ± 1.27% for 30% DOX. Statistical analyses revealed significant differences in the amount of encapsulated doxycycline, encapsulation efficiency, and drug loading among the three groups ($p < 0.001$).

As determined by dry weight (Table 5), the doxycycline that was encapsulated into HNT was 0.18 ± 0.01 g for 10% DOX, 0.28 ± 0.01 g for 20% DOX, and 0.37 ± 0.02 g for 30% DOX. The encapsulation efficiency was 34.73 ± 1.93% for 10% DOX, 27.46 ± 1.43% for 20% DOX, 24.74 ± 1.39% for 30% DOX. The drug loading (DOX: HNT ratio) was 14.16 ± 0.90% for 10% DOX, 22.02 ± 1.17% for 10% DOX, and 29.70 ± 1.67% for 10% DOX. One-way ANOVA showed no significant differences in the amount of encapsulated doxycycline, encapsulation efficiency, and drug loading among the three groups ($p < 0.001$).

The results of doxycycline encapsulation determined by both techniques showed a similar trend. Generally, the increases in the concentration of doxycycline significantly increased the amount of doxycycline that was encapsulated into HNT and drug loading

into the HNT. On the other hand, the increases in the concentration of doxycycline significantly decreased the encapsulation efficiency.

Degree of conversion

The degree of conversion of control (SBMP) and modified adhesives that were polymerized for 10 sec, 20 sec or 40 sec is shown in Table 6 and Figure 12. Increasing curing times led to an increase in the degree of conversion: 61.40–64.68 % (10 sec), 64.15–68.65 % (20 sec), and 70.44–73.26 % (40 sec). No significant differences were found with each curing time between each of the modified adhesives and the control (SBMP, $p > 0.05$).

Knoop microhardness

Results of Knoop microhardness of control (SBMP) and modified adhesives are shown in Figure 13. The Knoop microhardness values were 20.72 ± 1.38 (SBMP), 21.21 ± 0.59 (HNT), 22.18 ± 0.97 (10% DOX), 21.87 ± 2.28 (20% DOX), and 20.89 ± 1.30 (30% DOX). No significant differences were found among the groups ($p > 0.05$).

Amount of doxycycline in adhesive disks

Table 7 shows the amount of doxycycline in one adhesive disk determined by mass spectrometry. When specimen disks were dissolved in DMSO, the doxycycline contents in one modified adhesive disk were 0.11 ± 0.16 μg (control, SBMP), 0.06 ± 0.08 μg (HNT), 292.51 ± 29.77 μg (10% DOX), 911.06 ± 48.20 μg (20% DOX), and 1644.17 ± 40.71 μg (30% DOX). When 7.5 mg of DOX-encapsulated HNT powder was dissolved in ethanol, the doxycycline content in one modified adhesive disk were 234.26 ± 11.31 μg (10% DOX), 846.15 ± 43.88 μg (20% DOX), and 1485.35 ± 115.88 μg (30% DOX).

Doxycycline release profiles

Table 8 and Figure 14 show the cumulative release of doxycycline from the control (SBMP) and modified adhesives over 28 days. Generally, the release of doxycycline from the control (SBMP) and modified adhesive disks had an initial burst at 24 h and gradually decreased overtime. The cumulative release of doxycycline (mean ± SE) from the adhesive over 28 days was 0.55 ± 0.00 μg (SBMP), 0.59 ± 0.01 μg (HNT), 4.04 ± 0.05 μg (10% DOX), 4.79 ± 0.07 μg (20% DOX), and 8.21 ± 0.088 μg (30% DOX). No significant differences in total cumulative doxycycline release were found among 10% DOX, 20% DOX, and 30% DOX ($p = 0.259$).

Amount of doxycycline in adhesive disks after 4 months

The amounts of doxycycline that remained in adhesive disks are shown in Table 9. The amounts were 39.77 ± 0.78 μg (10% DOX), 55.50 ± 10.97 μg (20% DOX), and 102.63 ± 11.71 μg (30% DOX). Compared to the original amounts of doxycycline, the percent of doxycycline that remained in an adhesive disk were 13.60% (10% DOX), 6.09% (20% DOX), and 6.24% (30% DOX), respectively.

Agar diffusion test

Agar diffusion test was performed on two main pathogens of dental caries *(S. mutans and L. casei)*. Figure 15 shows representative images of agar diffusion at 72 h of incubation.

The inhibition zones for *S. mutans* (Table 10) were 2.3 ± 3.6 mm (10% DOX), 8.1 ± 0.9 mm (20% DOX), 11.5 ± 2.6 mm (30% DOX), and 16.0 ± 1.1 mm (0.12% chlorhexidine, positive control). The inhibition zones for *L. casei* (Table 10) were 5.1 ± 4.0 mm (10% DOX), 7.2 ± 3.7 mm (20% DOX), 11.3 ± 1.8 mm (30% DOX), and 14.4 ±

0.5 mm (0.12% chlorhexidine, positive control). No inhibition zones were observed for sterile PBS (negative control), SBMP, and HNT.

Figure 16 shows representative images for the agar diffusion test for doxycycline containing eluates of control (SBMP) and modified adhesive disks against *S. mutans* and *L. casei* at 72 h of incubation. The doxycycline containing eluates of 28 days of incubation did not inhibit the growth of either bacterial strain. These results indicated that the amount of doxycycline released from the modified adhesives were subantimicrobial levels (below the minimum inhibitory concentration).

FITC labeled type I collagen cleavage assay

Figure 17 shows representative images of Western blotting of inactive pro-MMP-1 and APMA activated MMP-1. The western blot results confirmed the activation of pro-MMP-1 by AMPA. The active MMP-1 is approximately 10 kDa smaller than the inactive forms. FITC labeled type I collagen cleavage assay demonstrated inhibition of MMP-1 activity by doxycycline containing eluates (Table 11 and Figure 18). Generally, the degree of MMP inhibition was the highest by doxycycline containing eluates from day 1 and gradually decreased overtime. 0.1% doxycycline (positive control) inhibited 44.11 ± 2.28% of MMP-1 activity. Doxycycline containing eluates from day 1 inhibited 16.20 ± 8.09% (10% DOX), 23.61 ± 3.33% (20% DOX), and 26.33 ± 5.01% (30% DOX) of MMP-1 activity. Inhibitions decreased to 3.05 ± 3.05% (10% DOX), 2.39 ± 2.39% (20% DOX), and 3.76 ± 1.46% (30% DOX) for the day 28 eluates. Eluates from the control (SBMP) and HNT inhibited 2.65–4.92 % (SBMP) and 1.27–8.88 % (HNT) of MMP-1 activity. Statistical analysis showed that there were significant differences between 0.1% doxycycline and all groups for all time points. At day 1, eluates of 30% DOX showed

significantly higher MMP inhibition than control (SBMP, $p < 0.05$). At day 7, eluates of 10% DOX and 30% DOX showed significantly higher MMP inhibition than control (SBMP) and HNT ($p < 0.05$). No other significant differences were found ($p > 0.05$).

Cytocompatibility

Figure 19 shows hDPSC viability (%) when exposed to eluates obtained from control (SBMP) and modified adhesive disks. The viability of hDPSCs incubated with various eluates ranged from 81.60% to 107.92% compared with that of cells that were not incubated with eluates (100% survival). The hDPSCs incubated with 0.3% phenol, which served as the negative control (total cell death), showed 0% viability. No significant differences were found among cells incubated with eluates of the same dilution of each group of samples compared with cells that were not incubated with eluate (100% survival, $p > 0.05$).

Transmission electron microscopy (TEM)

Representative TEM micrographs of the interface between resin composite and HNT modified adhesive are shown in Figure 20. Small clusters of HNT were observed at the interface between resin composite and HNT modified adhesive (Figure 20A and 20B). Conversely, HNT was not found in control (SBMP). Fillers of the resin composite were only found along the interface in control (SBMP, Figure 20C and 20D).

DISCUSSION

Over the past few years, MMPs have been shown to play a major role in hybrid layer degradation. Several approaches have been proposed to inhibit MMP activity within the hybrid layer such as using MMP inhibitors (Almahdy et al., 2012; Breschi et al., 2010) and chelating agents (chlorhexidine) (Carrilho et al., 2007; Ricci et al., 2010; Stanislawczuk et al., 2014). This study is a proof of concept that doxycycline, an MMP inhibitor, could be encapsulated into aluminosilicate clay nanotubes (HNT) and the doxycycline released overtime could inhibit MMP activity. Doxycycline was chosen in this study because it is the only MMP inhibitor that is approved by the FDA and subantimicrobial doses of doxycycline have been widely used as an adjunctive systemic therapy for periodontal disease (Giannobile, 2008). HNT was used as a drug carrier in this study because it has been used for drug encapsulation for controlled release of many drugs and other agents [e.g., tetracycline (Qi et al., 2013), dexamethasone (Veerabadran et al., 2009), Nifedipine and Furosemide (Lvov et al., 2008)]. Furthermore, HNT is safe, biocompatible and has high mechanical strength. Therefore, the use of doxycycline by encapsulating it into HNT would provide a sustained release for MMP inhibition. Furthermore, the mechanical properties of the dental adhesive loaded with HNT would not be compromised due to the high strength of HNT (Bottino et al., 2013).

This study was conducted with two specific aims. The first specific aim focused mainly on the potential use of doxycycline for MMP inhibition in the hybrid layer and its effects on the immediate resin-dentin microtensile bond strength. The concentration of doxycycline used for encapsulation was 10% (w/v). The data suggested that the concentration of doxycycline that was encapsulated into HNT and then incorporated into

the dental adhesive reached the minimum inhibitory concentration (MIC, 0.25–0.50 mg/mL (Al-Ahmad et al., 2014) and inhibited the growth of *S. mutans* when the specimen disks were directly contacting the bacteria. This result indicated successful encapsulation of doxycycline into HNT. On the other hand, the eluates containing doxycycline released from modified adhesive disks did not inhibit the growth of *S. mutans* but inhibited 13.4% of the MMP-1 activity (day 14 eluates). The results from antibacterial and anti-MMP activity led to the conclusion that doxycycline released from modified adhesive disks was at subantimicrobial levels.

It is very important to know the effects of doxycycline on monomer conversion of the adhesive because the incorporation of doxycycline led to significant darkening of the adhesives. This study investigated the degree of conversion of the modified adhesives by curing them not only for 10 sec as recommended by manufacturer, but also for 20 sec and 40 sec. Results showed no significant impact ($p > 0.05$) of different concentrations of doxycycline on monomer conversion when the specimens were polymerized with the same curing time between the modified adhesives and the control (SBMP). Furthermore, the release of doxycycline was not due to underpolymerization.

Regarding the resin-dentin microtensile bond strength, the incorporation of either HNT or DOX-encapsulated HNT did not jeopardize microtensile bond strength as no significant differences were found ($p = 0.07$). This finding was supported by a previously published study that the incorporation of HNT at 15% (w/v) did not increase nor compromise the resin-dentin bond strength (Bottino et al., 2013). This is because the degree of conversion of the modified adhesives was not jeopardized by the incorporation

of doxycycline. SEM micrographs confirmed the presence of HNT in the hybrid layer (Figure 11).

In conclusion, the results of the first specific aim established successful encapsulation and release of doxycycline from modified adhesives at subantimicrobial levels. Furthermore, the resin-dentin bonding was not compromised by the use of doxycycline. However, the amount of doxycycline that was encapsulated into HNT and the amount of doxycycline-released from the modified adhesives were unknown. These limitations were evaluated in specific aim 2.

Specific aim 2 was focused on the encapsulation of various concentrations of doxycycline (10–30%, w/v). The amount of doxycycline released and encapsulated into the HNT was also determined. In this part, drug encapsulation was evaluated by both HPLC and dry weight. The results from both techniques are in agreement with each other that increased concentrations of doxycycline significantly increased the amount of doxycycline that was encapsulated into the HNT. Conversely, higher concentrations of doxycycline significantly decreased the encapsulation efficiency. This reduction is possibly due to the threshold limit because the amount of HNT used for the encapsulation was constant (1.25 g of HNT in 5 mL of doxycycline solution) regardless of the concentration of doxycycline used. A study conducted by Qi et al reported a similar trend when HNT was encapsulated by tetracycline (Qi et al., 2010).

Since HNT is positively charged on the inner surface and negatively charged on the outer surface, the driving force for drug encapsulation on the surfaces of HNT could possibly be due to the differences in charges between the cationic drug (i.e., doxycycline) (Seleem et al., 2009) and the negatively charged HNT. Moreover, when vacuum is

applied, doxycycline could be pushed into the lumen of HNT due to the negative pressure regardless of the charge of the materials.

Regarding the physico-chemical properties of modified adhesives, one-way ANOVA revealed no statistically significant differences between the modified adhesives compared to the control (SBMP) when tested with the same curing time. Nevertheless, it is important to point out that even though doxycycline incorporation led to a darker adhesive, it did not compromise resin monomer conversion. Therefore, these modified adhesives could potentially be handled and used in the same fashion as the commercial ones. This study further evaluated the Knoop microhardness of each of the modified adhesives with the same dimension as that used for drug release profile (6.2 mm × 1 mm) by curing specimens for 20 sec (each side) to ensure that the polymerization of modified adhesives is not compromised due to thicker specimens. Moreover, it was reported that there is a strong correlation ($r^2 > 0.9$) between the degree of conversion and microhardness (Ferracane, 1985). Statistical analysis showed no significant differences among the groups. These results suggested that curing the modified adhesives would not jeopardize monomer conversion. Therefore, the release of doxycycline was not due to undercuring of the adhesives.

Regarding the release profile of doxycycline from modified adhesives, higher concentrations of doxycycline led to higher release of doxycycline from the modified adhesives although no significant differences ($p = 0.259$) were found among groups (10%, 20% and 30% DOX). Although higher concentration of doxycycline (> 30%, w/v) could provide higher release, the concentration used in this study was limited by the solubility and the pH of doxycycline that was dissolved in 50 mM HEPES (pH 7.2).

Doxycycline was not completely dissolved in 50 mM HEPES with a concentration higher than 30% (w/v). Moreover, the increased concentration of doxycycline significantly decreased pH of the doxycycline solution (i.e., pH of 30% DOX solution was approximately 3.5 whereas pH of 50% DOX was approximately 1). Since the pH of the dental adhesive (SBMP) is approximately 3.5–4.0, the increased concentration of doxycycline could significantly drop pH of the modified adhesive leading to changes in the properties of the adhesive or interactions between adhesive and demineralized dentin.

The cumulative release of doxycycline over 28 days was approximately 1–2% of the amount of doxycycline in the adhesive disks. Therefore, the doxycycline remaining in the adhesive disks would serve as a reservoir for sustained release over time. After 4 months of incubation, the doxycycline left in the adhesive was approximately 6–13% of the original concentration. Theoretically, most doxycycline should remain in the adhesive or almost all of the doxycycline should be released into the incubation medium. However, a portion of the doxycycline was lost during the incubation. This is possibly due to the half-life of the doxycycline that was reported to be approximately 24 h *in vivo* or in cell culture media (Centlivre et al., 2010; Strickman et al., 1995; Wang et al., 2003). It is important to point out that doxycycline was encapsulated in HNT and the DOX-encapsulated HNT was used for adhesive fabrication. In other words, doxycycline was in the solid form in adhesive disks. This condition should protect doxycycline from degradation.

As expected, results of agar diffusion tests revealed successful incorporation of DOX-encapsulated HNT into modified adhesives. The modified adhesive disks inhibited the growth of both *S. mutans* and *L. casei*. Overall, higher concentrations of doxycycline

showed larger inhibition zones. Conversely, the doxycycline containing eluates of 28 days of incubation did not inhibit the growth of either bacterial strain. This result indicated that the concentration of doxycycline released from the specimens was below the minimum inhibitory concentration (*S. mutans* = 0.25–0.50 mg/mL and *L. casei* = 0.38–1.5 mg/mL (Al-Ahmad et al., 2014). In other words, the eluates obtained from DOX-encapsulated specimens contained subantimicrobial levels of doxycycline.

To evaluate anti-MMP properties of doxycycline containing eluates, an FITC labeled type I collagen was used as the substrate for MMP-1. MMP-1 was used in this study because only MMP-1, MMP-8 and MMP-13 are true collagenases and can cleave fibrillar collagen more efficiently than the other types of MMPs. Furthermore, MMP-1 is also found in dentin along with MMP-2, MMP-3, MMP-8, and MMP -9 (Sulkala et al., 2007; van Strijp et al., 2003; Wang et al., 2012). The results demonstrated MMP-1 inhibition by the doxycycline containing eluates. Overall, doxycycline containing eluates from day 1 showed the highest MMP inhibition (16.20–26.33%), and the degree of MMP-1 inhibition by doxycycline containing eluates gradually decreased overtime compared to the negative control (Tris buffer). The positive control (0.1% doxycycline) inhibited 44.11 % of MMP-1 activity that was significantly higher than all other groups. This led to the conclusion that doxycycline was released from specimen disks at subantimicrobial levels. TEM micrographs of the interface between resin composite and the modified adhesive (Figure 20) showed the presence of small clusters of HNT, similar to SEM images of the fracture surfaces of the microtensile beams (Figure 11, specific aim 1). This finding indicated that HNT could serve as a reservoir for drug release.

Cytocompatibility tests revealed that the viability of hDPSCs cultured in doxycycline containing eluates ranged from 81.60% to 107.92%, compared to those cultured without eluate (100% survival). This is considered as slight toxicity (60–90% cell viability) or non-cytotoxicity (>90% cell viability) according to Dahl et al. (Dahl et al., 2006).

These findings led to the conclusion that doxycycline containing eluates had subantimicrobial properties and the ability to inhibit MMPs without toxicity and without compromising the physico-chemical properties of the adhesives. However, this study lacks the information regarding the resin-dentin bond strength especially the immediate bond strength of modified adhesives at 20% DOX and 30% DOX. Since the degree of conversion of the modified adhesives was not compromised by the incorporation of DOX-encapsulated HNT, the immediate dentin bond strength should not significantly decrease compared to the control (SBMP). Moreover, the data from specific aim 1 showed that the adhesive modified with 10% DOX-encapsulated HNT did not significantly decrease the microtensile bond strength to dentin evaluated after 24 h of bonding (Feitosa et al., 2014). Nevertheless, it would be informational to further investigate the immediate and the long-term bond durability of the resin-dentin bonding using the microtensile bond strength test along with nanoleakage and TEM studies of the resin-dentin interface after aging (i.e., 6 months or 1 year). Furthermore, the other MMP inhibitors, such as epigallocatechin gallate (EGCG), that do not change the color of the adhesive and are more stable in the oral environment, should be investigated.

SUMMARY AND CONCLUSIONS

The ultimate goal of this project was to evaluate doxycycline for its effects on preventing the degradation of hybrid layer through the modification of dental adhesive with aluminosilicate clay nanotubes (HNT) loaded with doxycycline. Doxycycline was chosen because it is an MMP inhibitor that is approved by the Food and Drug Administration (FDA). Doxycycline was encapsulated into HNT at three distinct concentrations (10%, 20% and 30% DOX, w/v). The increases in the concentration of doxycycline significantly increased the amount of doxycycline that was encapsulated into HNT and the drug loading into HNT. Conversely, the encapsulation efficiency was significantly decreased with increasing concentrations of doxycycline. The modified adhesives were fabricated by incorporation of DOX-encapsulated HNT into a commercially available three-step etch-and-rinse dental adhesive (Adper Scotchbond Multi-Purpose). The degree of conversion, Knoop microhardness, doxycycline release profiles, the biological activity (antibacterial and anti-MMP activity), and cytocompatibility of the modified adhesives were investigated. There were no statistically significant differences ($p > 0.05$) in the degree of conversion and Knoop microhardness compared to the control (SBMP). None of the adhesives eluates was cytotoxic to the human dental pulp stem cells. Higher concentrations of doxycycline led to generally higher release of doxycycline from the modified adhesives, although no significant differences ($p = 0.259$) were found among the groups (10%, 20% and 30% DOX). A significant growth inhibition of *S. mutans* and *L. casei* by direct contact illustrated successful encapsulation of doxycycline into the modified adhesives. Doxycycline released from the modified adhesives (doxycycline containing eluates) did not inhibit the

growth of both cariogenic bacteria but inhibited MMP-1 activity. The results suggested subantimicrobial levels of doxycycline were released. The immediate microtensile bond strengths were not significantly different compared to the control (SBMP) suggesting no negative effects of doxycycline on dentin bonding (only 10% DOX was investigated).

Collectively, the results suggested that HNT could be used as a drug carrier for release of doxycycline and possibly other MMP inhibitors without compromising the physico-chemical properties of modified adhesives or toxic effects to the human cells. This study lacks information regarding the long-term resin-dentin bond durability (i.e, 6 months or 1 year bond strength). However, it provides a solid background for the use of other MMP inhibitors that do not change the color of the adhesive and are more stable in the oral environment.

TABLES

Table 1. Classification of matrix metalloproteinases (MMPs).

Subgroup	
Collagenases	MMP-1, MMP-8, MMP-13, and MMP-18
Gelatinases	MMP-2 and MMP-9
Stromelysins	MMP-3, MMP-10, and MMP-11
Matrilysins	MMP-7, and MMP-26
Membrane-type MMPs	MMP-14, MMP-15, MMP-16, MMP-17, MMP-24, and MMP-25
Others	MMP-12, MMP-19, MMP-20, MMP-21, MMP-23, MMP- 27, and MMP-28

Table 2. Degree of conversion of control (SBMP) and the modified adhesives that were polymerized for 10 sec, 20 sec or 40 sec.

Group	Degree of conversion (%)		
	10 sec	**20 sec**	**40 sec**
SBMP	62.67 ± 2.74	63.74 ± 5.38	72.62 ± 1.72
HNT	64.10 ± 5.43	65.72 ± 4.33	70.79 ± 1.93
10% DOX	60.68 ± 4.51	69.70 ± 3.93	72.62 ± 5.89

The energies applied during light curing of 10 sec, 20 sec and 40 sec were 10.92 J/cm^2, 22.49 J/cm^2 and 46.18 J/cm^2, respectively. No statistically significant differences were found ($p > 0.05$) with each curing time between the modified adhesives and the control (SBMP).

Table 3. Mean microtensile bond strength (μTBS, mean ± SD) and failure modes.

Group	μTBS (MPa)	Failure modes (%)			
		Adhesive	Mixed	Cohesive-dentin	Cohesive-resin
SBMP	51.7 ± 23.3	25.00	52.78	2.78	19.44
HNT	44.6 ± 15.2	31.71	60.98	4.88	2.44
10% DOX	54.3 ± 19.1	23.26	53.49	11.63	11.63

Microtensile bond strengths showed no statistically significant differences among the groups ($p = 0.07$).

Table 4. Encapsulation of doxycycline determined by HPLC.

Group	Un-encapsulated DOX (g)	Encapsulated DOX (g)	Encapsulation efficiency (%)	Drug Loading (%)
10% DOX	0.26 ± 0.00	0.24 ± 0.00	47.08 ± 1.68	19.17 ± 0.28
20% DOX	0.64 ± 0.01	0.36 ± 0.01	36.24 ± 0.54	29.05 ± 0.48
30% DOX	1.03 ± 0.02	0.47 ± 0.02	31.54 ± 1.05	37.85 ± 1.27

There was a significant difference ($p < 0.001$) in the amount of encapsulated doxycycline, encapsulation efficiency and drug loading among the 3 concentrations of doxycycline. The amount of doxycycline used for encapsulation was 0.5 g (10% DOX), 1.0 g (20% DOX) and 1.5 g (30% DOX). Drug loading (DOX:HNT) is the ratio between encapsulated doxycycline and added HNT (1.25 g).

Table 5. Encapsulation of doxycycline determined by dry weight.

Group	Un-encapsulated DOX (g)	Encapsulated DOX (g)	Encapsulation efficiency (%)	Drug Loading (%)
10% DOX	0.32 ± .01	0.18 ± 0.01	34.73 ± 1.93	14.16 ± 0.90
20% DOX	0.72 ± .02	0.28 ± 0.01	27.46 ± 1.43	22.02 ± 1.17
30% DOX	1.12 ± 0.02	0.37 ± 0.02	24.74 ± 1.39	29.70 ± 1.67

There was a significant difference ($p < 0.001$) in the amount of encapsulated doxycycline, encapsulation efficiency and drug loading among the 3 concentrations of doxycycline. The amount of doxycycline used for encapsulation was 0.5 g (10% DOX), 1.0 g (20% DOX) and 1.5 g (30% DOX). Drug loading (DOX:HNT) is the ratio between encapsulated doxycycline and added HNT (1.25 g).

Table 6. Degree of conversion of control (SBMP) and modified adhesives that were polymerized for 10 sec, 20 sec or 40 sec.

Group	Degree of conversion (%)		
	10 sec	**20 sec**	**40 sec**
SBMP	64.68 ± 3.35	68.20 ± 1.19	70.61 ± 1.42
HNT	64.12 ± 2.80	66.93 ± 3.63	70.44 ± 1.16
10% DOX	61.40 ± 3.07	64.15 ± 3.08	73.26 ± 3.21
20% DOX	64.15 ± 3.09	66.19 ± 4.97	71.79 ± 4.16
30% DOX	62.31 ± 4.86	68.65 ± 4.71	72.03 ± 2.25

The energies applied during light curing of 10 sec, 20 sec and 40 sec were 10.92 J/cm^2, 22.49 J/cm^2 and 46.18 J/cm^2, respectively. No significant differences were found with each curing time between the modified adhesives and SBMP ($p > 0.05$).

Table 7. Amount of doxycycline (μg, mean ± SD) that was incorporated into the modified adhesive disks determined by two techniques.

Group	Doxycycline in the adhesive disk determined by	
	Adhesive disk dissolved in DMSO (μg)	**7.5 mg DOX-encapsulated HNT powder dissolved in ethanol (μg)**
SBMP	0.11 ± 0.16	N/A
HNT	0.06 ± 0.08	N/A
10% DOX	292.51 ± 29.77	234.26 ± 11.31
20% DOX	911.06 ± 48.20	846.15 ± 43.88
30% DOX	1644.17 ± 40.71	1485.35 ± 115.88

7.5 mg of DOX-encapsulated HNT powder was calculated based on the fact that an adhesive disk needs approximately 50 μL of modified adhesive solution. DOX-encapsulated HNT powder was mixed with the adhesive solution at 15% (w/v, 150 mg in 1 mL of adhesive solution). Therefore, 50 μL of modified adhesive solution had approximately 7.5 mg of DOX-encapsulated HNT powder.

Table 8. Cumulative release profile (μg, mean ± SE) of control (SBMP) and modified adhesives determined by mass spectrometry.

Groups	Cumulative release of doxycycline (μg)				
	Day 1	**Day 7**	**Day 14**	**Day 21**	**Day 28**
SBMP	0.19 ± 0.02	0.30 ± 0.01	0.39 ± 0.00	0.47 ± 0.00	0.55 ± 0.00
HNT	0.24 ± 0.01	0.34 ± 0.02	0.42 ± 0.02	0.50 ± 0.01	0.59 ± 0.01
10% DOX	1.71 ± 0.45	2.69 ± 0.19	3.29 ±0.09	3.70 ± 0.06	4.04 ± 0.05
20% DOX	2.30 ± 0.55	3.26 ± 0.20	2.94 ± 0.13	4.41 ± 0.09	4.79 ± 0.07
30% DOX	4.81 ± 1.96	6.38 ± 0.51	7.24 ± 0.23	7.80 ± 0.14	8.21 ± 0.08

No significant differences in total cumulative doxycycline release were found among 10% DOX, 20% DOX, and 30% DOX ($p = 0.259$).

Table 9. Amount of doxycycline remaining in modified adhesive disks after 4 months of incubation in phosphate buffer saline (PBS).

Group	DOX remaining in adhesive disk (µg)	Percent remaining (%)
SBMP	0.15 ± 0.17	N/A
HNT	1.60 ± 1.87	N/A
10% DOX	39.77 ± 0.78	13.60
20% DOX	55.50 ± 10.97	6.09
30% DOX	102.63 ± 11.71	6.24

Table 10. Agar diffusion test of control (SBMP) and modified adhesive disks against *S. mutans* and *L. casei* at 72 h of incubation.

Group	Average inhibition zone (mm)	
	S. mutans	***L. casei***
0.12% CHX	16.0 ± 1.1	14.4 ± 0.5
10% DOX	2.3 ± 3.6	5.1 ± 4.0
20% DOX	8.1 ± 0.9	7.2 ± 3.7
30% DOX	11.5 ± 2.6	11.3 ± 1.8

0.12% chlorhexidine (CHX) and sterile PBS were used as positive and negative controls, respectively. No inhibition zones were observed with SBMP, HNT and sterile PBS.

Table 11. Inhibition of MMP-1 by doxycycline (DOX) containing eluates (mean ± SE) compared with negative control (Tris buffer) and positive control (0.1% doxycycline solution).

Group	Inhibition by doxycycline containing eluates (%, mean ± SE)				
	Day 1	**Day 7**	**Day 14**	**Day 21**	**Day 28**
0.1% DOX	44.11 ± 2.28				
SBMP	3.99 ± 3.44	3.53 ± 2.74	2.65 ± 2.47	4.92 ± 2.08	2.86 ± 1.98
HNT	8.88 ± 3.17	3.06 ± 3.06	4.32 ± 2.68	4.86 ± 2.55	1.27 ± 1.27
10% DOX	16.20 ± 8.09	18.25 ± 1.78	8.39 ± 3.25	11.17 ± 2.61	3.05 ± 3.05
20% DOX	23.61 ± 3.33	17.36 ± 2.08	14.68 ± 3.24	8.83 ± 1.01	2.39 ± 2.39
30% DOX	26.33 ± 5.01	25.18 ± 1.49	15.10 ± 2.13	14.82 ± 3.41	3.76 ± 1.46

Statistical analysis showed significant difference between 0.1% doxycycline and each sample at all time points ($p < 0.05$). At day 1, eluates of 30% DOX had significantly higher MMP inhibition than those of control (SBMP, $p < 0.05$). At day 7, eluates of 10% DOX and 30% DOX showed significantly higher MMP inhibition than those of control (SBMP) and HNT ($p < 0.05$). No significant differences were found with other samples ($p > 0.05$). The negative control (Tris buffer) was 50 mM Tris with 0.2 M NaCl, 10 mM $CaCl_2$, and 1 μM $ZnCl_2$, pH 7.4).

FIGURES

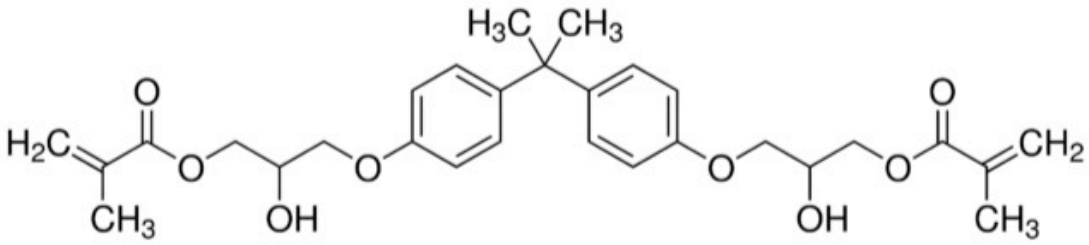

bisphenol A diglycidyl ether diemthacrylate (Bis-GMA)

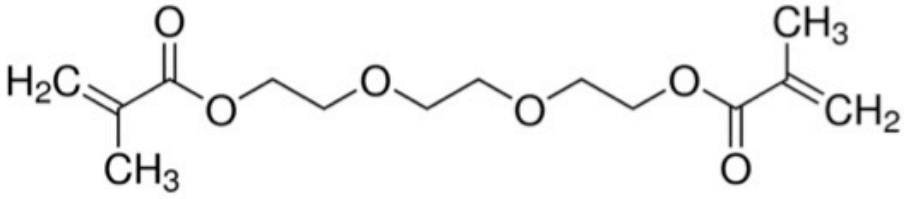

triethylene glycol dimethacrylate (TEGDMA)

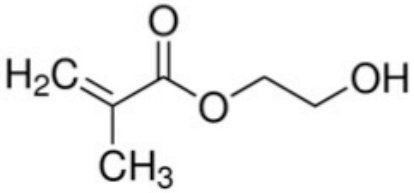

2-hydroxyethyl methacrylate (HEMA)

Figure 1. Monomers commonly used in dental resin composites and dental adhesives. These monomers contain ester-linkages that are vulnerable to hydrolysis.

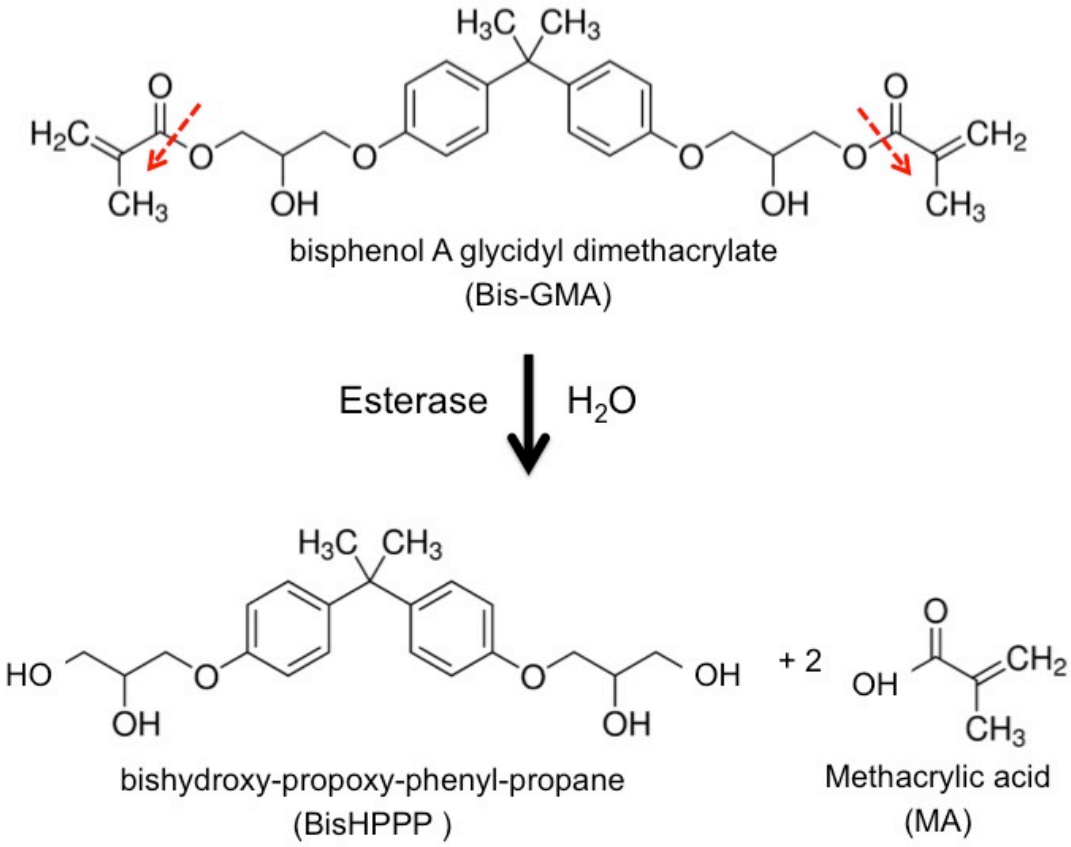

Figure 2. Biodegradation of the dental monomer Bisphenol A glycidyl dimethacrylate (Bis-GMA) to Bis-hydroxy-propoxy-phenyl-propane (BisHPPP) and methacrylic acid (MA).

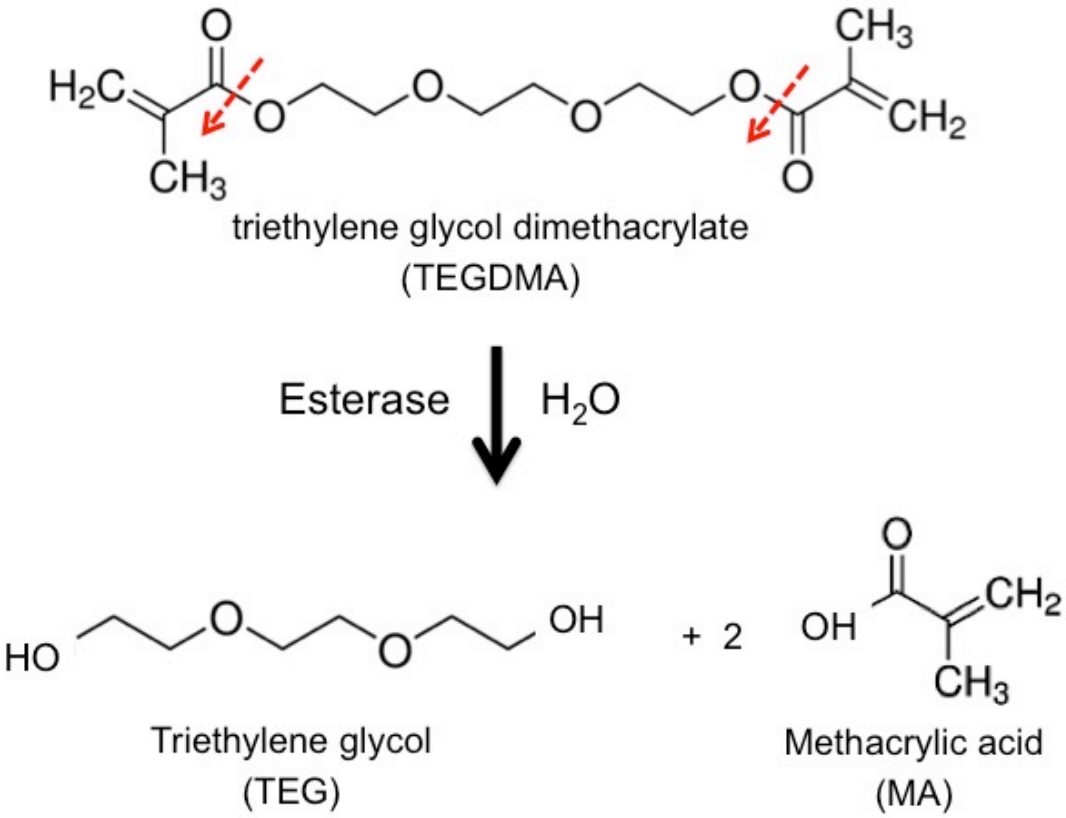

Figure 3. Biodegradation of the dental monomer triethylene glycol dimethacrylate (TEGDMA) to triethylene glycol (TEG) and methacrylic acid (MA).

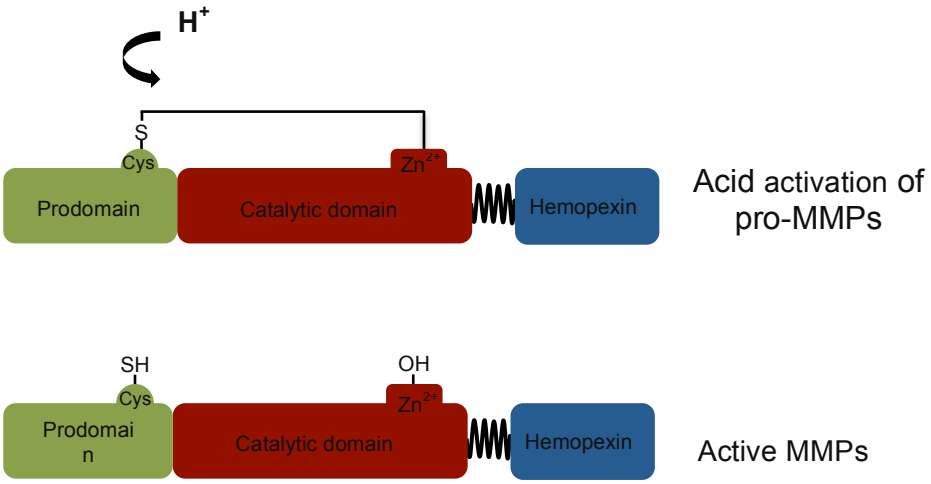

Figure 4. Activation of pro-MMPs by acid (H^+) that reduces the bond between cysteine in the prodomain and Zn^{2+} in the catalytic domain of MMPs.

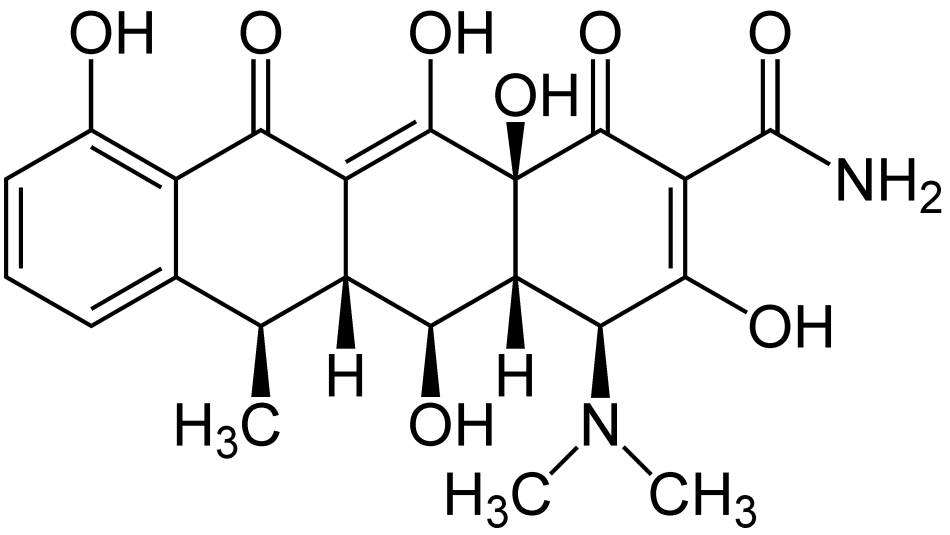

Figure 5. Chemical structure of doxycycline ($C_{22}H_{24}N_2O_8$).

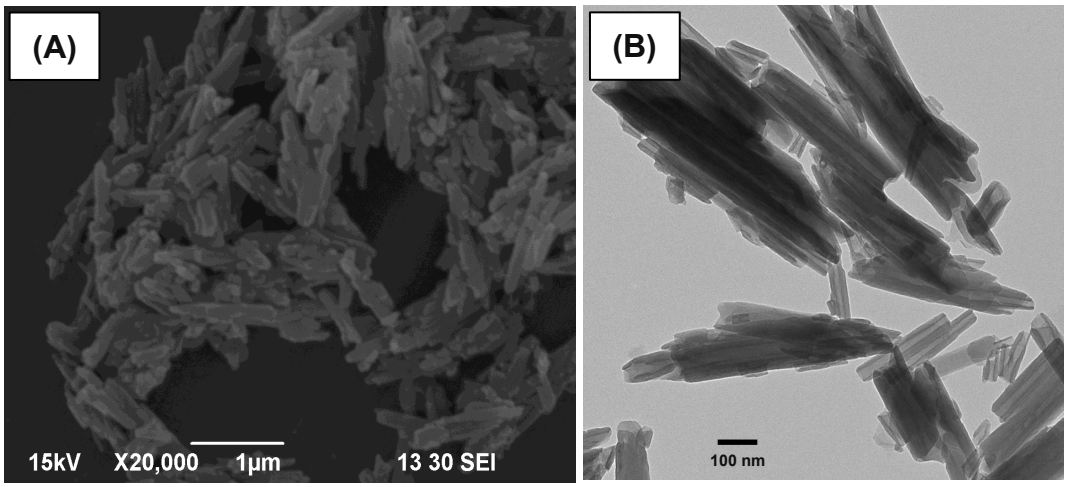

Figure 6. Scanning electron micrograph at 20,000× (A) and Transmission electron micrograph at 68,000× (B, HV=80.0 kV, bar 100 nm) of aluminosilicate clay nanotubes (Halloysite, HNT, Dragonite 1415JM, Applied Minerals Inc., New York, NY, USA).

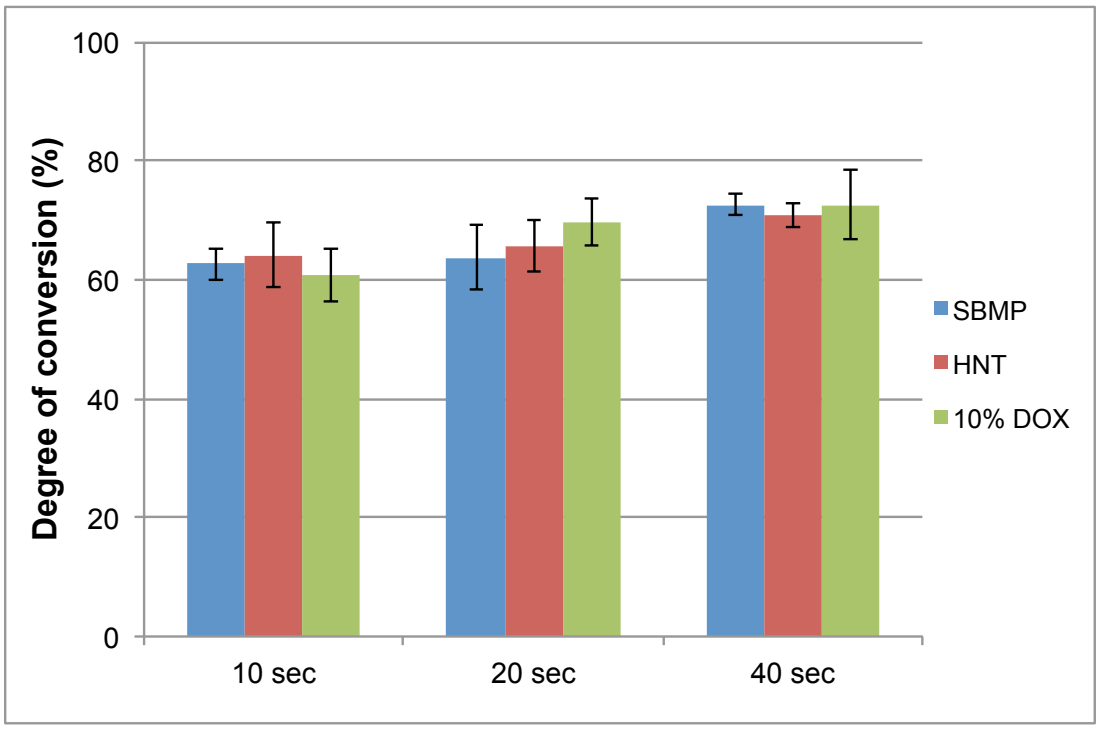

Figure 7. Degree of conversion of control (SBMP) and modified adhesives that were polymerized for 10 sec, 20 sec or 40 sec. The energy applied during light curing of 10 sec, 20 sec and 40 sec were 10.92 J/cm^2, 22.49 J/cm^2 and 46.18 J/cm^2, respectively. Increasing curing times led to an increase in degree of conversion values: 60.7–64.1% (10 sec), 63.7–69.7% (20 sec), and 70.8–72.6% (40 sec). There were no statistically significant differences ($p > 0.05$) in degree of conversion with each curing time between each of the modified adhesives and the control (SBMP).

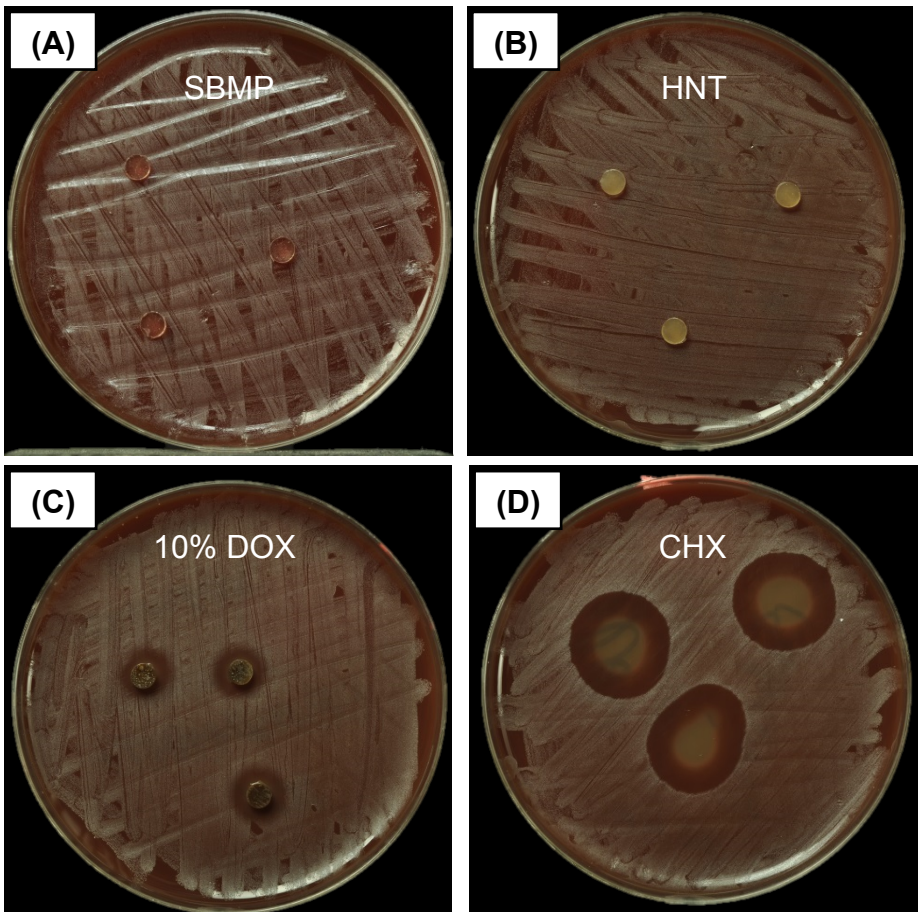

Figure 8. Representative macrophotographs of agar diffusion test of control (SBMP) and modified adhesive disks against *S. mutans* at 72 h of incubation. **(A)** control (SBMP), **(B)** HNT, **(C)** 10% DOX, and **(D)** 0.12% chlorhexidine (positive control). Mean inhibition zones of 10% DOX and 0.12% chlorhexidine were 12.0 ± 0.0 mm and 21.0 ± 1.0 mm, respectively. No inhibition zone was observed with control (SBMP) and HNT.

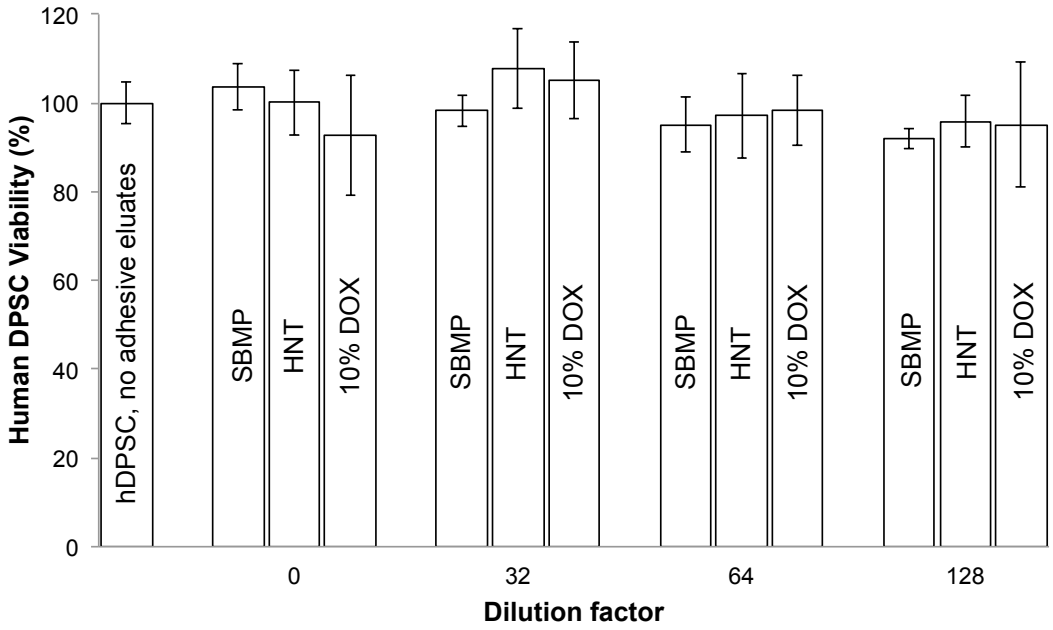

Figure 9. Cytotoxicity of eluates from control (SBMP) and modified adhesive specimens tested on human dental pulp stem cells (hDPSCs).

No significant differences ($p = 0.225$) in cytotoxicity were found among all groups of study and dilutions tested.

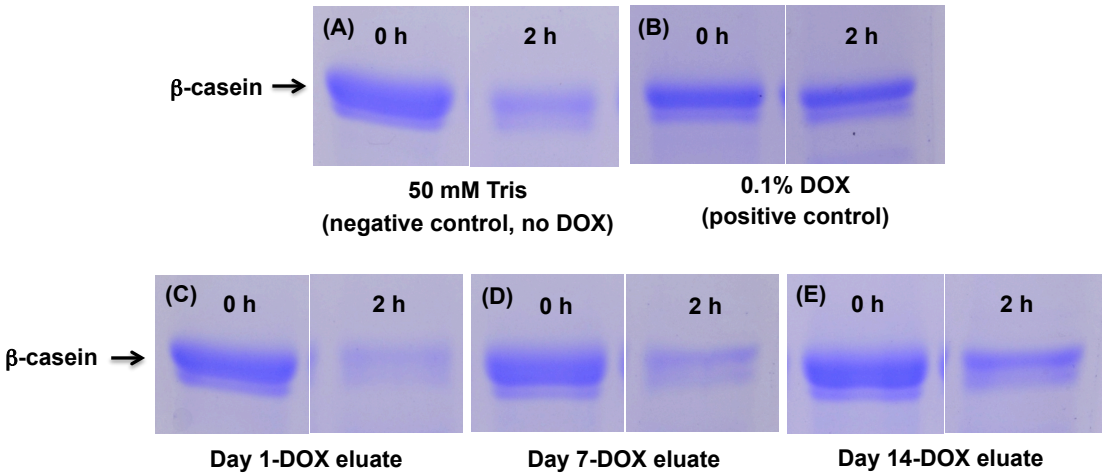

Figure 10. Representative images of Coomassie blue stained SDS-PAGE gels of β-casein cleavage inhibition assays. **(A)** Negative control: 50 mM Tris with 0.2 M NaCl, 10 mM $CaCl_2$, and 1 μM $ZnCl_2$ (pH 7.4), **(B)** Positive control: 0.1% DOX solution (Sigma), **(C)** DOX-eluates (Day 1), **(D)** DOX-eluates (Day 7), and **(E)** DOX-eluates (Day 14). More β-casein is present in Panel E compared to the negative control (50 mM Tris) at 2 hours.

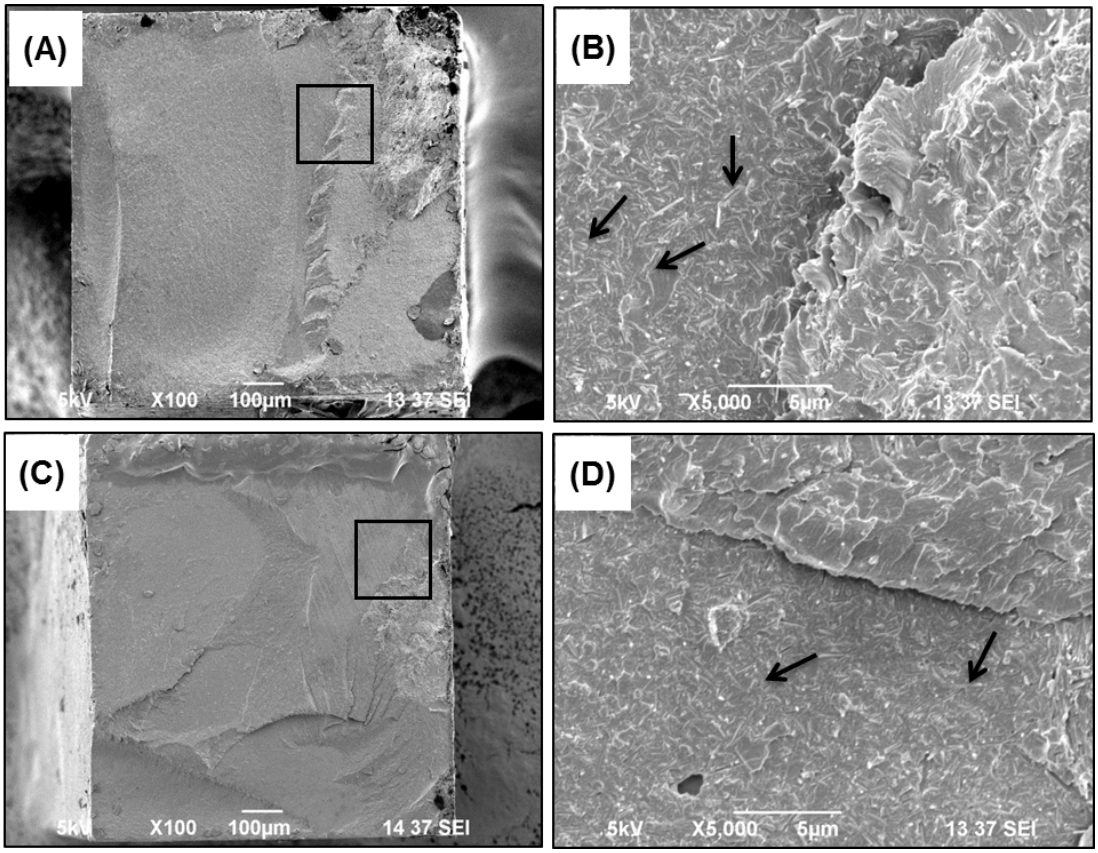

Figure 11. Representative scanning electron micrographs of fractured microtensile beams. **(A, B)** HNT (100×, 5000×), **(C, D)** HNT+DOX (100×, 5000×). Arrows show rod-like structure of approximately 1–2 µm in length indicating HNT incorporation into the modified adhesives.

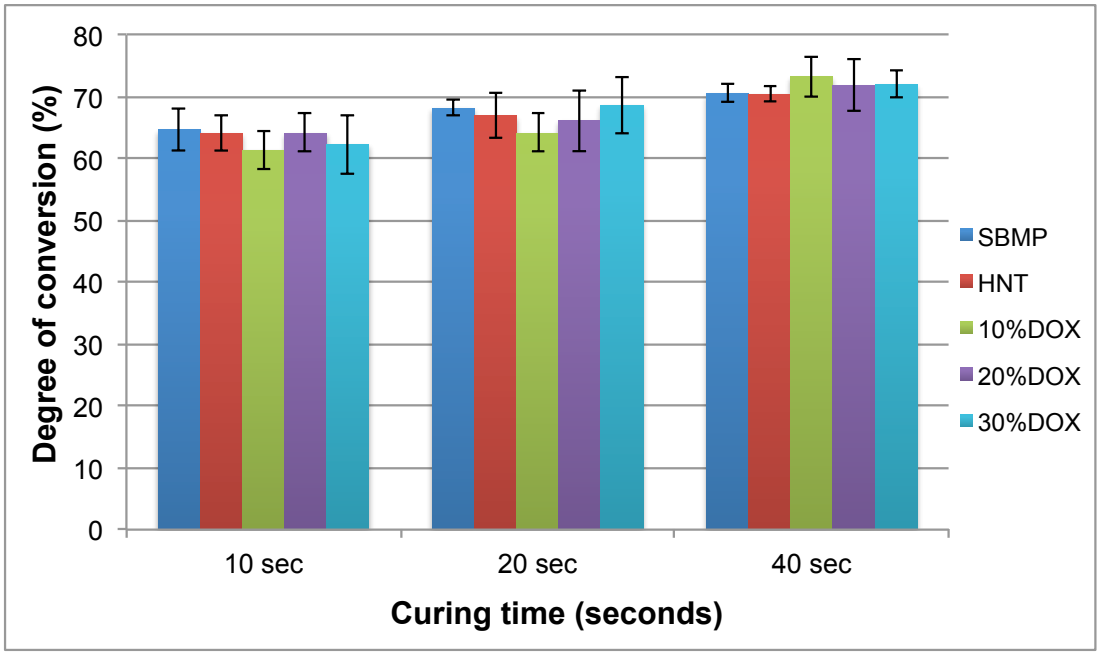

Figure 12. Degree of conversion of control (SBMP) and modified adhesives that were polymerized for 10 sec, 20 sec or 40 sec. The energies applied during light curing of 10 sec, 20 sec and 40 sec were 10.92 J/cm^2, 22.49 J/cm^2 and 46.18 J/cm^2, respectively. Increasing curing times led to an increase in degree of conversion values: 61.40–64.68% (10 sec), 64.15–68.65% (20 sec), and 70.44–73.26% (40 sec). No significant difference was found with each curing time between each of the modified adhesives and SBMP ($p > 0.05$).

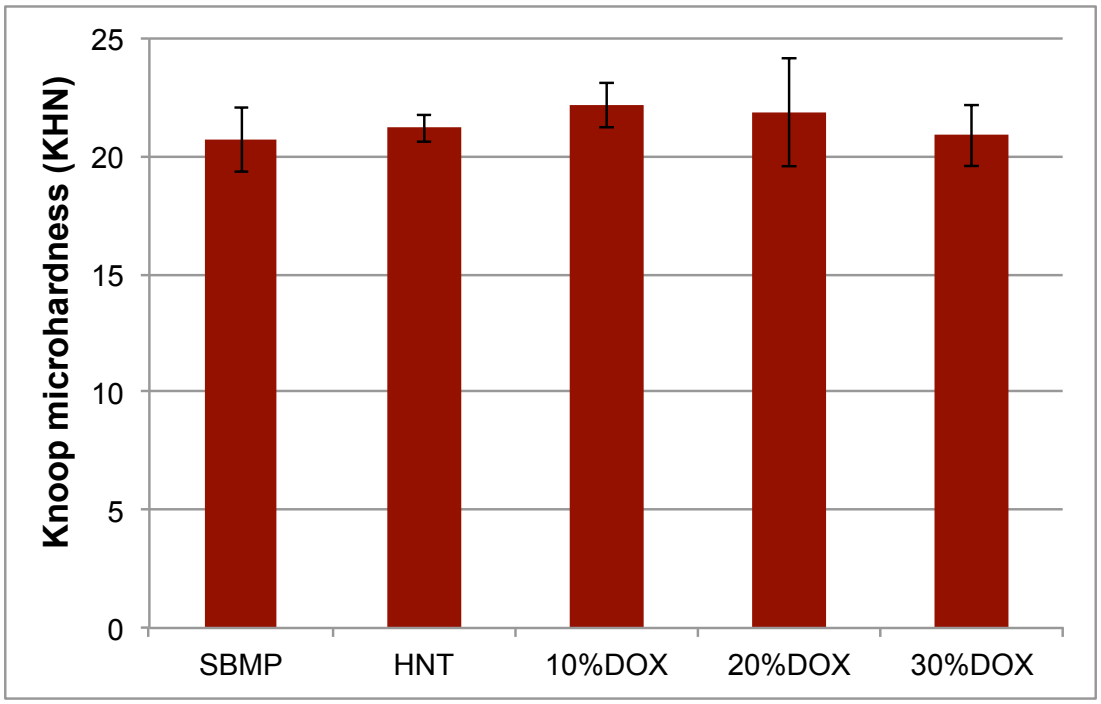

Figure 13. Knoop microhardness number (KHN) of control (SBMP) and modified adhesives polymerized for 20 sec. KHN was 20.72 ± 1.38 (SBMP), 21.21 ± 0.59 (HNT), 22.18 ± 0.97 (10% DOX), 21.87 ± 2.28 (20% DOX) and 20.89 ± 1.30 (30% DOX). No significant differences were found among groups of the study ($p > 0.05$).

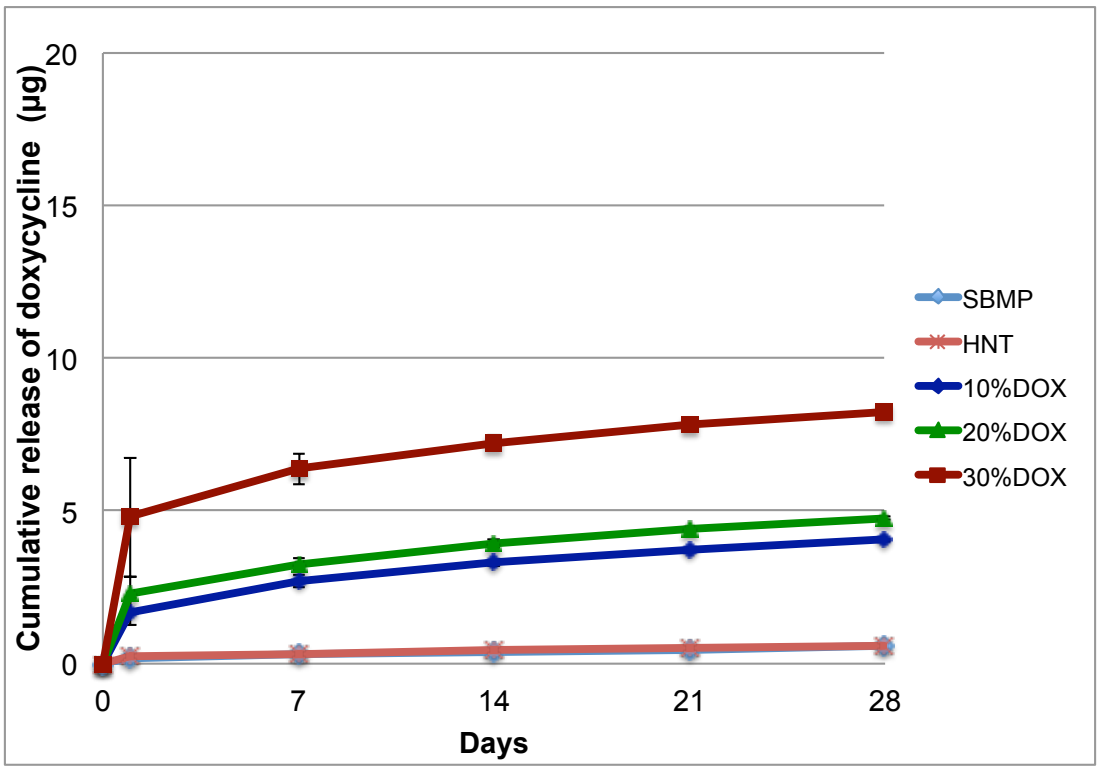

Figure 14. Release profiles (mean ± SE) of doxycycline of control (SBMP) and modified adhesives at day 1, 7, 14, 21, and 28. No significant differences in total cumulative doxycycline release were found among 10% DOX, 20% DOX, and 30% DOX ($p = 0.259$).

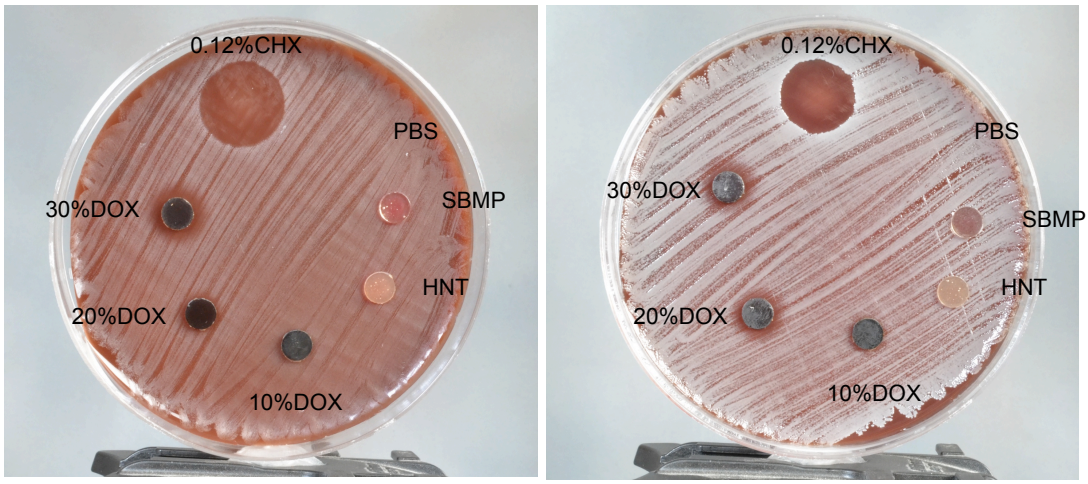

Figure 15. Representative images of agar diffusion test of control (SBMP) and modified adhesive disks against *S. mutans* (left) and *L. casei* (right) at 72 h of incubation. The average inhibition zones on *S. mutans* were 16.0 ± 1.1 mm (0.12% chlorhexidine), 2.3 ± 3.6 mm (10% DOX), 8.1 ± 0.9 mm (20% DOX), and 11.5 ± 2.6 mm (30% DOX). The average inhibition zones on *L. casei* were 14.4 ± 0.5 mm (0.12% chlorhexidine), 5.1 ± 4.0 mm (10% DOX), 7.2 ± 3.7 mm (20% DOX), and 11.3 ± 1.8 mm (30% DOX). No inhibition zones were observed with SBMP, HNT, and sterile PBS. 0.12% chlorhexidine (CHX) and sterile PBS served as the positive and negative controls, respectively.

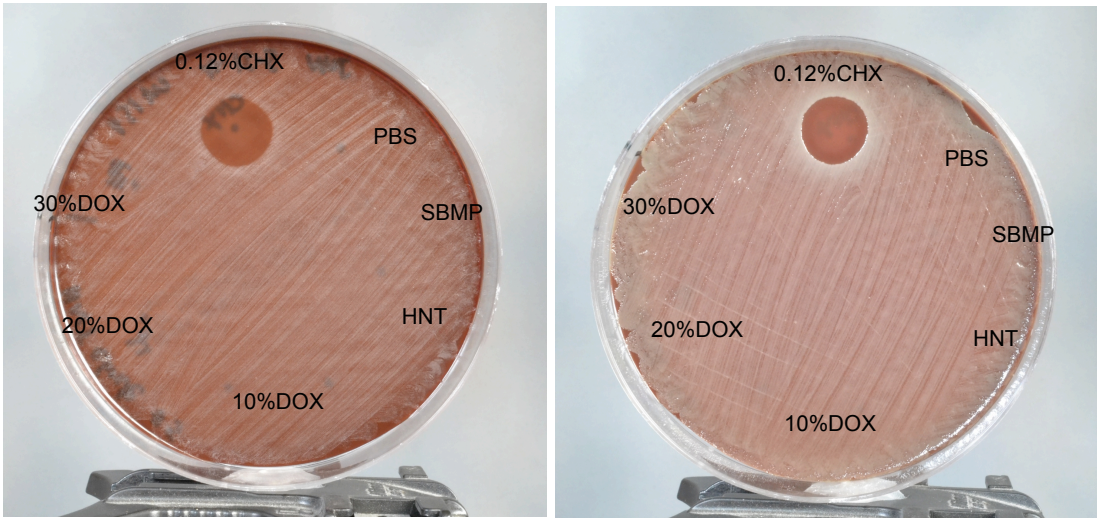

Figure 16. Representative images of agar diffusion test of adhesive disk eluates against *S. mutans* (left) and *L. casei* (right) at 72 h of incubation.

The average inhibition zones of 0.12% chlorhexidine on *S. mutans* and *L. casei* were 15.5 ± 1.5 mm and 13.4 ± 1.6 mm, respectively. No inhibition zone was observed with other samples. 0.12% chlorhexidine (CHX) and sterile PBS served as the positive and negative controls, respectively.

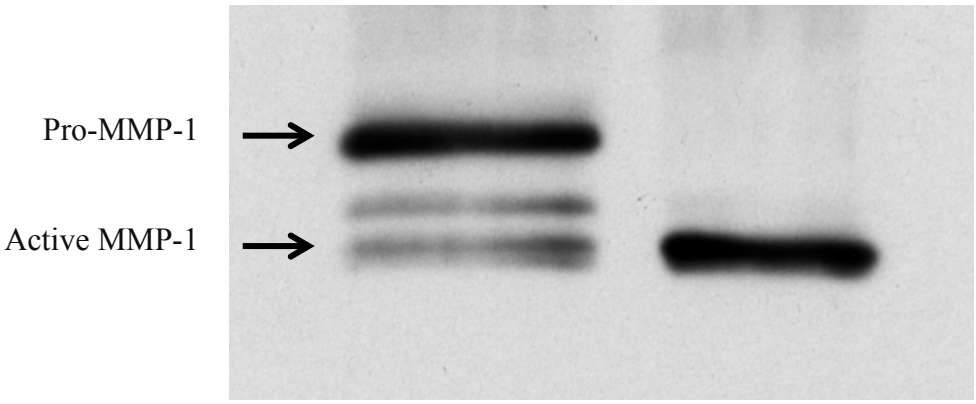

Figure 17. Western blot analysis of unactivated MMP-1 (left) and APMA activated MMP-1 (right).

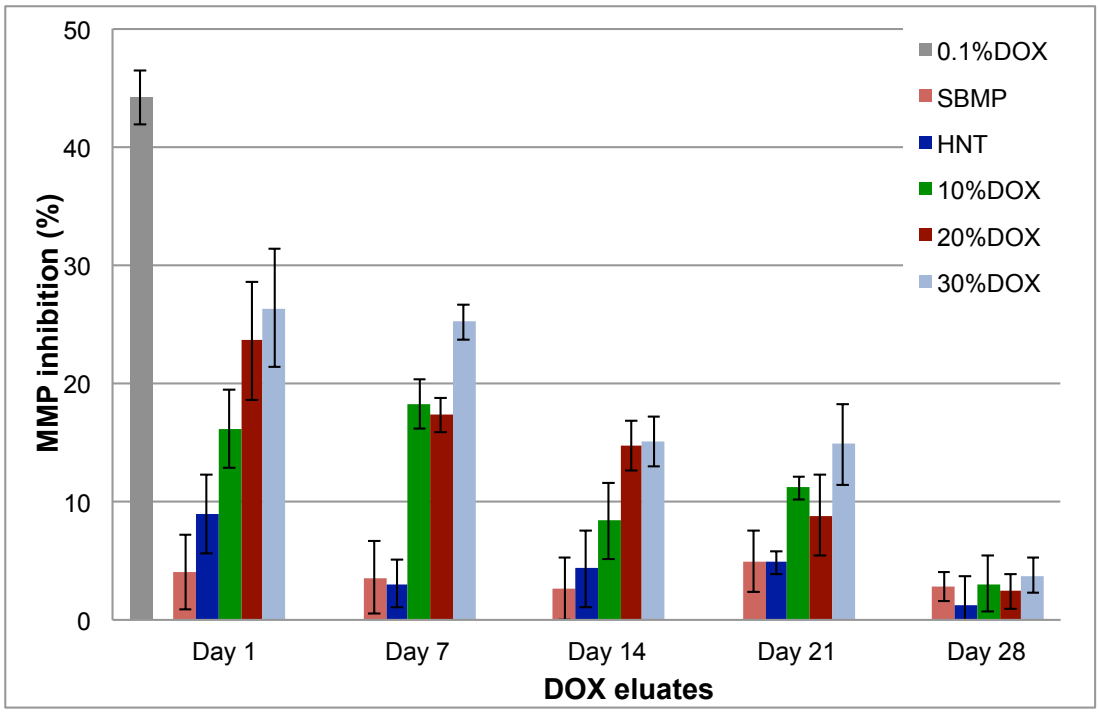

Figure 18. Inhibition of MMP-1 by doxycycline containing eluates (%, mean ± SE) compared to that by the negative control (Tris buffer), and the positive control (0.1% doxycycline solution). Statistical analysis showed significant difference between 0.1% doxycycline and each of the samples from various time points. At day 1, eluates of 30% DOX showed significantly higher MMP inhibition than those of control (SBMP, $p < 0.05$). At day 7, eluates of 10% DOX and 30% DOX showed significantly higher MMP inhibition than those of control (SBMP) and HNT ($p < 0.05$). No other significant differences in MMP-1 inhibition among other eluates were found ($p > 0.05$). The negative control (Tris buffer) was 50 mM Tris with 0.2 M NaCl, 10 mM $CaCl_2$, and 1 μM $ZnCl_2$, pH 7.4).

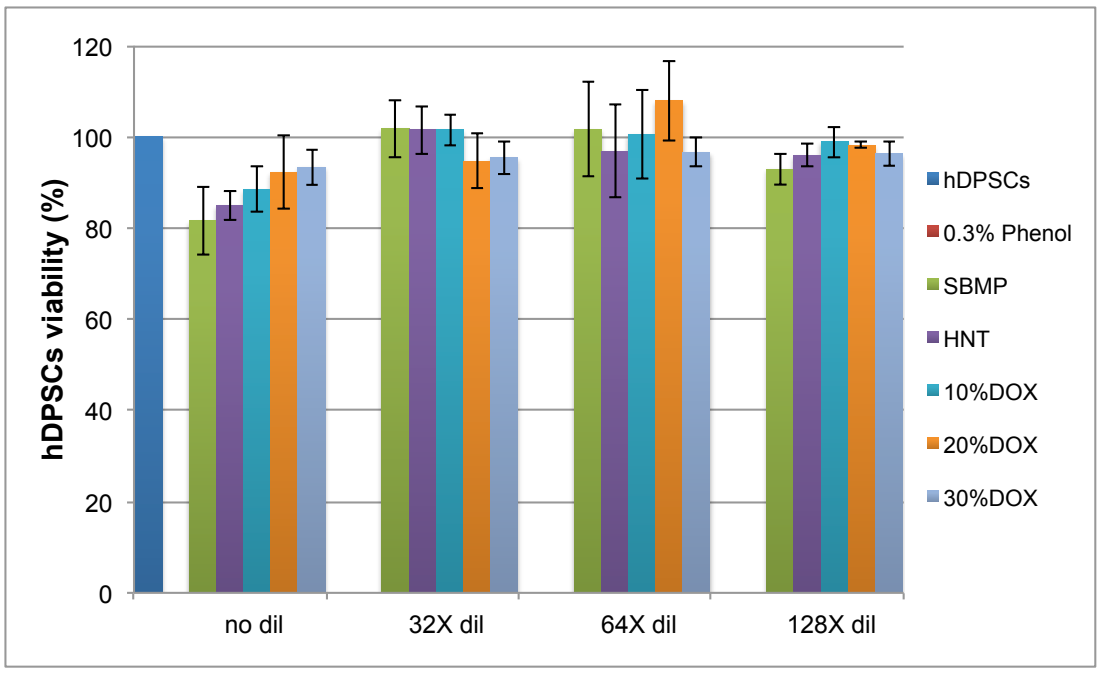

Figure 19. Viability of human dental pulp stem cells (hDPSCs, %). hDPSCs were exposed to eluates of the control (SBMP) and modified adhesive disks. The viability of the cells incubated with various eluates ranged from 81.60% to 107.92% compared to that of the cells not incubated with eluate (100% survival). Cells incubated with 0.3% phenol serving as the negative control (total cell death) showed 0% viability. No significant differences were found among cells incubated with eluates of the same dilution of each group of samples compared with cells that were not incubated with eluates (100% survival, $p > 0.05$).

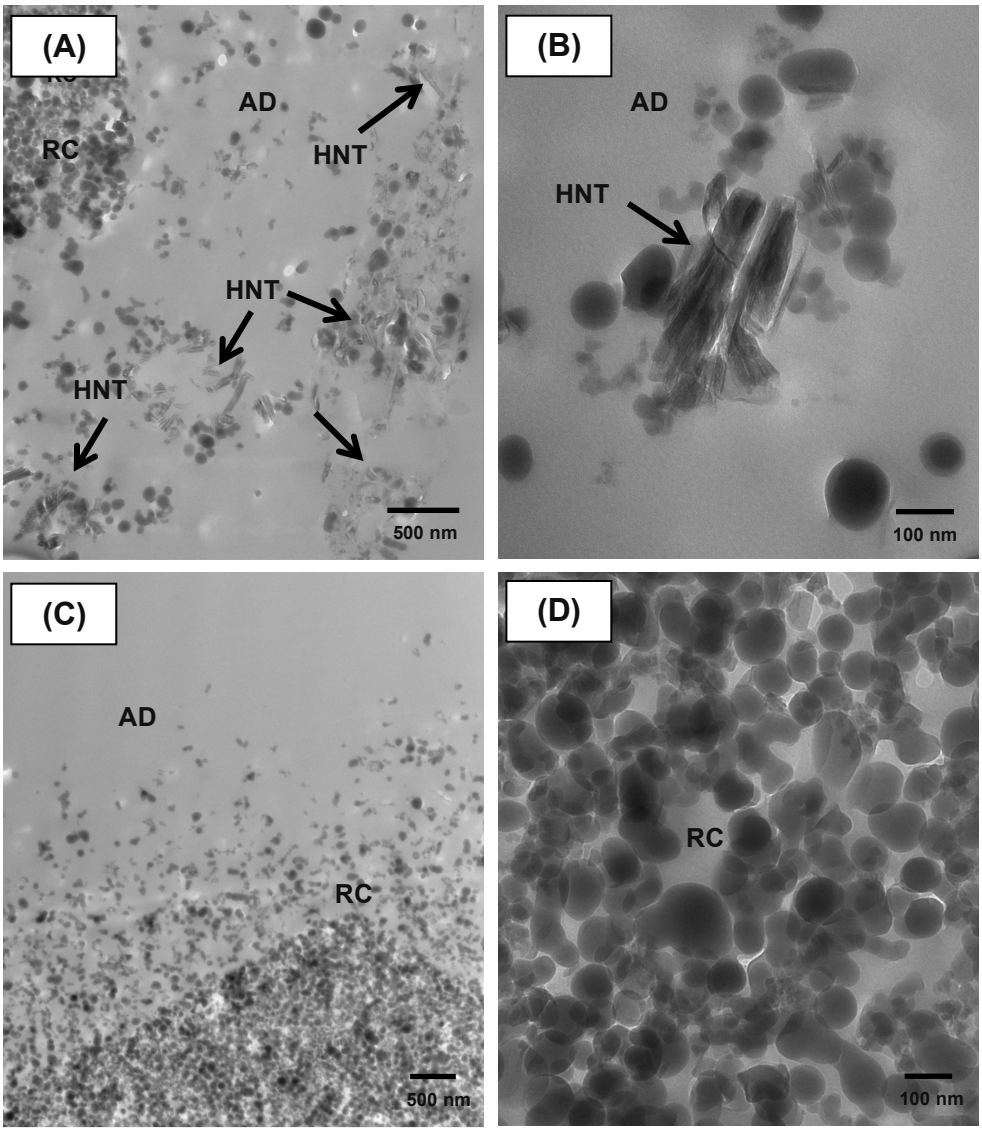

Figure 20. Transmission electron micrographs (HV=80kV) of the interface between resin composite and HNT modified adhesive at 20,000× (A), 120000× (B); and resin composite and SBMP at 18,500× (C), 98,000× (D). RC: Resin composite, AD: Dental adhesive, HNT: Halloysite nanotubes.

REFERENCES

Al-Ahmad A, Ameen H, Pelz K, Karygianni L, Wittmer A, Anderson AC *et al.* (2014). Antibiotic resistance and capacity for biofilm formation of different bacteria isolated from endodontic infections associated with root-filled teeth. *J Endod* 40(2)*:*223-230.

Almahdy A, Koller G, Sauro S, Bartsch JW, Sherriff M, Watson TF *et al.* (2012). Effects of MMP inhibitors incorporated within dental adhesives. *J Dent Res* 91(6)*:*605-611.

Ariga K, Lvov YM, Kawakami K, Ji Q, Hill JP (2011). Layer-by-layer self-assembled shells for drug delivery. *Adv Drug Deliv Rev* 63(9)*:*762-771.

Armstrong SR, Keller JC, Boyer DB (2001). The influence of water storage and C-factor on the dentin-resin composite microtensile bond strength and debond pathway utilizing a filled and unfilled adhesive resin. *Dent Mater* 17(3)*:*268-276.

Armstrong SR, Vargas MA, Fang Q, Laffoon JE (2003). Microtensile bond strength of a total-etch 3-step, total-etch 2-step, self-etch 2-step, and a self-etch 1-step dentin bonding system through 15-month water storage. *J Adhes Dent* 5(1)*:*47-56.

Armstrong SR, Vargas MA, Chung I, Pashley DH, Campbell JA, Laffoon JE *et al.* (2004). Resin-dentin interfacial ultrastructure and microtensile dentin bond strength after five-year water storage. *Oper Dent* 29(6)*:*705-712.

Birkedal-Hansen H, Yamada S, Windsor J, Poulsen AH, Lyons G, Stetler-Stevenson W *et al.* (2003). Matrix metalloproteinases. *Curr Protoc Cell Biol* Chapter 10(Unit 10 18.

Bottino MC, Batarseh G, Palasuk J, Alkatheeri MS, Windsor LJ, Platt JA (2013). Nanotube-modified dentin adhesive--physicochemical and dentin bonding characterizations. *Dent Mater* 29(11)*:*1158-1165.

Bourbia M, Ma D, Cvitkovitch DG, Santerre JP, Finer Y (2013). Cariogenic bacteria degrade dental resin composites and adhesives. *J Dent Res* 92(11)*:*989-994.

Breschi L, Mazzoni A, Ruggeri A, Cadenaro M, Di Lenarda R, De Stefano Dorigo E (2008). Dental adhesion review: aging and stability of the bonded interface. *Dent Mater* 24(1)*:*90-101.

Breschi L, Martin P, Mazzoni A, Nato F, Carrilho M, Tjaderhane L *et al.* (2010). Use of a specific MMP-inhibitor (galardin) for preservation of hybrid layer. *Dent Mater* 26(6)*:*571-578.

Buonocore MG (1955). A simple method of increasing the adhesion of acrylic filling materials to enamel surfaces. *J Dent Res* 34(6)*:*849-853.

Carrilho MR, Geraldeli S, Tay F, de Goes MF, Carvalho RM, Tjaderhane L *et al.* (2007). In vivo preservation of the hybrid layer by chlorhexidine. *J Dent Res* 86(6)*:*529-533.

Carvalho RM, Chersoni S, Frankenberger R, Pashley DH, Prati C, Tay FR (2005). A challenge to the conventional wisdom that simultaneous etching and resin infiltration always occurs in self-etch adhesives. *Biomaterials* 26(9)*:*1035-1042.

Centlivre M, Zhou X, Pouw SM, Weijer K, Kleibeuker W, Das AT *et al.* (2010). Autoregulatory lentiviral vectors allow multiple cycles of doxycycline-inducible gene expression in human hematopoietic cells in vivo. *Gene Ther* 17(1)*:*14-25.

Chen Q, Zhao Y, Wu W, Xu T, Fong H (2012). Fabrication and evaluation of Bis-GMA/TEGDMA dental resins/composites containing halloysite nanotubes. *Dent Mater* 28(10)*:*1071-1079.

Conde MC, Zanchi CH, Rodrigues-Junior SA, Carreno NL, Ogliari FA, Piva E (2009). Nanofiller loading level: Influence on selected properties of an adhesive resin. *J Dent* 37(5)*:*331-335.

Dahl JE, Frangou-Polyzois MJ, Polyzois GL (2006). In vitro biocompatibility of denture relining materials. *Gerodontology* 23(1)*:*17-22.

De Munck J, Van Meerbeek B, Yoshida Y, Inoue S, Vargas M, Suzuki K *et al.* (2003). Four-year water degradation of total-etch adhesives bonded to dentin. *J Dent Res* 82(2)*:*136-140.

De Munck J, Van Landuyt K, Peumans M, Poitevin A, Lambrechts P, Braem M *et al.* (2005). A critical review of the durability of adhesion to tooth tissue: methods and results. *J Dent Res* 84(2)*:*118-132.

De Munck J, Mine A, Poitevin A, Van Ende A, Cardoso MV, Van Landuyt KL *et al.* (2012). Meta-analytical review of parameters involved in dentin bonding. *J Dent Res* 91(4)*:*351-357.

Dickinson DP (2002). Cysteine peptidases of mammals: their biological roles and potential effects in the oral cavity and other tissues in health and disease. *Crit Rev Oral Biol Med* 13(3)*:*238-275.

Dutra-Correa M, Saraceni CH, Ciaramicoli MT, Kiyan VH, Queiroz CS (2013). Effect of chlorhexidine on the 18-month clinical performance of two adhesives. *J Adhes Dent* 15(3)*:*287-292.

Feitosa SA, Palasuk J, Kamocki K, Geraldeli S, Gregory RL, Platt JA *et al.* (2014). Doxycycline-encapsulated nanotube-modified dentin adhesives. *J Dent Res* 93(12)*:*1270-1276.

Ferracane JL (1985). Correlation between hardness and degree of conversion during the setting reaction of unfilled dental restorative resins. *Dent Mater* 1(1)*:*11-14.

Finer Y, Santerre JP (2003). Biodegradation of a dental composite by esterases: dependence on enzyme concentration and specificity. *J Biomater Sci Polym Ed* 14(8)*:*837-849.

Finer Y, Santerre JP (2004). The influence of resin chemistry on a dental composite's biodegradation. *J Biomed Mater Res A* 69(2)*:*233-246.

Fukushima T, Inoue Y, Miyazaki K, Itoh T (2001). Effect of primers containing N-methylolacrylamide or N-methylolmethacrylamide on dentin bond durability of a resin composite after 5 years. *J Dent* 29(3)*:*227-234.

Garnero P, Borel O, Byrjalsen I, Ferreras M, Drake FH, McQueney MS *et al.* (1998). The collagenolytic activity of cathepsin K is unique among mammalian proteinases. *J Biol Chem* 273(48)*:*32347-32352.

Giannobile WV (2008). Host-response therapeutics for periodontal diseases. *J Periodontol* 79(8 Suppl)*:*1592-1600.

Gonçalves PF, Sallum EA, Sallum AW, Casati MrZ, Toledo Srd, Junior FHN (2005). Dental cementum reviewed: development, structure, composition, regeneration and potential functions. *Braz J Oral Sci* 4(12)*:*651-658.

Goracci G, Mori G, Baldi M (1999). Terminal end of the human odontoblast process: a study using SEM and confocal microscopy. *Clin Oral Investig* 3(3)*:*126-132.

Greenstein G (1995). Clinical significance of bacterial resistance to tetracyclines in the treatment of periodontal diseases. *J Periodontol* 66(11)*:*925-932.

Gregson KS, Terrence O'Neill J, Platt JA, Jack Windsor L (2008). In vitro induction of hydrolytic activity in human gingival and pulp fibroblasts by triethylene glycol dimethacrylate and monocyte chemotatic protein-1. *Dent Mater* 24(11)*:*1461-1467.

Gregson KS, Jack Windsor L, Platt JA (2009). Biodegradation of a dental resin material by fibroblast conditioned media. *Dent Mater* 25(11)*:*1358-1362.

Gu Y, Walker C, Ryan ME, Payne JB, Golub LM (2012). Non-antibacterial tetracycline formulations: clinical applications in dentistry and medicine. *J Oral Microbiol* 4(

Guimaraes L, Enyashin AN, Seifert G, Duarte HA (2010). Structural, Electronic, and Mechanical Properties of Single-Walled Halloysite Nanotube Models. *J Phys Chem* 114(26)*:*11358-11363.

Hall R, Septier D, Embery G, Goldberg M (1999). Stromelysin-1 (MMP-3) in forming enamel and predentine in rat incisor-coordinated distribution with proteoglycans suggests a functional role. *Histochem J* 31(12)*:*761-770.

Hansel C, Leyhausen G, Mai UE, Geurtsen W (1998). Effects of various resin composite (co)monomers and extracts on two caries-associated micro-organisms in vitro. *J Dent Res* 77(1)*:*60-67.

Heikinheimo K, Salo T (1995). Expression of basement membrane type IV collagen and type IV collagenases (MMP-2 and MMP-9) in human fetal teeth. *J Dent Res* 74(5)*:*1226-1234.

Holmes NE, Charles PG (2009). Safety and Efficacy Review of Doxycycline. *Clin Med Insights Ther* 1(1)*:*471-482.

Humphrey SP, Williamson RT (2001). A review of saliva: normal composition, flow, and function. *J Prosthet Dent* 85(2)*:*162-169.

Imazato S, Kinomoto Y, Tarumi H, Ebisu S, Tay FR (2003). Antibacterial activity and bonding characteristics of an adhesive resin containing antibacterial monomer MDPB. *Dent Mater* 19(4)*:*313-319.

Jaffer F, Finer Y, Santerre JP (2002). Interactions between resin monomers and commercial composite resins with human saliva derived esterases. *Biomaterials* 23(7)*:*1707-1719.

Jokstad A, Bayne S, Blunck U, Tyas M, Wilson N (2001). Quality of dental restorations. FDI Commission Project 2-95. *Int Dent J* 51(3)*:*117-158.

Kanca J, 3rd (1992). Improving bond strength through acid etching of dentin and bonding to wet dentin surfaces. *J Am Dent Assoc* 123(9)*:*35-43.

Kermanshahi S, Santerre JP, Cvitkovitch DG, Finer Y (2010). Biodegradation of resin-dentin interfaces increases bacterial microleakage. *J Dent Res* 89(9)*:*996-1001.

Khalichi P, Cvitkovitch DG, Santerre JP (2004). Effect of composite resin biodegradation products on oral streptococcal growth. *Biomaterials* 25(24)*:*5467-5472.

Khalichi P, Singh J, Cvitkovitch DG, Santerre JP (2009). The influence of triethylene glycol derived from dental composite resins on the regulation of Streptococcus mutans gene expression. *Biomaterials* 30(4)*:*452-459.

Khamverdi Z, Rezaei-Soufi L, Rostamzadeh T (2015). The Effect of Epigallocatechin Gallate on the Dentin Bond Durability of Two Self-etch Adhesives. *J Dent (Shiraz)* 16(2)*:*68-74.

Kim JS, Cho BH, Lee IB, Um CM, Lim BS, Oh MH *et al.* (2005). Effect of the hydrophilic nanofiller loading on the mechanical properties and the microtensile bond strength of an ethanol-based one-bottle dentin adhesive. *J Biomed Mater Res B Appl Biomater* 72(2)*:*284-291.

Kogawa AC, Salgado HRN (2012). Doxycycline hyclate: A review of properties, applications and analytical methods. *Int J Life Sci Pharma Res* 2(4)*:*11-25.

Koibuchi H, Yasuda N, Nakabayashi N (2001). Bonding to dentin with a self-etching primer: the effect of smear layers. *Dent Mater* 17(2)*:*122-126.

Li X, Liu W, Sun L, Aifantis KE, Yu B, Fan Y *et al.* (2014). Resin composites reinforced by nanoscaled fibers or tubes for dental regeneration. *Biomed Res Int* 2014(542958.

Liu Y, Tjaderhane L, Breschi L, Mazzoni A, Li N, Mao J *et al.* (2011). Limitations in bonding to dentin and experimental strategies to prevent bond degradation. *J Dent Res* 90(8)*:*953-968.

Llano E, Pendas AM, Knauper V, Sorsa T, Salo T, Salido E *et al.* (1997). Identification and structural and functional characterization of human enamelysin (MMP-20). *Biochemistry* 36(49)*:*15101-15108.

Loguercio AD, Moura SK, Pellizzaro A, Dal-Bianco K, Patzlaff RT, Grande RH *et al.* (2008). Durability of enamel bonding using two-step self-etch systems on ground and unground enamel. *Oper Dent* 33(1)*:*79-88.

Lohbauer U, Nikolaenko SA, Petschelt A, Frankenberger R (2008). Resin tags do not contribute to dentin adhesion in self-etching adhesives. *J Adhes Dent* 10(2)*:*97-103.

Lohbauer U, Wagner A, Belli R, Stoetzel C, Hilpert A, Kurland HD *et al.* (2010). Zirconia nanoparticles prepared by laser vaporization as fillers for dental adhesives. *Acta Biomater* 6(12)*:*4539-4546.

Luo Z, Song H, Feng X, Run M, Cui H, Wu L *et al.* (2013). Liquid crystalline phase behavior and sol-gel transition in aqueous halloysite nanotube dispersions. *Langmuir* 29(40)*:*12358-12366.

Lvov Y, Aerov A, Fakhrullin R (2014). Clay nanotube encapsulation for functional biocomposites. *Adv Colloid Interface Sci* 207(189-198.

Lvov YM, Shchukin DG, Mohwald H, Price RR (2008). Halloysite clay nanotubes for controlled release of protective agents. *ACS Nano* 2(5)*:*814-820.

Mach L, Mort JS, Glossl J (1994). Maturation of human procathepsin B. Proenzyme activation and proteolytic processing of the precursor to the mature proteinase, in vitro, are primarily unimolecular processes. *J Biol Chem* 269(17)*:*13030-13035.

Manhart J, Chen H, Hamm G, Hickel R (2004). Buonocore Memorial Lecture. Review of the clinical survival of direct and indirect restorations in posterior teeth of the permanent dentition. *Oper Dent* 29(5)*:*481-508.

Martin-De Las Heras S, Valenzuela A, Overall CM (2000). The matrix metalloproteinase gelatinase A in human dentine. *Arch Oral Biol* 45(9)*:*757-765.

Mazzoni A, Breschi L, Carrilho M, Nascimento FD, Orsini G, Ruggeri Jr A *et al.* (2009). A review of the nature, role, and function of dentin non-collagenous proteins. Part II: enzymes, serum proteins, and growth factors. *Endod Top* 21(1)*:*19-40.

Mazzoni A, Papa V, Nato F, Carrilho M, Tjaderhane L, Ruggeri A, Jr. *et al.* (2011). Immunohistochemical and biochemical assay of MMP-3 in human dentine. *J Dent* 39(3)*:*231-237.

Mazzoni A, Nascimento FD, Carrilho M, Tersariol I, Papa V, Tjaderhane L *et al.* (2012). MMP activity in the hybrid layer detected with in situ zymography. *J Dent Res* 91(5)*:*467-472.

Mazzoni A, Scaffa P, Carrilho M, Tjaderhane L, Di Lenarda R, Polimeni A *et al.* (2013). Effects of etch-and-rinse and self-etch adhesives on dentin MMP-2 and MMP-9. *J Dent Res* 92(1)*:*82-86.

Mazzoni A, Apolonio FM, Saboia VP, Santi S, Angeloni V, Checchi V *et al.* (2014). Carbodiimide inactivation of MMPs and effect on dentin bonding. *J Dent Res* 93(3)*:*263-268.

Mazzoni A, Tjaderhane L, Checchi V, Di Lenarda R, Salo T, Tay FR *et al.* (2015). Role of dentin MMPs in caries progression and bond stability. *J Dent Res* 94(2)*:*241-251.

Metzger Z, Belkin D, Kariv N, Dotan M, Kfir A (2008). Low-dose doxycycline inhibits bone resorption associated with apical periodontitis. *Int Endod J* 41(4)*:*303-309.

Miyazaki M, Ando S, Hinoura K, Onose H, Moore BK (1995). Influence of filler addition to bonding agents on shear bond strength to bovine dentin. *Dent Mater* 11(4)*:*234-238.

Mjor IA, Nordahl I (1996). The density and branching of dentinal tubules in human teeth. *Arch Oral Biol* 41(5)*:*401-412.

Mjor IA, Moorhead JE, Dahl JE (2000). Reasons for replacement of restorations in permanent teeth in general dental practice. *Int Dent J* 50(6)*:*361-366.

Montagner AF, Sarkis-Onofre R, Pereira-Cenci T, Cenci MS (2014). MMP Inhibitors on Dentin Stability: A Systematic Review and Meta-analysis. *J Dent Res* 93(8)*:*733-743.

Nagase H, Visse R, Murphy G (2006). Structure and function of matrix metalloproteinases and TIMPs. *Cardiovasc Res* 69(3)*:*562-573.

Nakabayashi N, Kojima K, Masuhara E (1982). The promotion of adhesion by the infiltration of monomers into tooth substrates. *J Biomed Mater Res* 16(3)*:*265-273.

Nascimento FD, Minciotti CL, Geraldeli S, Carrilho MR, Pashley DH, Tay FR *et al.* (2011). Cysteine cathepsins in human carious dentin. *J Dent Res* 90(4)*:*506-511.

Nishitani Y, Yoshiyama M, Wadgaonkar B, Breschi L, Mannello F, Mazzoni A *et al.* (2006). Activation of gelatinolytic/collagenolytic activity in dentin by self-etching adhesives. *Eur J Oral Sci* 114(2)*:*160-166.

Obermajer N, Jevnikar Z, Doljak B, Kos J (2008). Role of cysteine cathepsins in matrix degradation and cell signalling. *Connect Tissue Res* 49(3)*:*193-196.

Palasuk J, Kamocki K, Hippenmeyer L, Platt JA, Spolnik KJ, Gregory RL *et al.* (2014). Bimix antimicrobial scaffolds for regenerative endodontics. *J Endod* 40(11)*:*1879-1884.

Pallan S, Furtado Araujo MV, Cilli R, Prakki A (2012). Mechanical properties and characteristics of developmental copolymers incorporating catechin or chlorhexidine. *Dent Mater* 28(6)*:*687-694.

Pallasch TJ (2003). Antibiotic resistance. *Dent Clin North Am* 47(4)*:*623-639.

Palosaari H, Wahlgren J, Larmas M, Ronka H, Sorsa T, Salo T *et al.* (2000). The expression of MMP-8 in human odontoblasts and dental pulp cells is down-regulated by TGF-beta1. *J Dent Res* 79(1)*:*77-84.

Palosaari H, Ding Y, Larmas M, Sorsa T, Bartlett JD, Salo T *et al.* (2002). Regulation and interactions of MT1-MMP and MMP-20 in human odontoblasts and pulp tissue in vitro. *J Dent Res* 81(5)*:*354-359.

Pashley DH, Tay FR, Breschi L, Tjaderhane L, Carvalho RM, Carrilho M *et al.* (2011). State of the art etch-and-rinse adhesives. *Dent Mater* 27(1)*:*1-16.

Patel BK, Parikh RH, Aboti PS (2013). Development of Oral Sustained Release Rifampicin Loaded Chitosan Nanoparticles by Design of Experiment. *Drug Deliv:*1-10.

Petersen PE, Lennon MA (2004). Effective use of fluorides for the prevention of dental caries in the 21st century: the WHO approach. *Community Dent Oral Epidemiol* 32(5)*:*319-321.

Peumans M, Kanumilli P, De Munck J, Van Landuyt K, Lambrechts P, Van Meerbeek B (2005). Clinical effectiveness of contemporary adhesives: a systematic review of current clinical trials. *Dent Mater* 21(9)*:*864-881.

Prakasam A, Elavarasu SS, Natarajan RK (2012). Antibiotics in the management of aggressive periodontitis. *J Pharm Bioallied Sci* 4(Suppl 2)*:*S252-255.

Prati C, Chersoni S, Mongiorgi R, Pashley DH (1998). Resin-infiltrated dentin layer formation of new bonding systems. *Oper Dent* 23(4)*:*185-194.

Qi R, Guo R, Shen M, Cao X, Zhang L, Xu J *et al.* (2010). Electrospun poly(lactic-co-glycolic acid)/halloysite nanotube composite nanofibers for drug encapsulation and sustained release. *J Mater Chem* 20(10622-10629.

Qi R, Cao X, Shen M, Guo R, Yu J, Shi X (2012). Biocompatibility of electrospun halloysite nanotube-doped poly(lactic-co-glycolic acid) composite nanofibers. *J Biomater Sci Polym Ed* 23(1-4)*:*299-313.

Qi R, Guo R, Zheng F, Liu H, Yu J, Shi X (2013). Controlled release and antibacterial activity of antibiotic-loaded electrospun halloysite/poly(lactic-co-glycolic acid) composite nanofibers. *Colloids Surf B Biointerfaces* 110(1)*:*148-155.

Reis A, de Carvalho Cardoso P, Vieira LC, Baratieri LN, Grande RH, Loguercio AD (2008). Effect of prolonged application times on the durability of resin-dentin bonds. *Dent Mater* 24(5)*:*639-644.

Ricci HA, Sanabe ME, de Souza Costa CA, Pashley DH, Hebling J (2010). Chlorhexidine increases the longevity of in vivo resin-dentin bonds. *Eur J Oral Sci* 118(4)*:*411-416.

Roberson TM, Heymann HO, Swift EJ (2006). Sturdevant's art and science of operative dentistry. 5th ed. St. Louis, MO: Mosby.

Rosa WL, Piva E, Silva AF (2015). Bond strength of universal adhesives: A systematic review and meta-analysis. *J Dent* 43(7)*:*765-776.

Sadat-Shojai M, Atai M, Nodehi A, Khanlar LN (2010). Hydroxyapatite nanorods as novel fillers for improving the properties of dental adhesives: Synthesis and application. *Dent Mater* 26(5)*:*471-482.

Sakaguchi RL, Powers JM (2012). Craig's restorative dental materials. 13th ed. Philadelphia, PA: Elsevier Mosby.

Sano H, Takatsu T, Ciucchi B, Horner JA, Matthews WG, Pashley DH (1995a). Nanoleakage: leakage within the hybrid layer. *Oper Dent* 20(1)*:*18-25.

Sano H, Yoshiyama M, Ebisu S, Burrow MF, Takatsu T, Ciucchi B *et al.* (1995b). Comparative SEM and TEM observations of nanoleakage within the hybrid layer. *Oper Dent* 20(4)*:*160-167.

Sano H (2006). Microtensile testing, nanoleakage, and biodegradation of resin-dentin bonds. *J Dent Res* 85(1)*:*11-14.

Santiago SL, Osorio R, Neri JR, Carvalho RM, Toledano M (2013). Effect of the flavonoid epigallocatechin-3-gallate on resin-dentin bond strength. *J Adhes Dent* 15(6)*:*535-540.

Sartori N, Stolf SC, Silva SB, Lopes GC, Carrilho M (2013). Influence of chlorhexidine digluconate on the clinical performance of adhesive restorations: a 3-year follow-up. *J Dent* 41(12)*:*1188-1195.

Sbardella D, Fasciglione GF, Gioia M, Ciaccio C, Tundo GR, Marini S *et al.* (2012). Human matrix metalloproteinases: an ubiquitarian class of enzymes involved in several pathological processes. *Mol Aspects Med* 33(2)*:*119-208.

Seleem MN, Jain N, Pothayee N, Ranjan A, Riffle JS, Sriranganathan N (2009). Targeting Brucella melitensis with polymeric nanoparticles containing streptomycin and doxycycline. *FEMS Microbiol Lett* 294(1)*:*24-31.

Sgolastra F, Petrucci A, Gatto R, Giannoni M, Monaco A (2011). Long-term efficacy of subantimicrobial-dose doxycycline as an adjunctive treatment to scaling and root planing: a systematic review and meta-analysis. *J Periodontol* 82(11)*:*1570-1581.

Shchukin DG, Sukhorukov GB, Price RR, Lvov YM (2005). Halloysite nanotubes as biomimetic nanoreactors. *Small* 1(5)*:*510-513.

Shchukin DG, Möhwald H (2007). Surface-engineered Nano- containers for Entrapment of Corrosion Inhibitors. *Adv Funct Mater* 17(9)*:*1451-1458.

Shokati B, Tam LE, Santerre JP, Finer Y (2010). Effect of salivary esterase on the integrity and fracture toughness of the dentin-resin interface. *J Biomed Mater Res B Appl Biomater* 94(1)*:*230-237.

Shono Y, Terashita M, Shimada J, Kozono Y, Carvalho RM, Russell CM *et al.* (1999). Durability of resin-dentin bonds. *J Adhes Dent* 1(3)*:*211-218.

Singh J, Khalichi P, Cvitkovitch DG, Santerre JP (2009). Composite resin degradation products from BisGMA monomer modulate the expression of genes associated with biofilm formation and other virulence factors in Streptococcus mutans. *J Biomed Mater Res A* 88(2)*:*551-560.

Solhi L, Atai M, Nodehi A, Imani M (2012). A novel dentin bonding system containing poly(methacrylic acid) grafted nanoclay: synthesis, characterization and properties. *Dent Mater* 28(10)*:*1041-1050.

Song F, Windsor LJ (2005). Novel nonmatrix-metalloproteinase-mediated collagen degradation. *Biochim Biophys Acta* 1721(1-3)*:*65-72.

Song F, Wisithphrom K, Zhou J, Windsor LJ (2006). Matrix metalloproteinase dependent and independent collagen degradation. *Front Biosci* 11(3100-3120.

Stanislawczuk R, Pereira F, Munoz MA, Luque I, Farago PV, Reis A *et al.* (2014). Effects of chlorhexidine-containing adhesives on the durability of resin-dentine interfaces. *J Dent* 42(1)*:*39-47.

Strickman D, Sheer T, Salata K, Hershey J, Dasch G, Kelly D *et al.* (1995). In vitro effectiveness of azithromycin against doxycycline-resistant and -susceptible strains of Rickettsia tsutsugamushi, etiologic agent of scrub typhus. *Antimicrob Agents Chemother* 39(11)*:*2406-2410.

Sulkala M, Larmas M, Sorsa T, Salo T, Tjaderhane L (2002). The localization of matrix metalloproteinase-20 (MMP-20, enamelysin) in mature human teeth. *J Dent Res* 81(9)*:*603-607.

Sulkala M, Tervahartiala T, Sorsa T, Larmas M, Salo T, Tjaderhane L (2007). Matrix metalloproteinase-8 (MMP-8) is the major collagenase in human dentin. *Arch Oral Biol* 52(2)*:*121-127.

Summitt JB, Robbins JW, Hilton TJ, Schwartz RS, Jr. JDS (2006). Fundamentals of Operative Dentistry: A Contemporary Approach. 3rd ed. Chicago: Quintessence.

Tallant C, Marrero A, Gomis-Ruth FX (2010). Matrix metalloproteinases: fold and function of their catalytic domains. *Biochim Biophys Acta* 1803(1)*:*20-28.

Talungchit S, Jessop JL, Cobb DS, Qian F, Geraldeli S, Pashley DH *et al.* (2014). Ethanol-wet bonding and chlorhexidine improve resin-dentin bond durability: quantitative analysis using raman spectroscopy. *J Adhes Dent* 16(5)*:*441-450.

Tan KR, Magill AJ, Parise ME, Arguin PM, Centers for Disease C, Prevention (2011). Doxycycline for malaria chemoprophylaxis and treatment: report from the CDC expert meeting on malaria chemoprophylaxis. *Am J Trop Med Hyg* 84(4)*:*517-531.

Tay FR, Carvalho R, Sano H, Pashley DH (2000). Effect of smear layers on the bonding of a self-etching primer to dentin. *J Adhes Dent* 2(2)*:*99-116.

Tay FR, Pashley DH, Yoshiyama M (2002). Two modes of nanoleakage expression in single-step adhesives. *J Dent Res* 81(7)*:*472-476.

Tay FR, Pashley DH, Garcia-Godoy F, Yiu CK (2004). Single-step, self-etch adhesives behave as permeable membranes after polymerization. Part II. Silver tracer penetration evidence. *Am J Dent* 17(5)*:*315-322.

Tersariol IL, Geraldeli S, Minciotti CL, Nascimento FD, Paakkonen V, Martins MT *et al.* (2010). Cysteine cathepsins in human dentin-pulp complex. *J Endod* 36(3)*:*475-481.

Tezvergil-Mutluay A, Agee KA, Uchiyama T, Imazato S, Mutluay MM, Cadenaro M *et al.* (2011). The inhibitory effects of quaternary ammonium methacrylates on soluble and matrix-bound MMPs. *J Dent Res* 90(4)*:*535-540.

Tjaderhane L, Salo T, Larjava H, Larmas M, Overall CM (1998). A novel organ culture method to study the function of human odontoblasts in vitro: gelatinase expression by odontoblasts is differentially regulated by TGF-beta1. *J Dent Res* 77(7)*:*1486-1496.

Tjaderhane L, Nascimento FD, Breschi L, Mazzoni A, Tersariol IL, Geraldeli S *et al.* (2013a). Strategies to prevent hydrolytic degradation of the hybrid layer-A review. *Dent Mater* 29(10)*:*999-1011.

Tjaderhane L, Nascimento FD, Breschi L, Mazzoni A, Tersariol IL, Geraldeli S *et al.* (2013b). Optimizing dentin bond durability: control of collagen degradation by matrix metalloproteinases and cysteine cathepsins. *Dent Mater* 29(1)*:*116-135.

Tjaderhane L, Buzalaf MA, Carrilho M, Chaussain C (2015). Matrix metalloproteinases and other matrix proteinases in relation to cariology: the era of 'dentin degradomics'. *Caries Res* 49(3)*:*193-208.

Van Landuyt KL, Yoshida Y, Hirata I, Snauwaert J, De Munck J, Okazaki M *et al.* (2008). Influence of the chemical structure of functional monomers on their adhesive performance. *J Dent Res* 87(8)*:*757-761.

Van Landuyt KL, Nawrot T, Geebelen B, De Munck J, Snauwaert J, Yoshihara K *et al.* (2011). How much do resin-based dental materials release? A meta-analytical approach. *Dent Mater* 27(8)*:*723-747.

Van Meerbeek B, De Munck J, Yoshida Y, Inoue S, Vargas M, Vijay P *et al.* (2003). Buonocore memorial lecture. Adhesion to enamel and dentin: current status and future challenges. *Oper Dent* 28(3)*:*215-235.

Van Meerbeek B, Peumans M, Poitevin A, Mine A, Van Ende A, Neves A *et al.* (2010). Relationship between bond-strength tests and clinical outcomes. *Dent Mater* 26(2)*:*e100-121.

Van Meerbeek B, Yoshihara K, Yoshida Y, Mine A, De Munck J, Van Landuyt KL (2011). State of the art of self-etch adhesives. *Dent Mater* 27(1)*:*17-28.

van Strijp AJ, Jansen DC, DeGroot J, ten Cate JM, Everts V (2003). Host-derived proteinases and degradation of dentine collagen in situ. *Caries Res* 37(1)*:*58-65.

Veerabadran NG, Mongayt D, Torchilin V, Price RR, Lvov YM (2009). Organized shells on clay nanotubes for controlled release of macromolecules. *Macromol Rapid Commun* 30(2)*:*99-103.

Vergaro V, Abdullayev E, Lvov YM, Zeitoun A, Cingolani R, Rinaldi R *et al.* (2010). Cytocompatibility and uptake of halloysite clay nanotubes. *Biomacromolecules* 11(3)*:*820-826.

Vidal CM, Tjaderhane L, Scaffa PM, Tersariol IL, Pashley D, Nader HB *et al.* (2014). Abundance of MMPs and cysteine cathepsins in caries-affected dentin. *J Dent Res* 93(3)*:*269-274.

Visse R, Nagase H (2003). Matrix metalloproteinases and tissue inhibitors of metalloproteinases: structure, function, and biochemistry. *Circ Res* 92(8)*:*827-839.

Vitalariu A, Caruntu ID, Bolintineanu S (2005). Morphological changes in dental pulp after the teeth preparation procedure. *Rom J Morphol Embryol* 46(2)*:*131-136.

Wang DY, Zhang L, Fan J, Li F, Ma KQ, Wang P *et al.* (2012). Matrix metalloproteinases in human sclerotic dentine of attrited molars. *Arch Oral Biol* 57(10)*:*1307-1312.

Wang J, Tekle E, Oubrahim H, Mieyal JJ, Stadtman ER, Chock PB (2003). Stable and controllable RNA interference: Investigating the physiological function of glutathionylated actin. *Proc Natl Acad Sci U S A* 100(9)*:*5103-5106.

Wang Y, Spencer P (2003). Hybridization efficiency of the adhesive/dentin interface with wet bonding. *J Dent Res* 82(2)*:*141-145.

Wang Y, Spencer P (2005). Continuing etching of an all-in-one adhesive in wet dentin tubules. *J Dent Res* 84(4)*:*350-354.

Wei W, Minullina R, Abdullayev E, Fakhrullin R, Millsa D, Lvov Y (2014). Enhanced efficiency of antiseptics with sustained release from clay nanotubes. *RSC Adv* 4(1)*:*488-494.

Windsor LJ, Bodden MK, Birkedal-Hansen B, Engler JA, Birkedal-Hansen H (1994). Mutational analysis of residues in and around the active site of human fibroblast-type collagenase. *J Biol Chem* 269(42)*:*26201-26207.

Windsor LJ, Steele DL, LeBlanc SB, Taylor KB (1997). Catalytic domain comparisons of human fibroblast-type collagenase, stromelysin-1, and matrilysin. *Biochim Biophys Acta* 1334(2-3):261-272.

Yah WO, Takahara A, Lvov YM (2012a). Selective modification of halloysite lumen with octadecylphosphonic acid: new inorganic tubular micelle. *J Am Chem Soc* 134(3):1853-1859.

Yah WO, Takahara A, Lvov YM (2012b). Selective Modification of Halloysite Lumen with Octadecylphosphonic Acid: New Inorganic Tubular Micelle. *J Am Chem Soc* 134(3):1853-1859.

Ye Y, Chen H, Wu J, Ye L (2007). High impact strength epoxy nanocomposites with natural nanotubes. *Polymer (Guildf)* 48(21):6426-6433.

Yoshida Y, Nagakane K, Fukuda R, Nakayama Y, Okazaki M, Shintani H *et al.* (2004). Comparative study on adhesive performance of functional monomers. *J Dent Res* 83(6):454-458.

Yoshiyama M, Carvalho R, Sano H, Horner J, Brewer PD, Pashley DH (1995). Interfacial morphology and strength of bonds made to superficial versus deep dentin. *Am J Dent* 8(6):297-302.

Yuan Y, Shimada Y, Ichinose S, Sadr A, Tagami J (2007). Effects of dentin characteristics on interfacial nanoleakage. *J Dent Res* 86(10)*:*1001-1006.

Zhang K, Cheng L, Imazato S, Antonucci JM, Lin NJ, Lin-Gibson S *et al.* (2013a). Effects of dual antibacterial agents MDPB and nano-silver in primer on microcosm biofilm, cytotoxicity and dentine bond properties. *J Dent* 41(5)*:*464-474.

Zhang K, Li F, Imazato S, Cheng L, Liu H, Arola DD *et al.* (2013b). Dual antibacterial agents of nano-silver and 12-methacryloyloxydodecylpyridinium bromide in dental adhesive to inhibit caries. *J Biomed Mater Res B Appl Biomater* 101(6)*:*929-938.

Zhang SC, Kern M (2009). The role of host-derived dentinal matrix metalloproteinases in reducing dentin bonding of resin adhesives. *Int J Oral Sci* 1(4)*:*163-176.

Zhang W, Song F, Windsor LJ (2010). Effects of tobacco and P. gingivalis on gingival fibroblasts. *J Dent Res* 89(5)*:*527-531.

CURRICULUM VITAE

Jadesada Palasuk

EDUCATION

Doctor of Philosophy (Ph.D. in Dental Science, 2016)

Indiana University, Indianapolis, IN, USA

Master of Science in Dentistry (M.S.D., Prosthodontics, 2010)

Indiana University, Indianapolis, IN, USA

Doctor of Dental Surgery (D.D.S., 2004)

Faculty of Dentistry, Chulalongkorn University, Bangkok, Thailand

APPOINTMENTS

Academic

Faculty member (Instructor, 2004-2007)

Faculty of Dentistry, Naresuan University, Phitsanulok, Thailand

Bench instructor (2010-2015)

Indiana University School of Dentistry, Indianapolis, IN, USA

Other

Dentist (private practice), Bangkok, Thailand

PEER-REVIEWED PUBLICATIONS

1. Palasuk J, Platt JA, Cho SD, Levon JA, Brown DT, Hovijitra ST. Effect of surface treatments on microtensile bond strength of repaired aged silorane resin composite. Oper Dent. 2013 Jan-Feb;38(1):91-9.
2. Bottino MC, Batarseh G, Palasuk J, Alkatheeri MS, Windsor LJ, Platt JA. Nanotube-modified dentin adhesive--physicochemical and dentin bonding characterizations. Dent Mater. 2013 Nov;29(11):1158-65.
3. Palasuk J, Kamocki K, Hippenmeyer L, Platt JA, Spolnik KJ, Gregory RL, Bottino MC. Bi-Mix Antimicrobial Scaffolds for Regenerative Endodontics. J Endod. 2014 Nov;40(11):1879-84.
4. Feitosa SA, Palasuk J, Kamocki K, Geraldeli S, Gregory RL, Platt JA, Windsor LJ, and Bottino MC. Doxycycline-Encapsulated Nanotube Modified Dentin Adhesive. J Dent Res. 2014 Dec;93(12):1270-6
5. Alkatheeri MS, Palasuk J, Eckert GJ, Platt JA, Bottino MC. Halloysite nanotube incorporation into adhesive systems-effect on bond strength to human dentin. Clin Oral Investig. 2015 Feb 10.
6. Kim-Park WK, Allam ES, Palasuk J, Kowolik M, Park KK, Windsor LJ. Green tea catechin inhibits the activity and neutrophil release of Matrix Metalloproteinase-9. J Tradit Complement Med.

CHAPTER

1. Allam ES, Feitosa SA, Palasuk J, Bottino MC, Windsor LJ. Chapter 2: Roles of matrix metalloproteinases in periodontal disease and dental caries. Book Title:

Matrix Metalloproteinases (MMPs): Classification, Molecular Mechanisms and Roles in Diseases. Nova Science Publishers.

AWARDS AND HONORS

1. Lester Furnas Scholarship Award (2008): Graduate prosthodontics program, Indiana University School of Dentistry, Indianapolis, IN, USA
2. Carl J. & Ida A. Andres Scholarship Award (2011): Graduate prosthodontics program, Indiana University School of Dentistry, Indianapolis, IN, USA

PUBLISHED ABSTRACTS (INTERNATIONAL)

1. Palasuk J, Platt JA. Effect of microtensile bond strength of repaired aged silorane resin composite. International Association of Dental Researches, 2011.
2. Palasuk J, Cho S, Platt J, Browning W. Nanofilled RMGI: Fracture Toughness, Surface Roughness and Gloss Testing. American Association of Dental Researches, 2012.
3. Palasuk J, Hippenmeyer L, Gregory RG, Platt JA, Spolnik KJ, Bottino MC. A Bi-Mix Antibacterial Drug-Delivery System for Regenerative Endodontics. International Association of Dental Researches, 2013.
4. Batarseh GS, Palasuk J, Platt JA, Windsor LJ, Bottino MC. A Novel Nanotube-Modified Dentin Bonding Agent. International Association of Dental Researches, 2013.

5. Palasuk J, Platt JA, Windsor LJ, Bottino MC. Development of Doxycycline-Encapsulated Nanotube-Modified Adhesives: Synthesis, Characterization and Drug Release. International Association of Dental Researches, 2015.

PUBLISHED ABSTRACTS (LOCAL)

1. Palasuk J, Platt JA. Microtensile Bond Strength of Repaired Aged Silorane Resin Composite. Indiana University School of Dentistry Nineteenth Annual Research Day Program 2011.
2. Palasuk J, Platt JA, Browning W, Cho S. Nanofilled RMGI: Fracture Toughness, Surface Roughness and Gloss Testing. Indiana University School of Dentistry Twentieth Annual Research Day Program 2012.
3. Palasuk J, Hippenmeyer L, Platt JA, Gregory RL, Spolnik KJ, Bottino MC. A Bi-Mix Antibacterial Drug-Delivery System for Regenerative Endodontics. Indiana University School of Dentistry twenty-first Annual Research Day Program 2013.
4. Palasuk J, Platt JA, Gregory RL, Windsor LJ, BOTTINO MC. Development of Doxycycline-Encapsulated Nanotube-Modified Adhesives: Synthesis, Characterization and Drug Release. Indiana University School of Dentistry twenty-third Annual Research Day Program 2015.